European Journal of Echocardiography (2011) **12**, 167–205
doi:10.1093/ejechocard/jer021

**EXPERT CONSENSUS STATEMENT**

# Current and Evolving Echocardiographic Techniques for the Quantitative Evaluation of Cardiac Mechanics: ASE/EAE Consensus Statement on Methodology and Indications Endorsed by the Japanese Society of Echocardiography

**Victor Mor-Avi, PhD, FASE*, Roberto M. Lang, MD, FASE†, Luigi P. Badano, MD, FESC, Marek Belohlavek, MD, PhD, FESC, Nuno Miguel Cardim, MD, PhD, FESC, Genevieve Derumeaux, MD, PhD, FESC, Maurizio Galderisi, MD, FESC, Thomas Marwick, MBBS, PhD, Sherif F. Nagueh, MD, FASE, Partho P. Sengupta, MBBS, FASE, Rosa Sicari, MD, PhD, FESC, Otto A. Smiseth, MD, PhD, FESC, Beverly Smulevitz, BS, RDCS, Masaaki Takeuchi, MD, PhD, FASE, James D. Thomas, MD, FASE, Mani Vannan, MBBS, Jens-Uwe Voigt, MD, FESC, and Jose Luis Zamorano, MD, FESC†**

*Chicago, Illinois; Padua, Naples, and Pisa, Italy; Scottsdale, Arizona; Lisbon, Portugal; Lyon, France; Cleveland and Columbus, Ohio; Houston, Texas; Irvine, California; Oslo, Norway; Kitakyushu, Japan; Leuven, Belgium; Madrid, Spain*

(J Am Soc Echocardiogr 2011;24:277–313.)

**From the University of Chicago, Chicago, Illinois (V.M.-A., R.M.L.); the University of Padua, Padua, Italy (L.P.B.); Mayo Clinic, Scottsdale, Arizona (M.B.); Hospital da Luz, Lisbon, Portugal (N.M.C.); Universite Claude Bernard Lyon 1, Lyon, France (G.D.); Federico II University Hospital of Naples, Naples, Italy (M.G.); Cleveland Clinic, Cleveland, Ohio (T.M., J.D.T.); Methodist DeBakey Heart and Vascular Center, The Methodist Hospital, Houston, Texas (S.F.N.); the University of California, Irvine, Irvine, California (P.P.S.); CNR Institute of Clinical Physiology, Pisa, Italy (R.S.); the University of Oslo, Oslo, Norway (O.a.S.); the University of Texas, Houston, Texas (B.S.); the University of Occupational and Environmental Health, Kitakyushu, Japan (M.T.); Ohio State University, Columbus, Ohio (M.V.); University Hospital, Leuven, Belgium (J.-U.V.); and University Clinic San Carlos, Madrid, Spain (J.L.Z.).**

**The following authors reported relationships with one or more commercial interests: Marek Belohlavek, MD, PhD, FESC, has had research supported in part by GE Healthcare (Milwaukee, WI), Siemens Medical Solutions (Erlangen, Germany), and Philips Medical Systems (Andover, MA). Mani Vannan, MBBS, received a per diem from Siemens Medical Solutions and served as a consultant with Lantheus Medical Imaging (North Billerica, MA). All other authors reported no actual or potential conflicts of interest in relation to this document.**

Reprint requests: American Society of Echocardiography, 2100 Gateway Centre Boulevard, Suite 310, Morrisville, NC 27560 (E-mail: ase@asecho.org). *Writing Group chair and † Writing Group co-chairs; Writing Group members are listed in alphabetical order. 0894-7317/$36.00

Echocardiographic imaging is ideally suited for the evaluation of cardiac mechanics because of its intrinsically dynamic nature. Because for decades, echocardiography has been the only imaging modality that allows dynamic imaging of the heart, it is only natural that new, increasingly automated techniques for sophisticated analysis of cardiac mechanics have been driven by researchers and manufacturers of ultrasound imaging equipment. Several such techniques have emerged over the past decades to address the issue of reader's experience and intermeasurement variability in interpretation. Some were widely embraced by echocardiographers around the world and became part of the clinical routine, whereas others remained limited to research and exploration of new clinical applications. Two such techniques have dominated the research arena of echocardiography: (1) Doppler-based tissue velocity measurements, frequently referred to as tissue Doppler or myocardial Doppler, and (2) speckle tracking on the basis of displacement measurements. Both types of measurements lend themselves to the derivation of multiple parameters of myocardial function. The goal of this document is to focus on the currently available techniques that allow quantitative assessment of myocardial function via image-based analysis of local myocardial dynamics, including Doppler tissue imaging and speckle-tracking echocardiography, as well as integrated back- scatter analysis. This document describes the current and potential clinical applications of these techniques and their strengths and weaknesses, briefly surveys a selection of the relevant published literature while highlighting normal and abnormal findings in the context of different cardiovascular pathologies, and summarizes the unresolved issues, future research priorities, and recommended indications for clinical use.

**Keywords** Ventricular function • Myocardial strain • Tissue Doppler • Myocardial Doppler • Tissue tracking • Speckle tracking • Integrated backscatter

# TABLE OF CONTENTS



## Abbreviations

| | |
|---|---|
| ASE | American Society of Echocardiography |
| CRT | Cardiac resynchronization therapy |
| DTI | Doppler tissue imaging |
| EAE | European Association of Echocardiography |
| EF | Ejection fraction |
| IBS | Integrated backscatter |
| IVPG | Intraventricular pressure gradient |
| LV | Left ventricular |
| RV | Right ventricular |
| SR | Strain rate |
| STE | Speckle-tracking echocardiography |
| 3D | Three-dimensional |
| 2D | Two-dimensional |

## 1. TERMS AND DEFINITIONS: BASIC PARAMETERS OF MYOCARDIAL FUNCTION

***Displacement,*** *d*, is a parameter that defines the distance that a certain feature, such as a speckle or cardiac structure, has moved between two consecutive frames. Displacement is measured in centimeters.

***Velocity,*** *v*, reflects displacement per unit of time, that is, how fast the location of a feature changes, and is measured in centimeters per second.

***Strain,*** e, describes myocardial deformation, that is, the fractional change in the length of a myocardial segment. Strain is unitless and is usually expressed as a percentage. Strain can have positive or negative values, which reflect lengthening or shortening, respectively. In its simplest one-dimensional manifestation, a 10-cm string stretched to 12 cm would have 20% positive strain.

***Strain rate,*** SR, is the rate of change in strain and is usually expressed as 1/sec or $sec^{-1}$.

Displacement and velocity are *vectors*; that is, in addition to magnitude, they have *direction*. Thus, one can examine their different spatial components along the x, y, and z directions, or alternatively along the anatomic coordinates of the cardiac chambers, longitudinal, radial, and circumferential components, which are especially relevant for the characterization of myocardial mechanics.

Similar logic applies to strain and SR, which provide local information on myocardial deformation. The important advantage of strain and SR over displacement is that they reflect regional function independently of translational motion. Nevertheless, deformation imaging cannot distinguish active from passive deformation. The term "principal strain" describes the local magnitude and direction of the shortening or lengthening of the myocardium. The term "global strain" or, more precisely, "global longitudinal strain" or "global circumferential strain" usually refers to the average longitudinal or circumferential component of strain in the entire myocardium, which can be approximated by the averaged segmental strain components in individual myocardial wall segments. Strain values can be expressed for each segment ("segmental strain"), as an average value for all segments ("global strain" mentioned above), or for each of the theoretical vascular distribution areas ("territorial strain").

The term left ventricular (LV) ***rotation*** refers to myocardial rotation around the long axis of the left ventricle. It is rotational displacement and is expressed in degrees. Normally, the base and apex of the ventricle rotate in opposite directions. The absolute apex-to-base difference in LV rotation is referred to as the net LV ***twist*** angle (also expressed in degrees). The term ***torsion*** refers to the base-to-apex gradient in the rotation angle along the long axis of the left ventricle, expressed in degrees per centimeter.

# 2. TECHNIQUES USED TO ASSESS LOCAL WALL DYNAMICS

## 2.1. Doppler Tissue Imaging (DTI)

Since the early attempts to implement the concept of tracking tissue motion using Doppler ultrasound[1] and the subsequent development of DTI over the past two decades,[2] this imaging technique has been used by multiple investigators to advance the understanding of cardiac pathophysiology and test a variety of potential new diagnostic techniques, as evidenced by a large body of literature. Although many of these techniques remained limited to the research arena, some have won widespread recognition and become mainstream tools in the arsenal of clinical echocardiography.

Although continuous-wave Doppler analyzes the *frequency shift* of the returning echoes compared with the original frequency of the ultrasound beam (*Figure 1A*), both pulsed-wave and color Doppler imaging use the *phase shift* between consecutive echoes for the velocity calculation.[3] In pulsed-wave Doppler mode, ultrasound

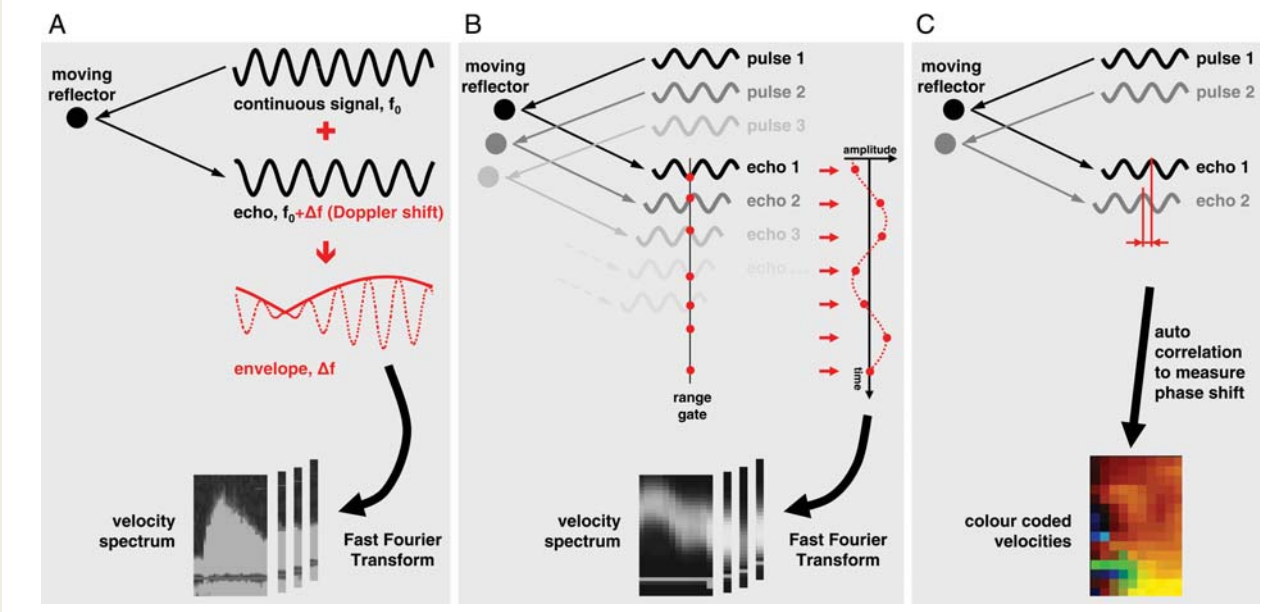


**Figure 1** (*A*) On continuous-wave Doppler, continuously emitted ultrasound with the frequency *f0* returns with the frequency *f0 + Df* when reflected by a moving object. The envelope of the mixture of the sent and received signal has a frequency equal to the frequency shift Df. In contrast, pulsed-wave and color Doppler analyze the phase shift between consecutive ultrasound pulses, while the frequency shift of the echoes is neglected. (*B*) On pulsed-wave Doppler, this phase shift is analyzed by sampling all echoes at the same point in time after emission (range gate). Sample amplitudes over time form a signal, which is converted into a velocity spectrum using the fast Fourier transform. (*C*) In color Doppler, the phase shift between consecutive pulses is measured by autocorrelation, resulting in velocities that are displayed in a color coded overlay. Modified with permission from Voigt.[179]

wavelets are emitted repeatedly at a certain repetition frequency along a single scan line, and the returning echoes are sampled at a preset time after each pulse is sent, allowing the determination of the distance between the target and the transducer. The amplitude of the sampled echoes over time is then converted into a velocity spectrum using a fast Fourier transform[3] (*Figure 1B*). In color Doppler mode, the echo of the entire scan line is received and divided into several range gates. To determine the phase shift between pulses in all range gates, an auto-correlation algorithm is used to convert the phase shifts into velocity values, which are displayed in a color overlay of the image[3] (*Figure 1C*). Although pulsed-wave Doppler has the advantage of offering a direct curve display during the examination, only color Doppler allows postprocessing, including tracking of the sample volume and calculating derived parameters (e.g., displacement or SR).

Tissue Doppler velocity estimation is based on the same principles as pulsed-wave and color Doppler echocardiography for blood flow. To distinguish between signals originating from moving tissue and blood flow, a so-called wall filter is used, which is a high-pass filter used to image blood velocities or a low-pass filter used to display tissue velocities. While the intensity of the signals generated by the myocardium is higher than that generated by blood, blood velocity usually exceeds that of the myocardium.

***DTI Acquisition: Spectral Doppler*** acquisition requires setting the sample volume size and position so that it remains within the region of interest inside the myocardium throughout the cardiac cycle. Scale and baseline should be adjusted in a way that the signal fills most of the display. Sweep speed must be adjusted according to the application for measuring slopes and time intervals: high sweep speed for measuring slopes in a few beats and low sweep speed for measuring peak values in several beats. Some imaging systems enable retrospective adjustments of sweep speed in stored data without a loss of data quality. Gain should be set to a value that produces an almost black background with just some weak noise speckles, to ensure that no important information is lost. On the other hand, caution should be taken to avoid excessive gain, as this causes spectral broadening and may cause overestimation of peak velocity. Although cardiac motion is three dimensional and complex, Doppler methods can measure only a single component of the regional velocity vector along the scan line. Care should therefore be taken to ensure that the ultrasound beam is aligned with the direction of the motion to be interrogated (*Figure 2A*). The angle of incidence should not exceed 15°, thereby keeping the velocity underestimation to $<4\%$. Only certain motion directions can be investigated with Doppler techniques (*Figure 2B*). In LV apical views, velocity samples are usually obtained at the annulus and at the basal end of the basal and mid levels and less frequently in the apical segments of the different walls.

**DTI *Acquisition: Color Doppler*** requires a high frame rate, preferably $>100$ frames/sec, and ideally $\geq 140$ frames/sec.[3] This can be achieved by reducing depth and sector width (ideally both grayscale and Doppler sectors) and by choosing settings that favor temporal over spatial resolution. Usually, the image is optimized in the grayscale display before switching to the color mode and acquiring images. Care should be taken to avoid reverberation artifacts by changing interrogation angle and transducer position, because such artifacts may affect SR estimations over a wide area (*Figure 3*). The velocity scale should be set to a range that just avoids aliasing in any region of the myocardium. Slowly scrolling through the image loop before storing allows recognition of possible aliasing. As with spectral Doppler, the motion direction to be interrogated should be aligned with the ultrasound beam. If needed, separate acquisitions should be made for each wall from slightly different transducer positions. Data should be acquired over at least three beats, that is, covering at least four QRS complexes and stored in a raw data format. Older imaging systems that store only color values in an image should not be used unless postprocessing is not planned. Acquisition of blood flow Doppler spectra of the inlet and outlet valves of the interrogated ventricle provides useful information for timing of opening and closing of the valves, and thus for hemodynamic timing of measurements obtained from the time curves of various parameters. For sufficient temporal matching, all acquisitions should have similar heart rate and show the same electrocardiographic lead.

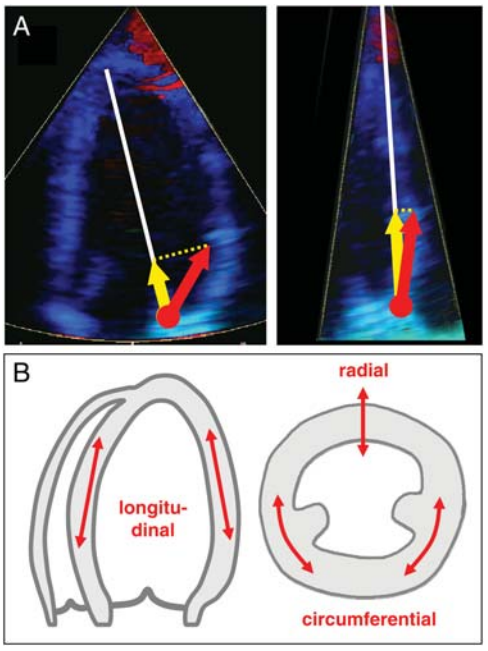


**Figure 2** Doppler techniques measure velocities in one dimension. (*A*) Alignment of the Doppler beam with the wall is therefore important. (Left) Measured velocities (yellow) are underestimated if the ultrasound beam is not well aligned with the motion to be interrogated (red). (Right) Narrow-sector single-wall acquisition may help minimize this problem. (*B*) Motion and deformation components that can be interrogated using Doppler techniques. Modified with permission from J.U. Voigt.[180]

***DTI Image Analysis: Spectral Doppler*** data cannot be further processed. Peak velocities, slopes, and time intervals are measured directly on the spectral display. *Figure 4* shows normal velocity time curves obtained from the LV basal septum and lateral wall.

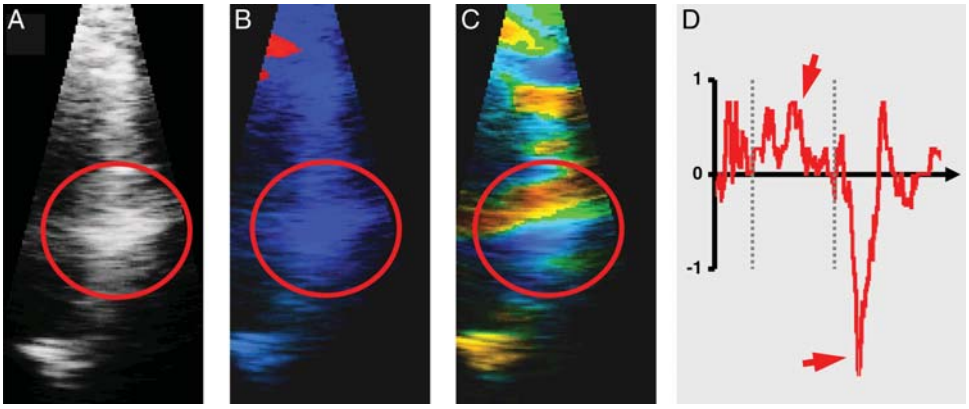


**Figure 3** Reverberation artifacts are best recognized in the grayscale image (*A*) and can be missed in the color Doppler display (*B*). They become again obvious in the color coded SR display as parallel yellow and blue lines of high intensity (*C*). If only the reconstructed time curve from such a region is considered (*D*), artifacts may be mistaken as highly pathologic curves mimicking "systolic lengthening" or "postsystolic shortening" (red arrows). Reproduced with permission from Voigt.[180]

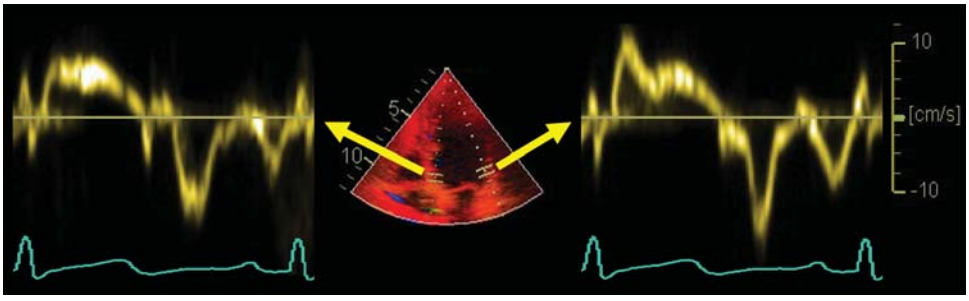


**Figure 4** Normal tissue Doppler spectra obtained from the basal septum (left) and the basal lateral wall (right). Note the different amplitudes and shapes of the curves. Reproduced with permission from Voigt.[180]

***DTI Image Analysis: Color Doppler*** data can be displayed and postprocessed in different ways. Various function parameters can be derived from a predefined region of interest within the same color Doppler data set, including velocity, displacement, SR, and strain (*Figure 5*). Two display concepts are used: color coding with or without a straight or curved M-mode and reconstructed curves of regional function. Color-coded data are best interpreted in still frames, particularly in M-mode displays. This way, there is easy visual access to the regional and temporal distribution of a particular parameter within the wall. Curve reconstructions are subsequently possible from any point within a stored data set (*Figure 5*). This allows displays of the exact time course of regional velocities and other parameters. An advantage of color Doppler processing over pulsed-wave Doppler is that with postprocessing, the sample volume can be adjusted to track the motion of the myocardium, thus staying in the same region throughout the entire cardiac cycle. Another advantage is that a sampling of the different myocardial regions is possible in the same time.

***Color Doppler Measurements of Myocardial Function:*** Because Doppler imaging generates velocity information, velocity, *v*, at any location and any time can be obtained directly from the color Doppler data.

Displacement, *d*, can be obtained by calculating the temporal integral of the tissue velocity, *v:*

$$d = \int V \, dt$$

Because of the nature of Doppler imaging, *d* describes only the motion component of the tissue in the sample volume toward or away from the transducer, while components perpendicular to the beam remain unknown. Thus, the motion curve of the mitral annulus derived from color Doppler data should have the same shape and magnitude as the M-mode tracing of the mitral annulus obtained in the same location.

SR is the temporal derivative of strain. Analytically, it is identical to the spatial gradient of tissue velocity and can therefore be obtained from the color Doppler data, as the difference between velocities measured in two samples 1 and 2 divided by the distance

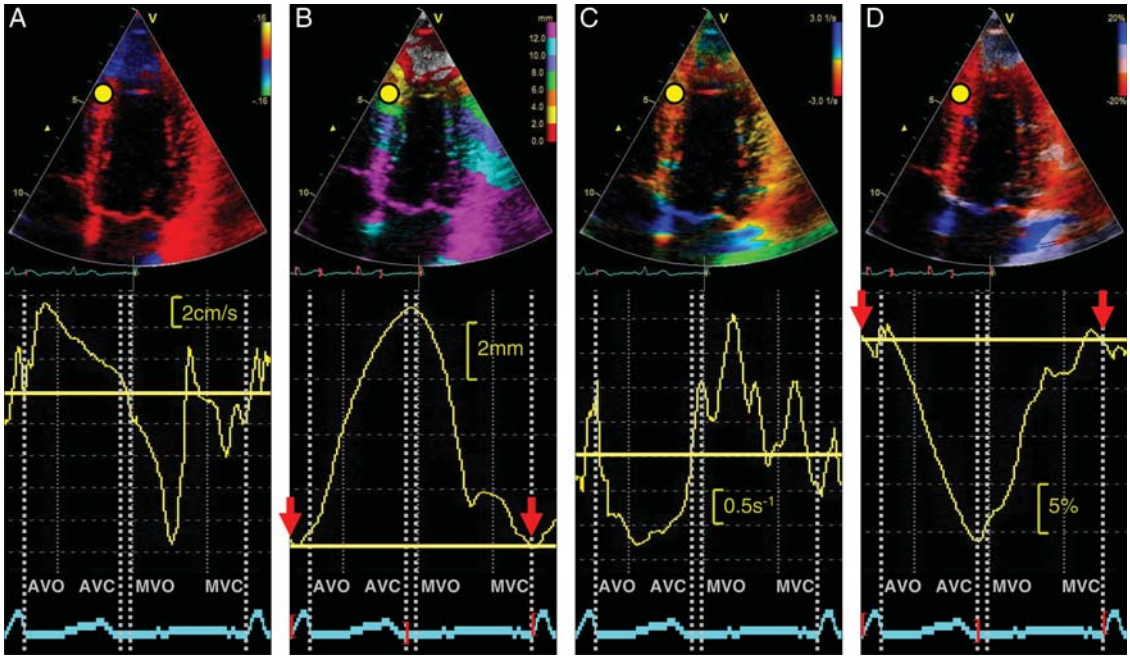


**Figure 5** Function parameters derived from one region of interest (yellow dot) within the same color Doppler data set: (*A*) velocity, (*B*) displacement, (*C*) SR, and (*D*) strain. (Top) Color coded displays. (Below) Corresponding time curves. (Bottom) Electrocardiogram. Opening and closing artifacts allow the exact definition of the cardiac time intervals. Note that in this case, the baseline is arbitrarily set to the curve value (red arrows) at the automatically recognized beginning of the QRS complex (red open bracket). *AVC*, Aortic valve closure; AVO, aortic valve opening; *MVC*, mitral valve closure; *MVO*, mitral valve opening. Reproduced with permission from Camm *et al.*[181]

r between the two samples[4]:

$$SR = \frac{V_2 - V_1}{r}$$

Strain can be calculated as the temporal integral of SR with appropriate mathematical adjustments[4,5]:

$$\varepsilon = \int SR\ dt$$

Time curves can be generated from color Doppler data for each spatial component (i.e., longitudinal, radial, and circumferential) of each of the above four parameters of cardiac function (*Figure 6*).

The time course of a spectral Doppler velocity curve is similar to a color Doppler-derived one. However, absolute values differ because the spectral curve is usually measured at the outer edge of the spectrum, whereas color Doppler data approximate the mean velocity of a region, so that reported pulsed Doppler peak velocity is typically 20% to 30% higher than that measured by color Doppler. Accordingly, it is recommended that the modal velocity (the brightest or darkest line in the spectral display, depending on display) be used for pulsed Doppler measurements.

***Potential Pitfalls of DTI:*** Tissue Doppler velocities may be influenced by global heart motion (translation, torsion, and rotation), by movement of adjacent structures, and by blood flow. These effects cannot be completely eliminated but may be minimized with the use of a smaller sample size (which may, however, result in noisier curves) and with careful tracking of the segment. To minimize the effects of respiratory variation, the patient should be asked to suspend breathing for several heartbeats.

The tissue Doppler signal can be optimized by making the width of the imaging beam as narrow as possible. Although temporal resolution is excellent with M-mode and spectral tissue Doppler, it is not as good with color tissue Doppler because of the lower frame rate.

The apical views are best for measuring the majority of LV, right ventricular (RV), and atrial segments in a parallel-to-motion fashion, although there may be some areas of deficient spatial resolution, for instance, near the apex, because of the prevalence of artifact and problems with proximal resolution. In the parasternal long-axis and short-axis views, tissue Doppler assessment is impossible in many segments (e.g., in the inferior interventricular septum and in the lateral wall) because the ultrasound beam cannot be aligned parallel to the direction of wall motion. Modified views should be used whenever necessary to achieve the optimal imaging angle.

Displacement and deformation of the myocardium are cyclic processes with no defined beginning or end. Therefore, the position of the baseline (zero line) is arbitrary. Most analysis packages define zero automatically as the value at the beginning of the QRS complex (red arrows in *Figures 5B* and *5D*) and report the actual position or length change relative to that value. Although useful for multiple applications, this approach may not

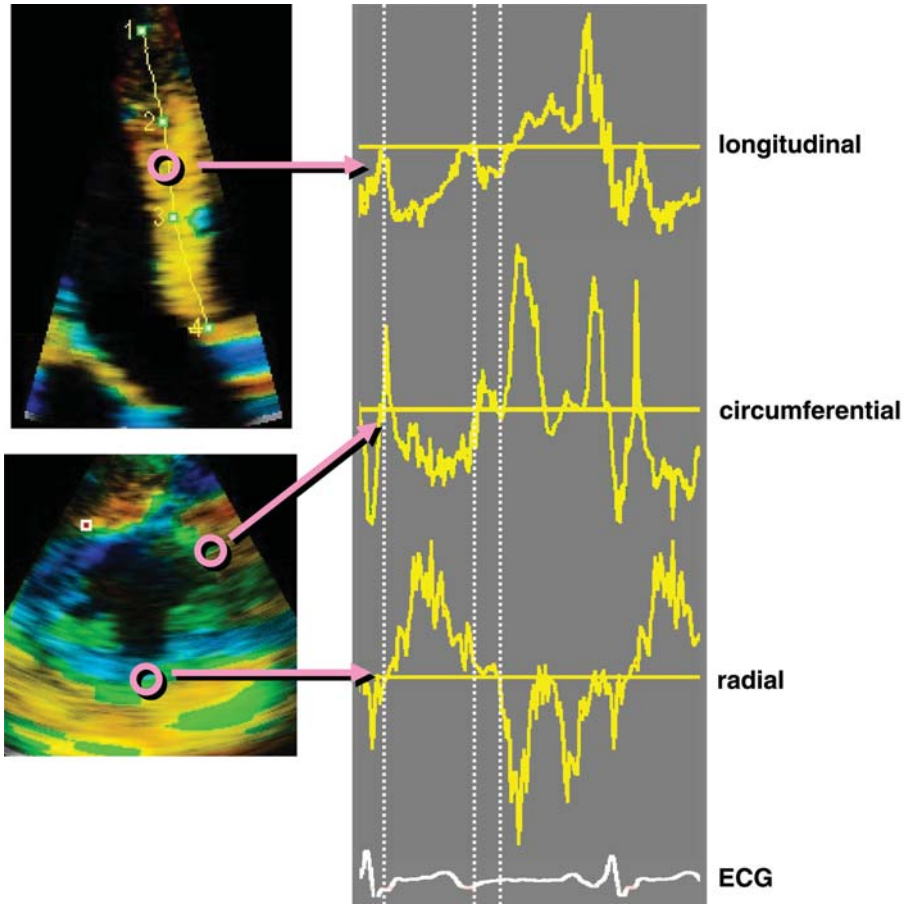


**Figure 6** Segmental SR curves in the longitudinal, circumferential, and radial directions. Besides the inversion of the radial curve, general patterns are similar.

work under certain circumstances (bundle branch blocks, wrong QRS detection on the electrocardiogram, atrial fibrillation, etc.). Care must be taken in such cases to clearly define and mark the beginning time point of deformation analysis or denote (perhaps by manual editing) the baseline (zero line) so that comparable references are used during repeated studies.

Furthermore, the integration used to calculate displacement and strain often results in an erroneous baseline shift. Most software programs automatically apply a linear correction, which is often referred to as drift compensation (*Figure 7*).

***Strengths and Weaknesses of DTI:*** The major strength of DTI is that it is readily available and allows objective quantitative evaluation of local myocardial dynamics. Over the past decade, this ability triggered extensive research in a variety of disease states that affect myocardial function, either globally or regionally, as reflected by the large body of literature involving this methodology. It is well established that peak tissue velocities are sufficiently reproducible, which is crucial for serial evaluations. Also, spectral pulsed DTI has the advantage of online measurements of velocities and time intervals with excellent temporal resolution, which is essential for the assessment of ischemia (see section 3.6) and diastolic function (see section 3.5). The major weakness of DTI is its angle dependency, as any Doppler-based methodology can by definition only measure velocities along the ultrasound beam, while velocity components perpendicular to the beam remain undetected. In addition, color Doppler-derived strain and SR are noisy, and as a result, training and experience are needed for proper interpretation and recognition of artifacts.

## 2.2. Two-Dimensional (2D) Speckle-Tracking Echocardiography (STE)

STE is a relatively new, largely angle-independent technique used for the evaluation of myocardial function. The speckles seen in grayscale B-mode images are the result of constructive and destructive interference of ultrasound backscattered from structures smaller than the ultrasound wavelength. With this technology, random noise is filtered out, while keeping small temporally stable and unique myocardial features, referred to as speckles.[6,7] Blocks or kernels of speckles can be tracked from frame to frame (simultaneously in multiple regions within an image plane) using block matching, and provide local displacement information, from which parameters of myocardial function such as velocity,

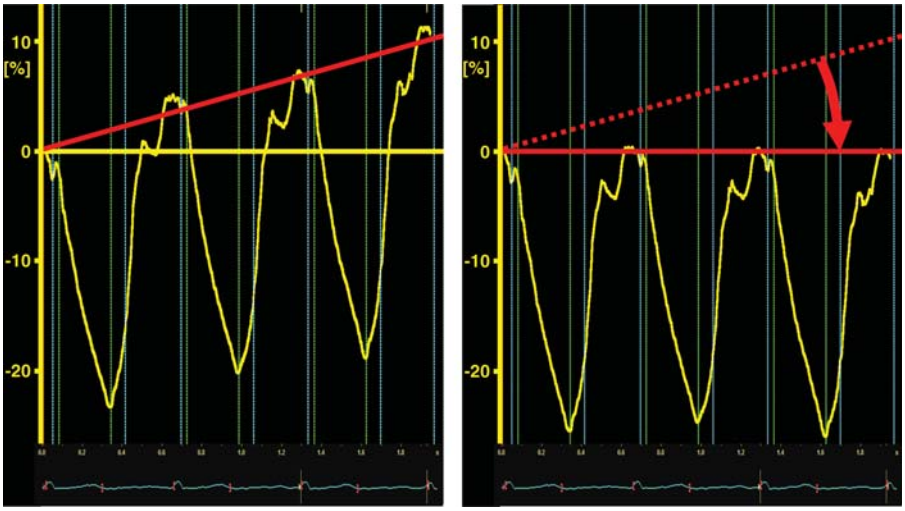


**Figure 7** Integration of velocity or SR data often results in considerable baseline shifts of the resulting motion or strain (left) curves. Most software programs allow a linear correction (right). Note that both systolic and diastolic values are influenced by this correction. Reproduced with permission from Voigt.[180]

strain, and SR can be derived (*Figure 8*). In addition, instantaneous velocity vectors can be calculated and superimposed on the dynamic images (*Figure 9*). In contrast to DTI, analysis of these velocity vectors allows the quantification of strain and SR in any direction within the imaging plane. Depending on spatial resolution, selective analysis of epicardial, midwall, and endocardial function may be possible as well.[8–10] STE has been validated for the assessment of myocardial deformation against sonomicrometry[7] and clinically against DTI.[11]

***2D STE Image Acquisition:*** Speckle tracking is an offline technique that is applied to previously acquired 2D images. The use of low frame rates may result in a loss of speckles, which in successive frames may move out of plane or beyond the search area. On the other hand, high frame rates may be achieved by reducing the number of ultrasound beams in each frame, thereby reducing the spatial resolution and image quality. Therefore, although frame rates of 40 to 80 frames/sec have been used in various applications involving normal heart rates,[12–14] higher frame rates are advisable to avoid undersampling in tachycardia.[15,16]

The focus should be positioned at an intermediate depth to optimize the images for 2D STE, and sector depth and width should be adjusted to include as little as possible outside the region of interest. Any artifact that resembles speckle patterns will influence the quality of speckle tracking, and thus care should be taken to avoid these. For software packages that process single beats, data sampling should start $\geq$ 100 msec before the peak R wave of the first QRS complex and end 200 msec after the last QRS to allow correct identification of the QRS complex, because failure to do so may result in erroneous drift compensation. Apical foreshortening seriously affects the results of 2D STE, and should therefore be minimized. Similarly, the short-axis cuts of the left ventricle should be circular shaped to assess the deformation in the anatomically correct circumferential and radial directions.

***2D STE Analysis of Myocardial Mechanics:*** Two-dimensional STE allows measurements of the above four parameters of myocardial mechanics by tracking groups of intramyocardial speckles (*d* or *v*) or myocardial deformation (e or SR) in the imaging plane. STE- derived measurements of these parameters have been validated against sonomicrometry[17,18] and magnetic resonance imaging.[15]

Assessment of 2D strain by STE is a semiautomatic method, which requires manual definition of the myocardium. Furthermore, the sampling region of interest needs to be adjusted to ensure that most of the wall thickness is incorporated in the analysis, while avoiding the pericardium. When automated tracking does not fit with the visual impression of wall motion, regions of interest need to be adjusted manually until optimal tracking is achieved. For the left ventricle, because end-systole can be defined by aortic valve closure as seen in the apical long-axis view, this view should be analyzed first. If valve closure is difficult to recognize accurately (e.g., because of aortic sclerosis), a spectral Doppler display of LV outflow may be helpful.

Assessment of 2D strain by STE can be applied to both ventricles and atria. However, because of the thin wall of the atria and right ventricle, signal quality may be suboptimal. In contrast, all LV segments can be analyzed successfully in most patients. Feasibility is best for longitudinal and circumferential strain and is more challenging for radial strain.

The timing at which peak strain is measured is not uniform across publications. Peak strain can be measured as peak systolic strain (positive or negative), peak strain at end-systole (at time of aortic valve closure), or peak strain regardless of timing (in systole or early diastole). The time point to be used to measure peak strain in the assessment of systolic function depends on the specific question one wishes to answer.

***Potential Pitfalls of 2D STE:*** Suboptimal tracking of the endocardial border may be a problem with STE. Another

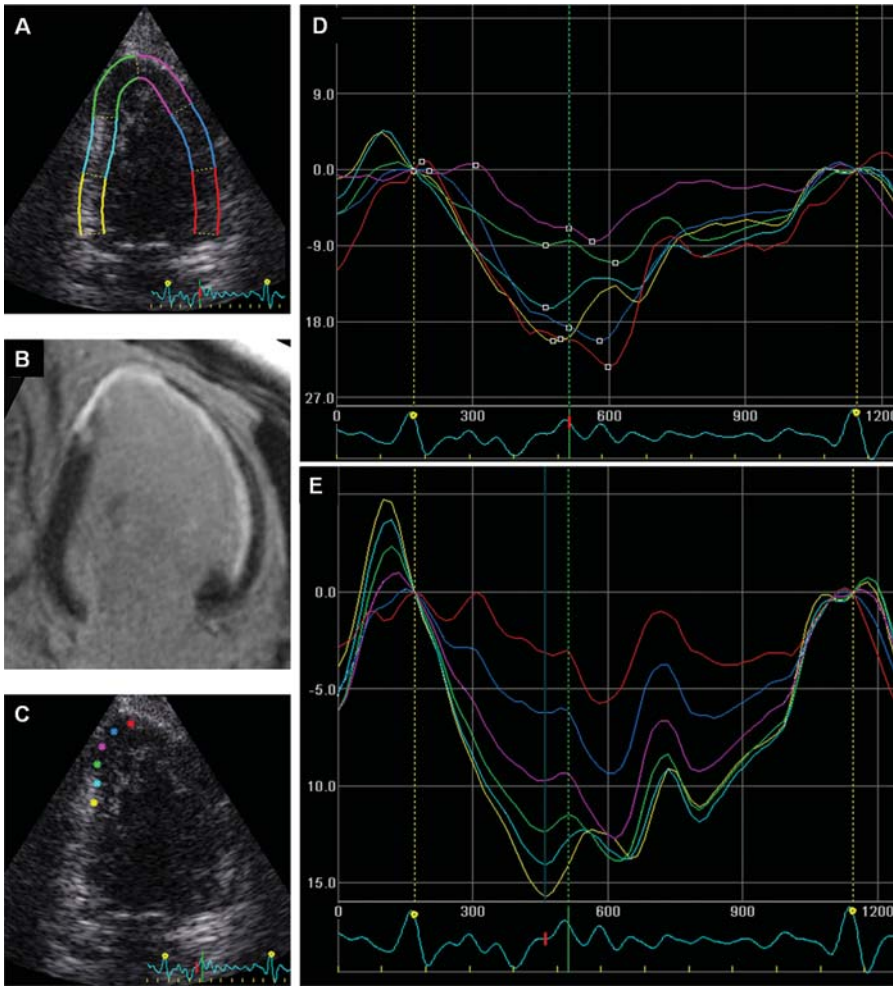


**Figure 8** Segmental strain curves (*D, E*) measured by 2D STE from an apical two-chamber view (*A, C*). Contrast-enhanced magnetic resonance image from the same patient shows white areas of delayed enhancement in the infarcted myocardium (*B*). (*A*) Myocardial segments corresponding to the segmental strain curves in (*C*). The green and purple strain curves are derived from transmural- infarcted segments, the red and blue curves represent subendocardial-infarcted segments, and the yellow and cyan curves are from noninfarcted segments. In (*C*), the colored circles correspond to the strain curves (*E*) within one segment (apical inferior) that mainly consist of transmural infarct. The yellow curve is from the border zone of the infarct and the red is within the transmural part. Reproduced with permission from Gjesdal *et al.*[19]

important limitation is its sensitivity to acoustic shadowing or reverberations, which can result in underestimation of the true deformation. Therefore, when strain traces appear nonphysiologic, signal quality and suboptimal tracking should be considered as potential causes. Tracking algorithms use spatial smoothing and a priori knowledge of "normal" LV function, which may erroneously indicate regional dysfunction or affect neighboring segmental strain values.

When using STE to measure LV twist, image quality of basal LV short-axis recordings can be a limitation. This is due in part to acoustic problems related to the depth of the basal part of the ventricle and to the wide sector angle that is necessary to visualize the entire LV base. Furthermore, measurements are complicated by out-of-plane motion when the base descends toward the apex in systole. Because LV rotation increases toward the apex, it is important to standardize the apical short-axis view. It is often easiest to find the correct circular apical short-axis view by tilting the probe from the apical four-chamber view rather than moving the probe in the apical direction from the parasternal short-axis view. The former also increases the chance of capturing a circular apical short-axis view when the endocardium nearly closes at end-systole.[19]

Global strain might be inaccurate if too many segmental strain values are discarded because of suboptimal tracking. This is particularly true in localized myocardial diseases where strain values are unevenly distributed.

Strengths and Weaknesses of 2D STE: Both DTI and STE: ***Both DTI and STE*** measure motion against a fixed external point in space (i.e., the transducer). However, STE has the advantage of being able to measure this motion in any direction within the image plane, whereas DTI is limited to the velocity component toward or away from the probe. This property of STE allows

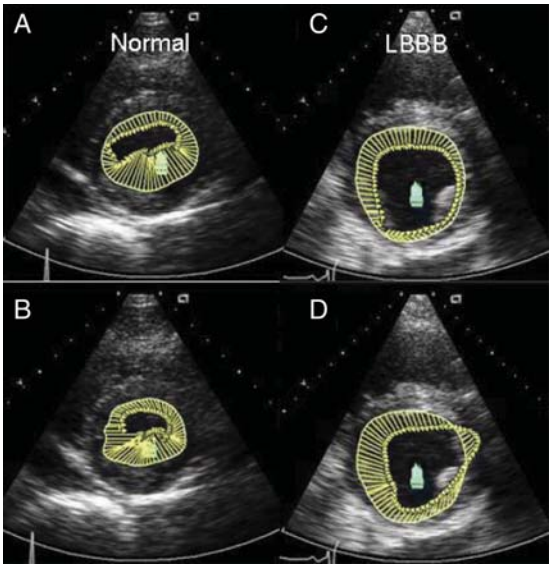


**Figure 9** Radial velocity vectors in the apical short-axis view from a normal subject (left) and a patient with left bundle branch block (LBBB) (right). In the normal subject, in early/mid-systole (*A*) and in late/end-systole (*B*), the radial vectors are of similar magnitude and direction. In contrast, in patient with LBBB, in early/mid-systole (*C*) the septal vectors are of higher magnitude than lateral radial velocities, in late systole (*D*) the septal vectors have peaked, whereas the lateral wall vectors are directed in the opposite direction (dyssynchronous).

measurement of circumferential and radial components irrespective of the direction of the beam. Of note, however, is that STE is not completely angle independent, because ultrasound images normally have better resolution along the ultrasound beam compared with the perpendicular direction. Therefore, in principle, speckle tracking works better for measurements of motion and deformation in the direction along the ultrasound beam than in other directions. Similar to other 2D imaging techniques, STE relies on good image quality as well as the assumption that morphologic details can be tracked from one frame to the next (i.e., that they can be identified in consecutive frames), which may not be true when out of plane motion occurs. Because speckle tracking relies on sufficiently high temporal resolution, DTI may prove advantageous when evaluating patients with higher heart rates (e.g., during stress echocardiography) or if short-lived events need to be tracked (isovolumic phases, diastole, etc.).

A significant limitation of the current implementation of 2D STE is the differences among vendors, driven by the fact that STE analysis is performed on data stored in a proprietary scan line (polar) format, which cannot be analyzed by other vendors' software. There are some implementations that operate on images stored in a raster (Cartesian) Digital Imaging and Communications in Medicine format, but there is only limited experience to date cross-comparing different vendors' images.[20] This issue needs further investigation before STE can become a mainstream methodology. There is currently a joint effort between the American Society of Echocardiography (ASE), European Association of Echocardiography (EAE), and the industry to address this issue.

## 2.3. Three-Dimensional (3D) STE

Although 2D STE is a useful technique, it has the intrinsic limitations of 2D imaging, such as the use of foreshortened views that affect the accuracy of the quantification of individual components of myocardial motion. In addition, the assumption that speckles remain within the 2D imaging plane and can be adequately tracked throughout the cardiac cycle may not always be valid, because of the complex 3D motion of the heart chambers. The inability of 2D STE to measure one of the three components of the local displacement vector is an important limitation, which affects the accuracy of the derived indices of local dynamics.

In contrast to 2D STE, which cannot track motion in and out of the imaging plane, the recently developed 3D STE can track motion of speckles irrespective of their direction, as long as they remain within the selected scan volume. Several recent studies showed that in individual patients, compared with 2D STE, 3D STE results in a more homogeneous spatial distribution of the measured parameters in normal ventricles. This finding is consistent with normal patterns of LV function and the fact that 3D STE can measure all three spatial components of the myocardial displacement vector[21,22] (*Figure 10*). As a result, 3D STE-based measurements of LV volumes were found to be in close agreement with magnetic resonance-derived reference values, and the levels of agreement were higher than those of 2D STE measurements obtained in the same patients, as reflected by higher correlation coefficients, smaller biases, and tighter limits of agreement.[21]

Although 3D STE generates >3,000 vectors per volume and its temporal resolution is the same as the frame rate of real-time 3D data sets (typically 20-30 volumes/sec), its use was found to considerably reduce the examination time to one third of that for 2D STE.[23] Furthermore, a significantly greater number of segments could be analyzed using 3D STE. This advantage of 3D STE stems from the fact that the entire left ventricle can be analyzed from a single volume of data obtained from the apical transducer position. These initial clinical results indicate that 3D STE may have important advantages over 2D STE, allowing a faster and potentially more complete and more accurate analysis of myocardial function, despite the relatively low temporal resolution.

***3D STE Image Acquisition:*** Three-dimensional STE can be applied to 3D echocardiographic images acquired using a matrix-array transducer from the apical position in a wide-angled acquisition "full-volume" mode. In this mode, a number of wedge-shaped subvolumes are acquired over consecutive cardiac cycles during a single breath hold and stitched together to create one pyramidal volume sample. It is likely that 3D STE will be applicable to 3D data sets acquired in a single-beat mode, when this mode allows imaging at sufficiently high frame rates. Special care must be taken to include the entire LV cavity within the pyramidal volume, which may have a detrimental effect on temporal resolution.

***3D STE Analysis of Myocardial Deformation:*** Pyramidal data sets are analyzed using dedicated, semiautomated 3D STE

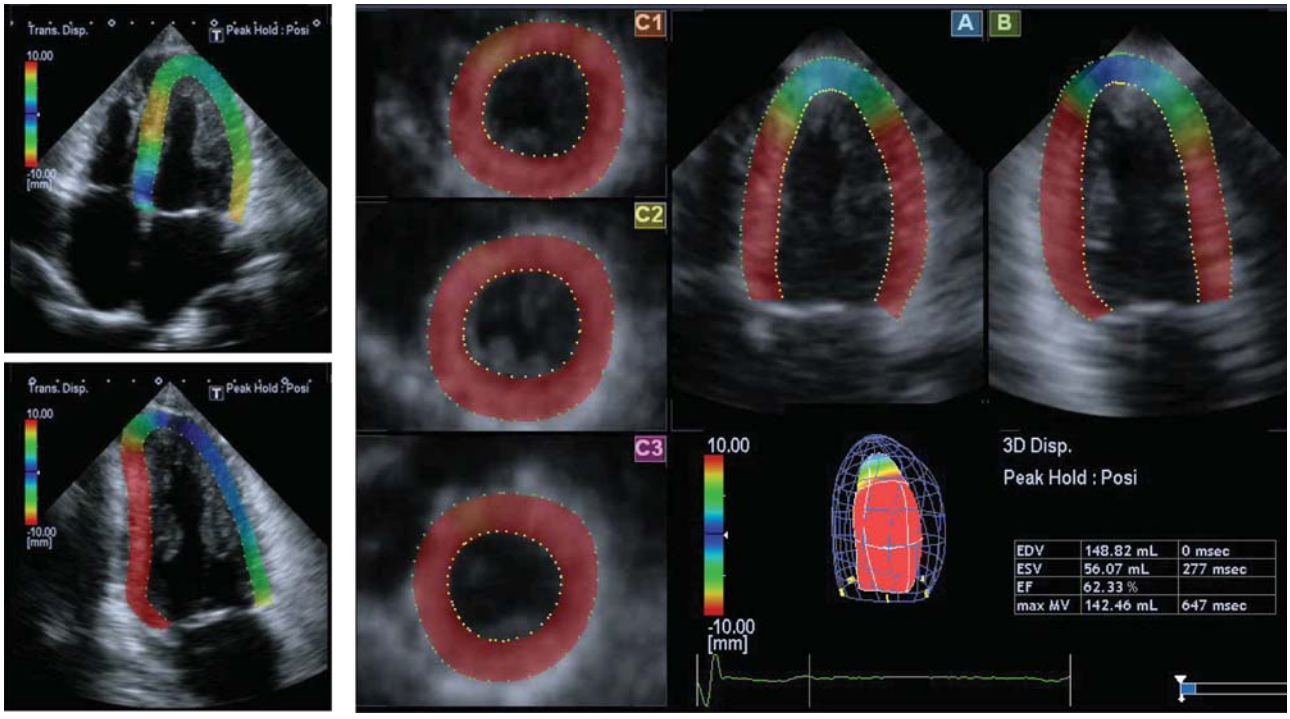


**Figure 10** Example of images obtained at end-systole in a patient with normal LV function and concentric hypertrophy: 2D STE (left top, apical-four chamber [A4C] view; left bottom, apical two-chamber [A2C] view) and 3D STE extracted from the real-time 3D echocardiography pyramidal data set (right, [*A*] and [*B*]: A4C and A2C views; [*C1–C3*]: short-axis views from apex to base). The color patterns in both 2D views showed considerable variability in the measured regional displacement, as reflected by different colors, despite the normal LV function, reflecting out-of-plane motion of the speckles. In contrast, the 3D slices showed considerably more uniform color patterns, consistent with normal LV wall motion, in the short-axis views and also in the apical views, where one can also appreciate the gradual decrease in endocardial displacement toward the LV apex. Reproduced with permission from Nesser *et al.*[21]

software. After anatomically correct, nonforeshortened apical views are identified at end-diastole and LVendocardial and epicardial boundaries are initialized, 3D endocardial and epicardial surfaces are automatically detected with manual adjustments as necessary. Subsequently, these borders are automatically tracked in 3D space throughout the cardiac cycle. To obtain regional information about LV motion and deformation, the ventricle is divided into 3D segments. Radial and longitudinal displacements and rotation, as well as radial, longitudinal, and circumferential strains, are automatically calculated for each segment over time. In addition, displacement in 3D space is calculated. Peak and time-to-peak values can also be obtained for each index similarly to 2D STE.

***Potential Pitfalls of 3D STE:*** The major pitfall of 3D STE is its dependency on image quality. Random noise and relatively low temporal and spatial resolution affecting its ability to define the endocardial and epicardial boundaries. These issues likely affect the frame-to-frame correlation of local image features and contribute to suboptimal myocardial tracking. As with 2D STE, tracking quality should therefore be carefully verified and adjusted as necessary.

***Strengths and Weaknesses of 3D STE:*** With the theoretical benefits gained by the addition of the third component of motion vector, which is "invisible" to either DTI or 2D STE, 3D STE promises to allow accurate assessment of regional ventricular dynamics. Nevertheless, it still requires rigorous validation and testing. On the downside, the much slower frame rates of 3DE compared with 2D STE may limit analysis of rapid events such as isovolumic contraction and relaxation. Future studies should assess the impact of these relatively low frame rates.

Another limitation is that although this methodology has been validated against sonomicrometry in animals,[24] there is no true noninvasive "gold standard" technique that can be used in humans to validate regional ventricular function in three dimensions. As a result, most of the literature on this topic published thus far represents feasibility studies and potential advantages of 3D STE but does not establish the accuracy of the method. The clinical value of this new technology in a wide variety of clinical scenarios such as chamber volume measurements,[21] evaluation of global and regional wall motion abnormalities[25] (*Figure 11*), and assessment of LV dyssynchrony[26] in patients with heart failure remains to be determined in future studies.

Even more than 2D STE, 3D STE is currently implemented in ways specific to individual vendors. Although this methodology is in its infancy of development, it will be important to move toward vendor interchangeability.

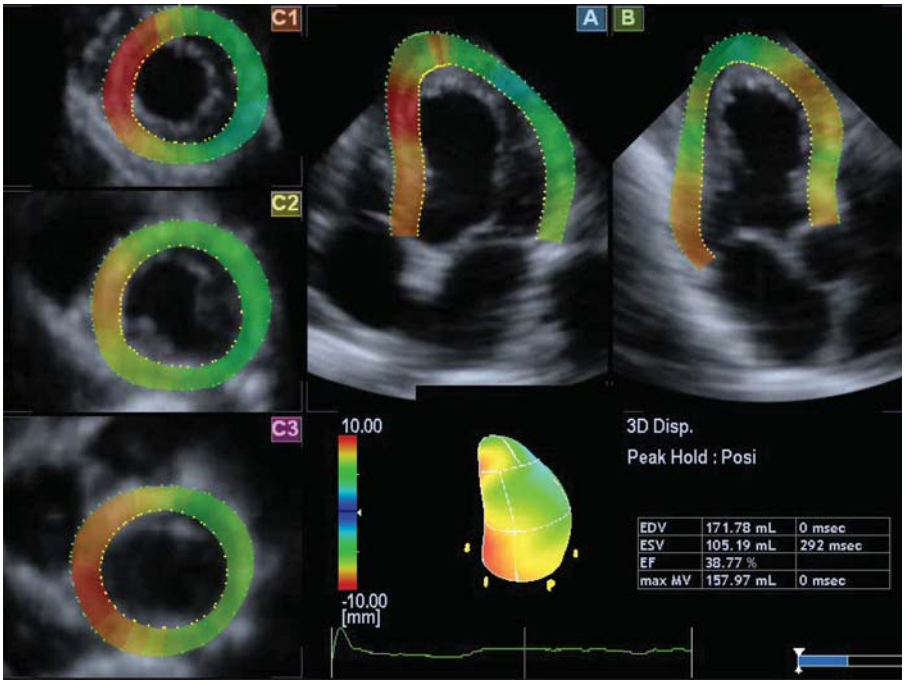


**Figure 11** Unlike the images in *Figure 10*, 3D speckle-tracking echocardiographic slices obtained at end-systole in this patient show reduced 3D displacement in the lateral wall (green hues), consistent with chronic inferolateral myocardial infarction. Reproduced with permission from Nesser *et al.*[21]

## 2.4. Integrated Backscatter (IBS) Analysis

IBS analysis can be considered the first technique used for myocardial imaging, with initial studies being described as the method evolved in parallel with the development of 2D imaging more than three decades ago.[27] IBS analysis describes a process of quantitative acoustic characterization of the myocardial structure.[28] In this analysis, the power of the reflected signal in each scan line is quantified before the radio-frequency signal is demodulated to construct a real-time image. The IBS signal reflects the interaction between the incidental ultrasound wave and the structural heterogeneity in the myocardium and can be analyzed in either the time or the frequency domain.

***IBS Signal Acquisition:*** The IBS signal is obtained from standard dynamic 2D images, usually in the parasternal long-axis view. However, images need to be saved in raw data format to allow IBS analysis before the image is processed.

***IBS Analysis of Myocardial Dynamics:*** This analysis is performed by dedicated software that may be used for two major purposes. Variation in backscatter during the cardiac cycle is thought to reflect the crossover of actin and myosin within the myofibrillar structure. This process results in changes of reflectivity, and the resulting cyclic variation has been shown to correlate with myocardial strain.[29] The problem is that because of the myocardial anisotropy (directional nonuniformity of myofibers), the pattern of this variation differs from wall to wall and view to view, such that specific normal ranges need to be documented for each wall and each view. Nonetheless, the signal has been used as a noninvasive marker of contractility, for example in the assessment of myocardial viability.[30] The second measurement approach relates to the comparison of myocardium with other tissues to document the reflectivity of

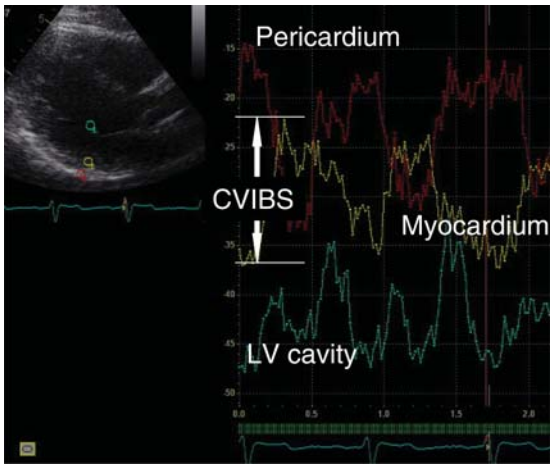


**Figure 12** Analysis of IBS. Calibrated backscatter is calculated from the difference between myocardial signal (yellow) and either pericardium (red) or LV cavity (blue). Cyclic variation of backscatter is measured by the variation of signal intensity throughout systole.

the myocardium (*Figure 12*). In the absence of a frame of reference, this parameter would be influenced by gain settings and patient habitus, so the provision of this material requires calibration with an intrinsic frame of reference (calibrated IBS),[28] such as the pericardium (which is brighter than myocardium) or blood pool (which is darker).

The results of clinical studies have been described at length in previous review articles.[28] Normal ranges of cyclic variation in IBS of the septum and posterior wall vary from 4.5 to 6.0 dB. Dilated cardiomyopathy has been associated with obstruction of cyclic variation, corresponding to areas of reduced function. Likewise, reduced cyclic variation has been documented in the setting of acute myocardial infarction. In viable myocardium, residual cyclic variation is detected even though the tissue may appear akinetic.[31] Cyclic variation in IBS is also reduced in early myocardial disease, for example because of diabetes or hypothyroidism.[32] Likewise, calibrated IBS has been used as a marker of fibrosis in a variety of cardiac conditions, including hypertensive heart disease and hypertrophic cardiomyopathy.[33] Biopsy studies have been performed to validate the presence of fibrous tissue in these settings.[34] Also, IBS can identify an increase in atrial degeneration that might predict the occurrence of atrial fibrillation before LA dilation.[35]

***Potential Pitfalls of IBS Analysis:*** In the image setup, care needs to be taken with the output power settings to ensure that the signal is not saturated. This is particularly a problem when using video signal, rather than the radiofrequency signal, because the relationship between signal intensity and brightness is nonlinear at the upper and lower extremes of signal intensity. The ultrasound beam should be perpendicular to the interrogated wall, and measurements should be performed within the myocardium while avoiding the endocardium, because the blood-tissue interface is much brighter than the in- tramyocardial signal and can lead to overestimation of the IBS signal.

***Strengths and Weaknesses of IBS Analysis:*** The attraction of this application is that myocardial texture may be analyzed from standard grayscale images. Potentially, this method could be used to quantify tissue characteristics independent of the usual parameters of LV shape and function. However, there are a variety of weaknesses. The technique is susceptible to poor image quality and signal noise. Measurements are generally restricted to the anteroseptal and posterior segments in the parasternal views. Although other segments and views may be imaged, the user should be aware that normal ranges are less well defined and that the variability of the signal is greater, related to angulation issues.[36]

The long history of this technique compared with its rare clinical use tells its own story in relation to its difficulty. This procedure is technically demanding, subject to artifacts related to the presence of other myocardial reflectors, image settings, and the exact location of the sample volume. In the era of strain measurement, there is little to recommend the ongoing measurement of cyclic variation as a marker of contractility. Calibrated backscatter still has value as a marker of fibrosis, but this appears to be most effective in more severe disease. Therefore, this methodology remains more of a research instrument than a clinical tool.

# 3. PHYSIOLOGIC MEASUREMENTS OF LEFT VENTRICULAR FUNCTION

## 3.1. LV Architecture and Vectors of Myocardial Deformation

Knowledge of the cardiac micro and macro architecture is useful in understanding the relative contributions of different myocardial layers to the 3D components of myocardial deformation. This information is important for optimizing motion analysis using DTI and STE.

Several studies have explored the 3D deformation of the ventricular tissue, describing myocyte arrangements as a continuum of two helical fiber geometries. The subendocardial region shows a right- handed helical myofiber geometry, which changes gradually into a left-handed helical geometry in the subepicardium.[37–39] Thus, the longitudinal axis of cardiac myofiber sheets rotates continuously. In the subendocardium, the fibers are roughly longitudinally oriented, with an angle of about 80° with respect to the circumferential direction. The angle decreases toward the midwall, where the fibers are oriented in the circumferential direction (0°), and decreases further to an oblique orientation of about −60° in the subepicardium (*Figure 13A*).[40]

This structural anisotropy of the LV wall affects the propagation and backscatter of ultrasound waves[6] and the appearance of cardiac tissue in echocardiographic images. Greater backscatter and brighter speckles are seen when myofibers and the ultrasound beam are perpendicular rather than parallel.[41,42] For example, in the apical four- chamber view, bright speckles in the middle of the interventricular septum represent the location of the middle layer of circumferentially oriented fibers that are perpendicular to the beam (*Figure 13B*). In short-axis views, bright speckles are seen in the anterior and posterior segments where myofiber sheets are perpendicular to the beam, while marked attenuation occurs within the septum and the lateral wall, where the myofiber sheets are relatively parallel to the scan lines (*Figure 14*).

The above myocardial structure broadly determines the components of myocardial deformation. The subendocardial region contributes predominantly to the longitudinal mechanics of the left ventricle, whereas the midwall and the subepicardium contribute predominantly to the rotational motion.

***Longitudinal and Circumferential Mechanics:*** During preejection, reshaping of LV geometry causes simultaneous shortening and stretch of the early and the late activated regions, respectively.[37,39,43] Thus, shortening of subendocardial fibers is accompanied by simultaneous subepicardial fiber stretching. Segmental stretch may also be seen in the late activated regions of the subendocardium, particularly near the basal posterolateral region, which is the last area of the ventricle to activate. The onset of longitudinal and circumferential shortening therefore shows substantial transmural and apex-to-base heterogeneity.[37,44]

Subendocardial and subepicardial layers shorten concurrently during ejection.[39,44] The magnitude of circumferential strains during ejection exceeds that of longitudinal strains.[44] Furthermore, longitudinal and circumferential shortening strains during ejection

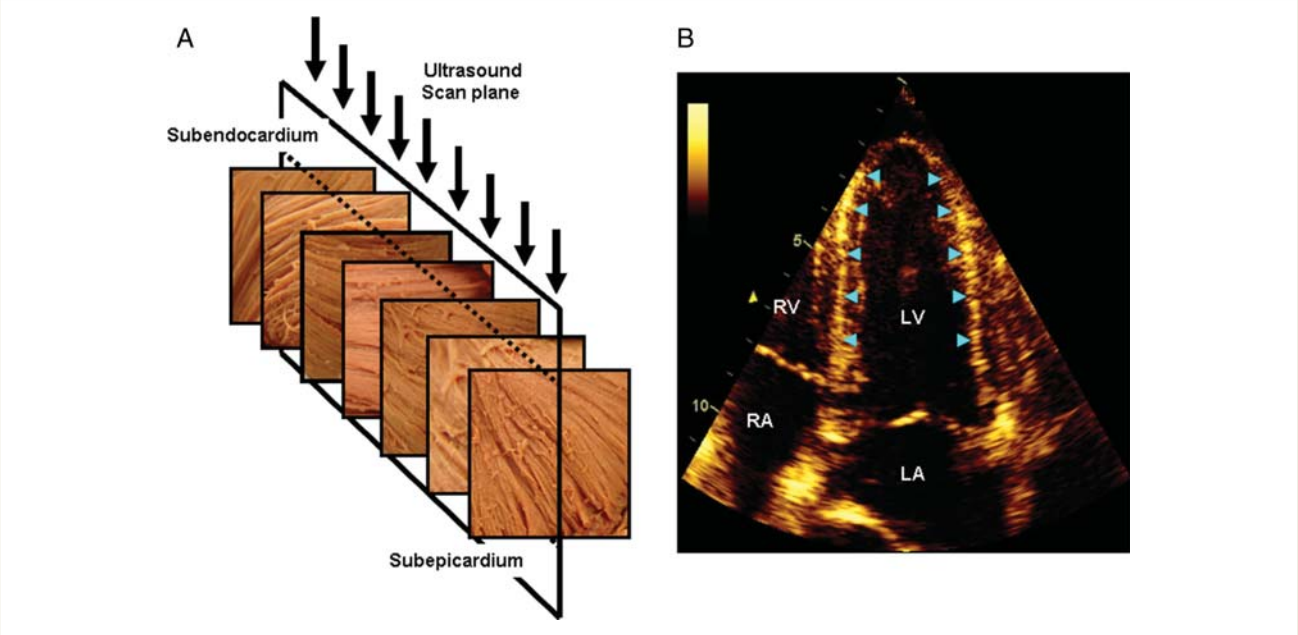


**Figure 13** Link between transmural variation of myocardial fiber direction (*A*) and speckle pattern generated in echocardiography (*B*). Fiber direction changes from right-handed (R) helix in subendocardium to left-handed (L) helix in subepicardium. Direction of myofibers is predominantly circumferential in midwall. Ultrasonic image plane in apical four-chamber view (*A*) (arrows) is therefore orthogonal to circumferentially oriented fibers in midwall. Region of LV wall where fibers are orthogonal to plane of ultrasound produce bright speckles and can be readily identified in the septum and LV lateral wall (*B*) (arrowheads). *LA*, Left atrium; *RA*, right atrium; *RV*, right ventricle.

show a small apex-to-base gradient, such that successive shortening strains are higher at apical and mid segments compared with the LV base.[44]

The postejection period also shows significant heterogeneity in the onset of myofiber relaxation. Lengthening of subepicardial fibers is accompanied by shortening of subendocardial fiber sheets.[37,44] This transient heterogeneity accounts for physiologic longitudinal postsystolic shortening of myocardial segments recorded in normal human subjects.[39]

***Radial Mechanics:*** Continuum mechanics would suggest that shortening in the longitudinal and circumferential direction would result in thickening in the radial direction for conservation of mass. However, LV wall thickening is not a result of simple shortening of individual myocytes but an effect of shearing of groups of myocytes across one another. One of the principal purposes of cardiac shearing deformation lies in amplifying the 15% shortening of myocytes into >40% radial LV wall thickening, which in turn results in a >60% change in LV ejection fraction (EF) in a normal heart.[38] Because the degree of shearing increases toward the subendocardium, higher thickening strains are seen at the subendocardium in comparison with the subepicardium. This difference does not reflect a difference in contractility between wall layers but is a consequence of geometry and tissue incompressibility. Transmural heterogeneity in the timing of wall thickening mechanics is also seen during the preejection and postejection phases of the cardiac cycle.[37]

***Twist Mechanics:*** The helical nature of the heart muscle determines its wringing motion during the cardiac cycle, with counterclockwise rotation of the apex and clockwise rotation of the base around the LV long axis, when observed from the apical perspective.

In a normal heart, the onset of myofiber shortening occurs earlier in the endocardium than the epicardium.[45] During preejection, subendocardial shortening and subepicardial stretch contribute to a brief clockwise rotation of the LV apex.[37,45] During ejection, the activation and contraction of the subepicardial region with a larger radius of arm of moment produces higher torque to dominate the direction of rotation, resulting in global counterclockwise LV rotation near the apex and clockwise rotation near the LV base. Twisting and shearing of the subendocardial fibers deform the matrix and result in storage of potential energy.

Subsequent recoil of twist, or untwist, which is associated with the release of restoring forces contributes to diastolic suction, which facilitates early LV filling. The onset of myofiber relaxation occurs earlier in epicardium than endocardium. Thus, at early diastole, both subepicardial lengthening and subendocardial shortening facilitates recoil in the clockwise direction. Nearly 50% to 70% of LV untwisting occurs within the period of isovolumic relaxation, while the rest is completed during early diastolic filling phase. One manifestation of this is that during systole, twisting occurs simultaneously with long-axis and radial shortening, while during diastole, untwisting distinctly precedes lengthening and expansion, a phenomenon that is even more marked with exercise.[46] This leads to a linear relation between twist and LV volume during ejection with a nonlinear curve in diastole.

***Components of Myocardial Deformation and Transmurality of Disease: In general, longitudinal LV mechanics, which are*** predominantly governed by the subendocardial layer, are the most vulnerable and most sensitive to the presence of myocardial disease. If unaffected, midmyocardial and epicardial function may

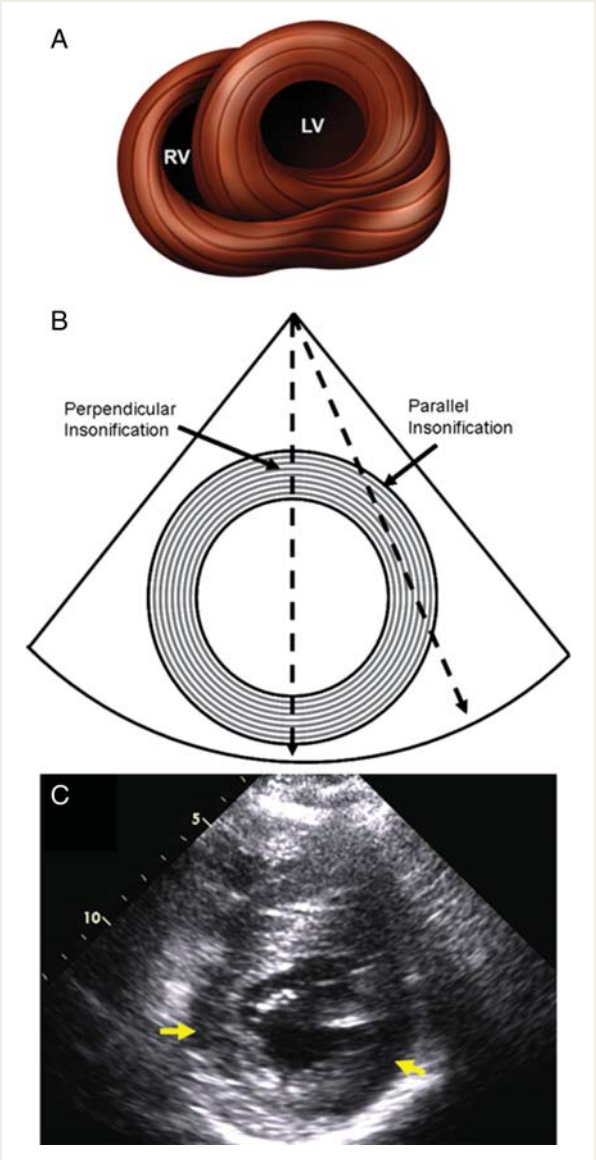


**Figure 14** Illustration showing the local angles of insonification between incident ultrasound beam and predominant myofiber orientation in the short-axis view. Short-axis view of left and right ventricles showing the myofiber anatomy as seen from the apical end of the left ventricle (*A*). Cross-sectional drawing of left ventricle shows parallel and perpendicular insonification in relation to the orientation of the myofibers (*B*). This results in marked attenuation and reduced speckles (arrows) in the septum and the lateral wall segments in short-axis views of the left ventricle (*C*).

result in normal or nearly normal circumferential and twist mechanics with relatively preserved LV pump function and EF. However, compromised early diastolic longitudinal mechanics and reduced and/or delayed LV untwisting may elevate LV filling pressures and result in diastolic dysfunction. On the other hand, an acute transmural insult or progression of disease results in concomitant midmyocardial and subepicardial dysfunction, leading to a reduction in LV circumferential and twist mechanics and a reduction in EF.[47,48] Thus understanding the layer- based contributions to the components of cardiac deformation helps in estimating the transmural disease burden correctly and provides pathophysiologic insight into the mechanisms of LV dysfunction.

## 3.2. Clinical Use of LV Displacement, Velocity, Strain, and SR

There is a wealth of literature on the use of the displacement and deformation indices of myocardial dynamics in multiple disease states. The following is a brief summary of the existing body of knowledge.

***Normal Values:*** Normal values of the parameters of LV myocardial mechanics vary depending on the specific LV wall and the specific 3D component of each index. For both DTI and STE, longitudinal measurements are more robust than radial ones. Because the apical window allows interrogation of all LV myocardial segments, most available clinical data pertain to longitudinal deformation. Longitudinal velocities in the lateral wall are higher than in the septum. There is also a base-to-apex gradient, with higher velocities recorded at LV base than near the apex. Minor differences are seen between LV segments for DTI-derived strain and SRs. STE-derived measurements generally show higher values in the apical segments than DTI. Within a segment, higher velocities and strains are usually recorded from the subendocardium than from the subepicardium. Velocities and deformation parameters are also affected by age and loading conditions. In a recent study in a large European population, the lower limits of normal range with the Doppler method were found to be 18.5% and 44.5% for longitudinal and radial strain and 1.00 and 2.45 $sec^{-1}$ for longitudinal and radial SR.[49] Normal deformation values vary among publications[49,50] and importantly depend on the brand of imaging equipment, which does not use the same algorithms to process measured data across vendors. Moreover, loading conditions and heart rate need to be taken into account when interpreting all functional data.

**Published Findings:** *Estimation of LV Filling Pressures.*— LV filling pressures obtained by cardiac catheterization show good correlation with the ratio of the mitral inflow E velocity to DTI-derived mitral annular wave (E/e′).[51] E/e′ (lateral) $\geq$12 and E/e′ (septal) $\geq$15 are correlated with elevated LV early diastolic pressure, and E/e′ (lateral, septal, or average) $<$8 is correlated with normal LV early diastolic pressure.

*Subclinical Disease.* — Strain and SR analysis increase sensitivity in detecting subclinical cardiac involvement in conditions such as amyloidosis, diabetes, and hypertensive heart disease,[52] as well as changes in LV function after cancer treatment,[53] because e′ velocity is reduced in patients with all these conditions.

*Constrictive Versus Restrictive Physiology.* — In the absence of myocardial disease, e′ velocities typically remain normal in patients with constrictive pericarditis (usually $>$8 cm/sec). In contrast, intrinsic myocardial abnormalities characteristic of restrictive cardiomyopathy result in impaired relaxation and reduced e′ velocities.[54]

*Athlete's Heart Versus Hypertrophic Cardiomyopathy.* — *The* presence of brisk e′ velocities is seen in athletes' hearts in contrast to the reduced e′ velocities seen in individuals with hypertrophic cardiomyopathy.[55]

*Mitral and Tricuspid Annular Motion.* — The mitral and tricuspid annuli are anatomic structures that may be distinctly visualized by 2D echocardiography in almost all patients, irrespective of endocardial visualization. As a result, annular longitudinal displacement can be accurately assessed in the majority of patients.

*Myocardial Strain and SR.* — In disease states, myocardial deformation patterns may either remain comparable with normal, but reach lower peak values,[53] or show striking changes as the disease progresses.

*Coronary Artery Disease.* — Changes in strain not only facilitate recognition of ischemic myocardium during stress echocardiography (*Figure 15*) but also may provide prognostic information.[56–60] Furthermore, assessment of cardiac strain helps in defining the transmural extent of myocardial infarction and the presence of viable myocardium.

*Cardiomyopathy.* — Cardiac strain and SRs may be reduced in cardiomyopathy and potentially could be used for monitoring disease progression and the impact of therapeutic interventions.[61,62] DTI and speckle-tracking echocardiographic measurements are helpful in quantifying LV dyssynchrony. However, there is currently a lack of consensus on how LV dyssynchrony indices should be measured in clinical practice.

*Congenital Heart Disease.* — Several studies have recently tested the use of DTI and STE to assess myocardial deformation and strain in children, both normal and with congenital abnormalities.[63–65] However very little is known to date as far as clinical usefulness of these techniques in the context of congenital heart disease.[66]

***Unresolved Issues and Research Priorities:*** A growing body of evidence suggests that the assessment of LV deformation by Doppler or speckle-tracking techniques provides incremental information in clinical settings. The areas that hold the greatest promise for potential applications include assessment of myocardial ischemia and viability (see below), detection of subclinical heart disease, and the serial assessment of different cardiomyopathies. One of the major challenges, however, is the rapid pace of technological growth, which has resulted in a variety of software packages and algorithms. Future clinical trials therefore need to include standardization of nomenclature, steps in data acquisition, and optimal training to reduce data variability.

***Summary and Recommended Indications:*** Clinical applications of DTI or STE derived myocardial displacement, velocity, strain, and SR measurements are gradually becoming established as tools for the assessment of LV diastolic function but still require further refinements. DTI-derived mitral annular velocities by pulsed-wave Doppler are recommended for the routine clinical evaluation of LV diastolic function, as described in detail below in the section 3.5. STE- derived and DTI-derived strain parameters are comparable, but STE has advantages with regard to ease of application and analysis and for data reproducibility. For both techniques, the accuracy of measurements, however, depends on image quality and the accuracy of tracking. In expert hands, strain and SR parameters can improve accuracy and prognostic value of stress

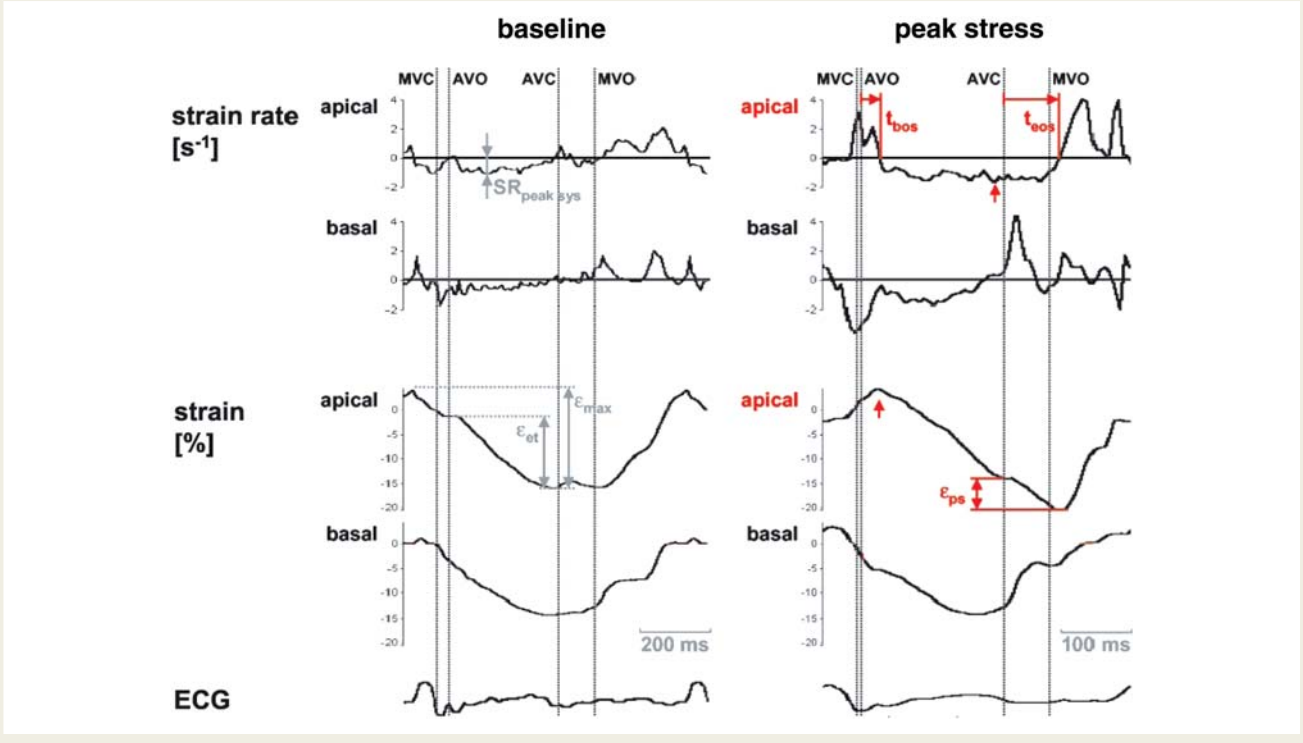


**Figure 15** Example of ischemic (apical segment) and nonischemic (basal segment) stress response in strain and SR curves. Note the reduced systolic shortening and the marked postsystolic shortening (eps) during stress-induced ischemia. AVC, Aortic valve closure; AVO, aortic valve opening; *MVC*, mitral valve closure; MVO, mitral valve opening. Adapted with permission from Voigt *et al.*[59]

echocardiograms. Further technical development and standardization of methodology are necessary before additional clinical application can be recommended.

## 3.3. LV Rotation

LV rotation or twisting motion has an important role in LV systolic and diastolic function. Although LV rotational deformation can be quantified using color DTI with high temporal resolution, this method is technically demanding and has not achieved widespread adoption.[67] In contrast, multiple recent studies have demonstrated that 2D STE represents a clinically feasible alternative to color DTI in evaluation of myocardial rotation and twist mechanics in the majority of patients.[46,68]

***Normal Values:*** Normal values for LV rotation and net twist angle show variability depending on the technique used for measurement, the location of the region of interest in the subendocardium or the subepicardium, the age of the subject, and the loading hemodynamics of the ventricle.[45] A recent study of a large group of healthy volunteers[69] reported a mean value of peak LV twist angle as $7.7 \pm 3.5^{\circ}$. Peak LV twist angle was significantly greater in subjects aged >60 years ($10.8 \pm 4.9^{\circ}$) compared with those aged <40 years ($6.7 \pm 2.9^{\circ}$) and even those aged 40 to 60 years ($8.0 \pm 3.0^{\circ}$). The increase in LV twist angle can be explained by less opposed apical rotation, resulting from a gradual decrease in subendocardial function with aging. Worsening of diastolic relaxation and reduced early diastolic suction is, however, associated with reduction in the rate and magnitude of untwisting.[70] In a study of patients from infancy to middle age, it was noted that twist increases from $5.8 \pm 1.3^{\circ}$ in infancy to $6.8 \pm 2.3^{\circ}$ in grade school, $8.8 \pm 2.6^{\circ}$ in the teenage years, and $13.8 \pm 3.3^{\circ}$ in middle age. Apical rotation was fairly constant in childhood, with basal rotation transition from counterclockwise in infancy to the adult clockwise rotation, causing most of the increase in twist in childhood. Subsequently, the twist increases, mainly because of a gradual increase in apical rotation with age.[71]

***Published Findings:*** Because apical rotation accounts for most of LV twist, apical wall motion abnormalities significantly impair peak LV twist parameters. This may be manifested by (1) a reduction of initial clockwise twist during early systole, (2) augmentation of peak counterclockwise twist, and (3) reduction in LV untwisting during early diastole (*Figure 16*). Major findings reported in published studies are described below and summarized in *Table 1*.

*Heart Failure Syndromes.* — In early stages of heart failure, diastolic dysfunction is associated with relatively preserved or even higher LV net twist angle in the presence of normal EF.[72] The onset of untwisting and peak untwisting in early diastole, however, is significantly delayed and can be further unmasked during exercise. Patients with heart failure and reduced EF show progressive reduction of LV twist angle and untwisting velocities. However, in patients with heart failure and preserved systolic function, peak untwisting is usually normal but may be delayed in a subset of patients.[72,73]

*Coronary Artery Disease.* — Although LV longitudinal strain is attenuated in the presence of subendocardial perfusion deficit, LV circumferential deformation and twist may remain unaltered in ischemic myocardium. Similarly, patients with subendocardial infarcts and preserved EF show reduced radial and longitudinal strain, although LV circumferential strains and twist mechanics remain relatively preserved. In contrast, a larger transmural infarction is associated with reduction in LV systolic twist angle and diastolic untwisting velocity, which correlates with the reduced EF.[74]

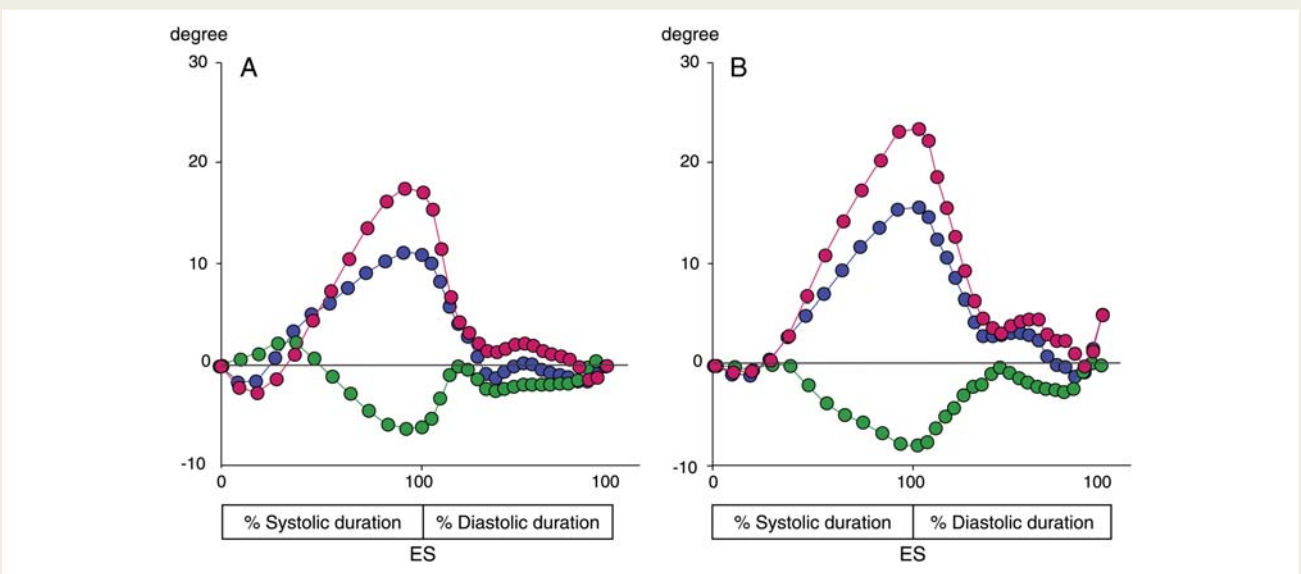


**Figure 16** Basal and apical rotation (green and blue curves, respectively) and LV twist (red) during one cardiac cycle in a normal subject (*A*) and a patient with diabetes without LV hypertrophy (*B*).Time axis was normalized to 100% of systolic duration (10% steps) followed by 100% of diastolic duration (5% steps). Note less prominent initial clockwise twist, higher peak twist, and lower untwisting during early diastole in the patient with diabetes compared with the normal subject. *ES*, End-systole.

**Table 1 LV twist dynamics in different pathologies**

| | LV twist | Untwisting | Time to peak untwisting |
|---|---|---|---|
| Heart failure[72,73] | | | |
| With preserved LV EF | → or ↑ | → or ↑ | Delayed |
| With reduced LV EF | ↓ | ↓ | Delayed |
| Coronary artery disease[74] | | | |
| Subendocardial MI | → | → | Delayed |
| Transmural MI | ↓ | ↓ | Delayed |
| Aortic stenosis[45] | ↓ | → or ↑ | Delayed |
| LV hypertrophy[77] | | | |
| Hypertension | → or ↑ | ↓ | Delayed |
| HCM | Variable | Variable | Delayed |
| Dilated cardiomyopathy[76] | ↓ | ↓ | Delayed |
| Pericardial disease[78] | ↓ | ↓ | No data provided |

*HCM*, Hypertrophic cardiomyopathy; *MI*, myocardial infarction; ↓, reduced; ↑, elevated; →, unchanged.

*Aortic Valve Disease.* — Net LV twist angle is significantly increased in aortic valve stenosis, although diastolic apical untwisting is prolonged in comparison with normal subjects. After aortic valve replacement, LV twist angle normalizes.[45]

*Mitral Valve Disease.* — Changes in LV twist angle have also been studied in patients with mitral regurgitation.[75] Chronic mitral regurgitation is associated with complex LV adaptive remodeling and eccentric hypertrophy. The effect of chronic mitral regurgitation on twist probably depends on the extent of subclinical LV systolic dysfunction. Peak untwisting velocity in mitral regurgitation remains normal but correlates negatively with end-systolic dimension and regurgitant volume, suggesting that peak untwisting velocity, like peak systolic twist, depends on the stage of the disease. This confirms the important effect of LV end-systolic volume on LV untwisting, because LV end- systolic volume was found to be an important determinant of peak untwisting velocity, irrespective of EF.[73]

*Cardiomyopathy.* — In dilated cardiomyopathy, the amplitude of peak LV systolic twist angle is impaired in proportion to global LV function. This reduction in LV twist angle is accounted for by marked attenuation of LV apical rotation, whereas basal rotation may be spared. In some cases, rotation of the apex may be abruptly interrupted, such that in the major part of systole, the LV base and apex rotate clockwise together in the same direction. For patients undergoing cardiac resynchronization therapy (CRT), an immediate improvement in LV twist angle has been reported to predict LV reverse remodeling at 6-month follow-up.[76]

*Dilated Versus Hypertrophic Cardiomyopathy.* — In contrast to dilated cardiomyopathy, patients with hypertrophic cardiomyopathy show variability in the extent of LV twist and untwisting, depending on the extent and distribution of hypertrophy and obstruction. Patients with LV hypertrophy due to systemic hypertension, however, show relatively preserved LV twist mechanics, although LV untwisting velocities, particularly during isovolumic relaxation, are both attenuated and delayed.[77] The marked endocardial dysfunction with relative sparing of epicardial function leads to abnormal longitudinal mechanics, with relative sparing of circumferential and twist mechanics in restrictive cardiomyopathy.

*Pericardial Disease.* — Like constrictive pericarditis, pericardial diseases show predominant impairment of circumferential and twist mechanics, while relatively sparing subendocardial longitudinal mechanics.[78]

*Diastolic Function.* — During systole, a significant amount of elastic energy is stored in the myocyte and the interstitium as torsion. The earliest mechanical manifestation of diastole is an abrupt untwisting that is largely completed before the mitral valve opens. This untwisting helps establish a base-to-apex intraventricular pressure gradient (IVPG), or diastolic suction, in early diastole that assists in the low-pressure filling of the heart. A study of normal controls and patients with hypertrophic cardiomyopathy examined the relationship between untwisting rate and IVPG at rest and with low-level (heart rate about 100beats/min) exercise.[71] IVPG has been shown to be calculable by applying the Euler equation to color M-mode transmitral flow propagation data in dogs[79] and humans.[80] In both normal controls and patients with hypertrophic cardiomyopathy, there was a linear relationship between ventricular untwisting rate and peak diastolic suction gradient ($r = 0.72$). This mirrors another exercise study that showed that the best determinant of maximal myocardial oxygen consumption in normal subjects and in patients with heart failure was the ability to augment diastolic suction with exercise,[81] while an animal study confirmed that untwisting was directly related to IVPG and inversely related to the ventricular relaxation time constant t.[82]

***Unresolved Issues and Research Priorities:*** The lack of standardization of imaging planes and different speckle-tracking algorithms among vendors make it difficult to make comparisons or establish normal values for LV twist with high levels of confidence. A multicenter study in a large number of normal subjects with different ultrasound machines is required to resolve this issue. Also, the development of 3D STE is likely to allow standardization of LV planes used for assessing twist torsion measurements. Moreover, population samples representing diseases affecting cardiac function should be studied to determine the diagnostic power and abnormal ranges of LV twist values.

Another issue that needs to be clarified relates to the definitions of "rotation," "twist," and "torsion." One may find in the recent literature that these terms are sometimes used interchangeably. Because the mathematical definitions clearly differentiate among these three entities, it is important that they are used correctly, as defined in section 1.1.

***Summary and Recommended Indications:*** Despite the growing evidence in support of clinical implications of LV twist measurements using 2D STE, routine clinical use of this methodology is not recommended at this time.

## 3.4. LV Dyssynchrony

Echocardiographic approaches to imaging dyssynchrony encompass several techniques, including M-mode, 2D, DTI (*Figures 17*

and *18*), STE, and 3D echocardiography. To date, several studies have examined the feasibility of using these techniques for predicting response to CRT. Current guidelines define the indications for CRT on the basis of clinical findings (heart failure symptoms and New York Heart Association class), LV function (EF), and electrocardiographic findings (QRS width) only.[83] However, approximately one third of patients treated with CRT do not respond to this treatment with improvement in LV function, reflecting the clinical need for better patient selection and means of therapy optimization.

Intraventricular dyssynchrony is commonly seen in patients with heart failure, which is believed to indicate more severe myocardial disease and poor prognosis.[84] Previously, a left bundle branch block pattern has been suggested as a main sign of systolic dyssynchrony. In left bundle branch block or RV pacing, septal activation occurs first and results in prestretch of the still quiescent lateral wall, shortens diastolic function, and reduces isovolumic contraction by reducing the peak rate of pressure increase ($dP/dt_{max}$). Afterward, the delayed lateral wall contraction generates forces that are partly dissipated by re- stretching the now early relaxing septal region,

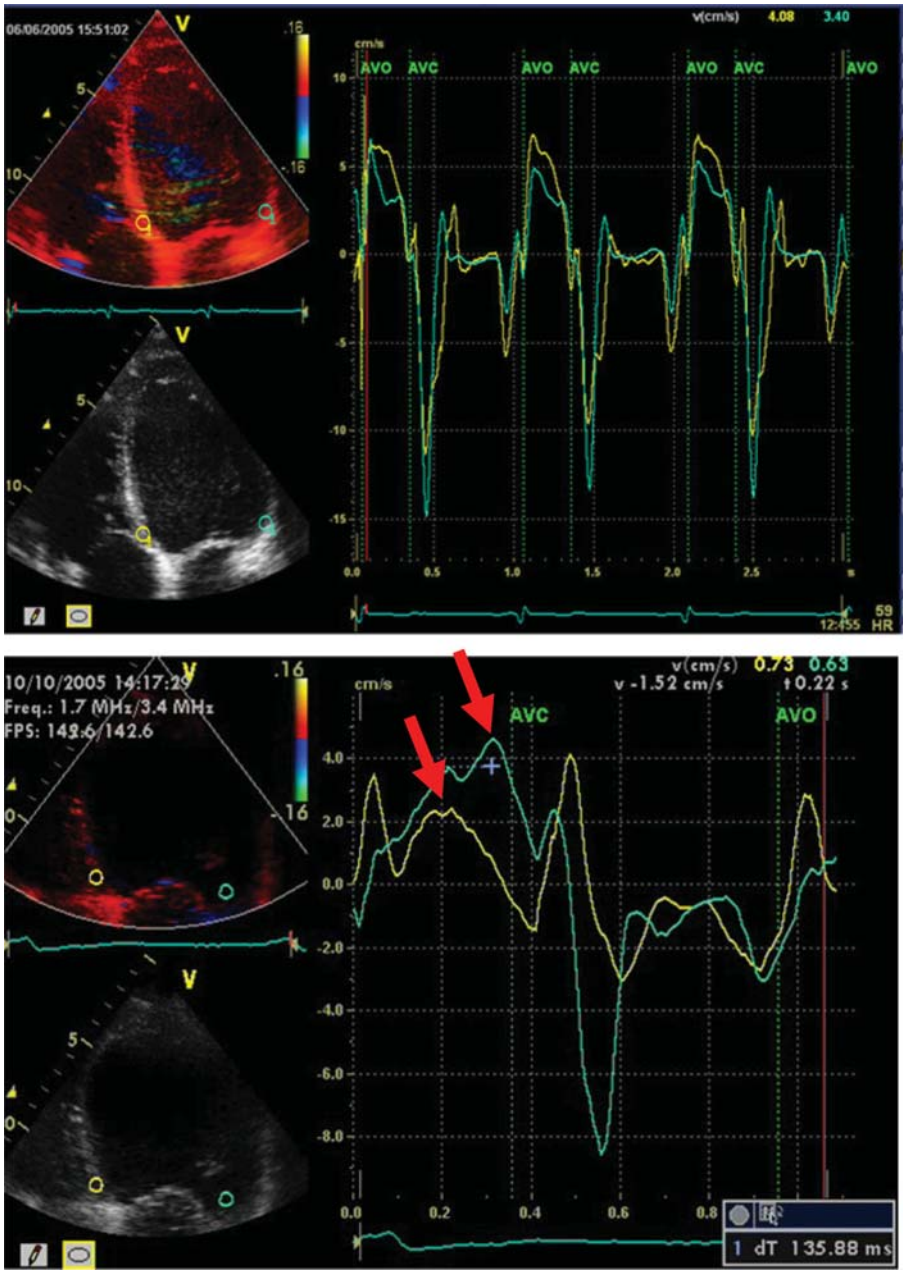


**Figure 17** Color DTI velocity tracings of the basal septal and lateral wall segments. Normal subject (top) and a patient with significant delay in lateral wall contraction (bottom). Red arrows indicate the difference in the timing of peak septal and lateral velocities.

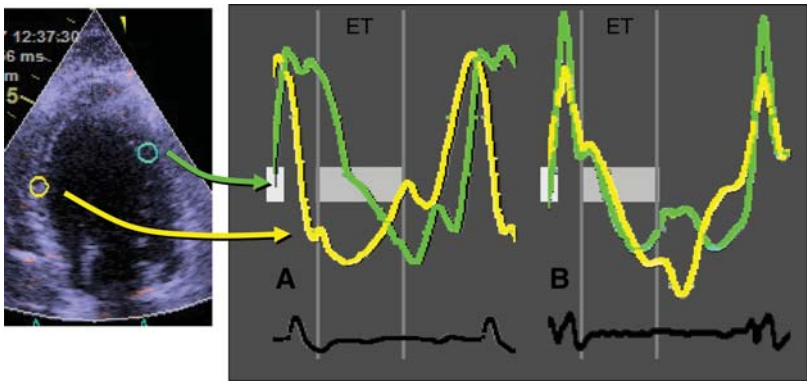


**Figure 18** Longitudinal strain curves clearly show asynchronous shortening of the different LV walls. (*A*) CRT off: note the off-phase shortening in the septum and the lateral wall resembling a typical left bundle branch block pattern. (*B*) CRT on: mostly synchronous shortening in both walls during ejection time (ET) indicating more efficient LV function under CRT. Reproduced with permission from Voigt.[180]

lowering net cardiac output. Dyscoordinate papillary muscle activation can further compromise overall LV performance by increasing the severity of mitral regurgitation. Dyssynchrony in relaxation prolongs isovolumic relaxation time and reduces filling further.

Several studies have shown an elusive relationship between QRS duration and mechanical dyssynchrony.[85] The transformation of electrical into mechanical dyssynchrony is modulated by calcium cycling, myofilament calcium interactions, regional loading, fibrosis, and other factors.[86,87] Therefore, disparities in the timing of regional mechanical function may not be strictly coupled to electrical stimulation delay.

***Normal Values:*** *Tables 2, 3*, and *4* provide a summary of DTI-based and STE-based parameters used to evaluate intraventricular dyssynchrony with published cutoff values that have been most frequently applied to predict reverse remodeling after CRT.

***Published Findings:*** The value of interventricular dyssynchrony was also recently tested for predicting response to CRT.[88] This study demonstrated that in addition to blood pool Doppler measurements in the RVand LV outflow tracts, DTI may be used to compare the onset of systolic motion in the basal RV free wall with the most delayed basal LV segment, concluding that delay >56 msec indicated dyssynchrony.[88] Nevertheless, it is agreed that intraventricular dyssynchrony is the important feature to evaluate in patients with heart failure. "Apical rocking" visualized on 2D echocardiographic images has also been recently suggested as a potential predictor of response to CRT.[89,90]

A recent consensus document[91] favored the use of opposite wall delay by color DTI and the delay between anteroseptal radial strain and posterior (or inferior lateral) radial strain by STE. The standard deviation in time to peak systolic velocity from 12 segments, or the Yu index, was also recommended.[91] Since the publication of this document, additional studies have shown that longitudinal strain measurements could be useful as well.[92] In particular, the approach of measuring both radial and longitudinal dyssynchrony seems to have a much higher accuracy in predicting the response to CRT[93] than each parameter separately. It is clear that a number of factors should be taken into consideration, aside from mechanical dyssynchrony, in trying to predict the response to CRT. These include QRS duration, interventricular mechanical delay, and the amount of scar tissue and its relation to the implanted LV pacing lead, in addition to implanting the LV pacing lead in close proximity to the site with the latest mechanical activation.[94]

An observational multicenter study (Predictors of Response to CRT) reported on the limited role of velocity dyssynchrony

**Table 2 DTI-based parameters used to evaluate intraventricular dyssynchrony with published cutoff values to predict response to CRT[88]**

| Parameter | Cutoff to predict response to CRT |
|---|---|
| Time to peak systolic velocity in four basal segments | Dispersion >65 msec |
| Time to peak systolic velocity in six basal segments | Dispersion >110 msec |
| Time to peak systolic velocity in six basal and six mid segments | Standard deviation >33 msec |
| Onset of basal motion in three segments (septal, lateral, posterior) | Dispersion >60 msec |

**Table 3 STE-based parameters to evaluate intraventricular dyssynchrony with published cutoff values to predict response to CRT[88]**

| Parameter | Cutoff to predict response to CRT |
|---|---|
| Time to peak radial strain in two basal segments (septal, posterior) | Dispersion >130 msec |
| Time to peak longitudinal strain in 12 basal and mid segments | Standard deviation >60 msec |
| Time of postsystolic contraction in 12 basal and mid segments | Sum of shortening time >760 msec |

**Table 4 DTI-based and STE-based measurements that have been most frequently applied to predict reverse remodeling after CRT**

| Measurement | Normal | Cutoff for predicting reverse remodeling |
|---|---|---|
| Opposite-wall peak systolic velocity delay by color DTI[84] | <50 msec | ≥65 msec |
| Yu index (12-segment model)[84] | <30 msec | ≥33 msec |
| Septal-to-posterior wall delay by radial strain derived by STE[84] | <40 msec | ≥130 msec |
| Interventricular delay[84] | <20 msec | ≥40 msec |
| Longitudinal strain delay index by STE[85] | <20% | ≥25% |

measurements by color DTI in predicting response to CRT.[95] However, the study had several important limitations, including enrollment of patients who did not meet criteria for CRT (20% of patients with EFs >35%), overall low feasibility and reproducibility of DTI measurements, and using ultrasound systems and software from different vendors, including systems that had lower temporal resolution than the time intervals to be measured.[87]

Currently, for patients with QRS durations <120 msec, the existing data do not support using DTI or M-mode measurements for the selection of patients for CRT.[96] On the other hand, a recent single- center study showed that radial dyssynchrony by STE can be of value in predicting changes in LV volumes and EF after CRT in patients with QRS durations of 100 to 130 msec.[97] It was also reported that the strain-derived dyssynchrony index distinguished patients with left bundle branch block or decreased LV EFs from those with normal systolic function and normal QRS durations with minimal overlap and appeared to identify patients with intraventricular dyssynchrony more reliably than DTI parameters.[98] Another recent study showed that the combination of timing and magnitude of longitudinal strain could predict response to resynchronization.[92]

***Unresolved Issues and Research Priorities:*** The assessment of mechanical dyssynchrony in patients treated with or planned for CRT is a recent concept that arose from the clinical need for better patient selection and means of therapy optimization. Although the concept is mostly accepted among experts despite recent challenges,[95,99] the clinical value of the approach remains to be better defined. Clearly, additional multicenter outcome studies are needed in patients with congestive heart failure. However, to avoid previous mistakes[95] and make different studies comparable, we first need a standardization of technical characteristics of the imaging systems used to assess dyssynchrony, trial end points (i.e., definition of CRTresponders), data to be collected to characterize patients both at baseline and during follow-up (myocardial scar quantification, LV volume quantification, need for device optimization, etc.), and implant characteristics (i.e., lead position in relation to scar and most delayed LV segment). Also, intermeasurement variability of the different techniques used to assess ventricular synchronicity needs to be evaluated in multicenter studies.

***Summary and Recommended Indications:*** Currently, after the Predictors of Response to CRT and the Mayo Clinic studies,[99] which support the indications in clinical guidelines, there is no definite role for the echocardiographic measurement of mechanical dyssynchrony to indicate the need for CRT in patients with heart failure. There is a potential role for dyssynchrony imaging in patients with borderline QRS duration, in which this additional information may help, and this methodology may aid in determining the site of latest mechanical activation which can be taken into consideration by the CRT implantation team.

## 3.5. LV Diastolic Function

The clinical utility of myocardial velocity measurements for the assessment of diastolic function is widely accepted and has been documented previously.[100] Myocardial strain and SR are also sensitive parameters for quantification of diastolic function. Diastolic SR signals can be recorded during isovolumic relaxation ($SR_{IVR}$), during early filling ($SR_E$), and in late diastole ($SR_A$). Both DTI and STE can be used to acquire diastolic strain signals.

***Normal Values:*** Normal values have been previously published for DTI mitral annular velocities in several populations. In adults, e′ velocity decreases with age; accordingly, age-based normal values should be used in drawing conclusions about LV diastolic function.[100] However, in general, septal e′ ≥8 cm/s and lateral e′ ≥10 cm/s are usually observed in normal subject, and are reduced in patients with impaired LV relaxation and increased LV filling pressures (*Figure 19*). Normal values of strain and SR are yet to be established.

***Published Findings:*** Diastolic SR provides important information about LV diastolic function. This includes assessment of postsystolic myocardial strain, which occurs in the setting of ischemia,[59] and with electrical and mechanical dyssynchrony. The closely related observation of delayed regional relaxation is also noted in the setting of ischemia and dyssynchrony.[101] The hemodynamic determinants of SRE include LV relaxation, regional diastolic stiffness, systolic function, end-systolic wall stress, and filling pressures.[102,103] In addition, $SR_E$ can assess interstitial fibrosis[103] and can be used to identify viable myocardium after stunning and infarction.[102–104]

Several studies have shown a significant relationship between segmental $SR_E$ and the time constant of LV relaxation.[105,106] However, there are problems with extrapolating conclusions from regional SRE to global LV diastolic function. This limitation can be circumvented by using data from all myocardial segments. In that regard, two studies were published looking at global $SR_{IVR}$ and $SR_E$ by STE.[73,107] Both studies showed that these measurements have good feasibility and reproducibility and are related to the time constant of LV relaxation. However, in the study that performed head-to-head comparison between $SR_{IVR}$ and $SR_E$, $SR_{IVR}$ correlated better with the time constant of LV relaxation.[73] The ratio of E to $SR_{IVR}$ was useful in predicting LV filling pressure in patients in whom the E/e′ ratio was inconclusive and was more accurate than E/e′ in patients with normal EFs and

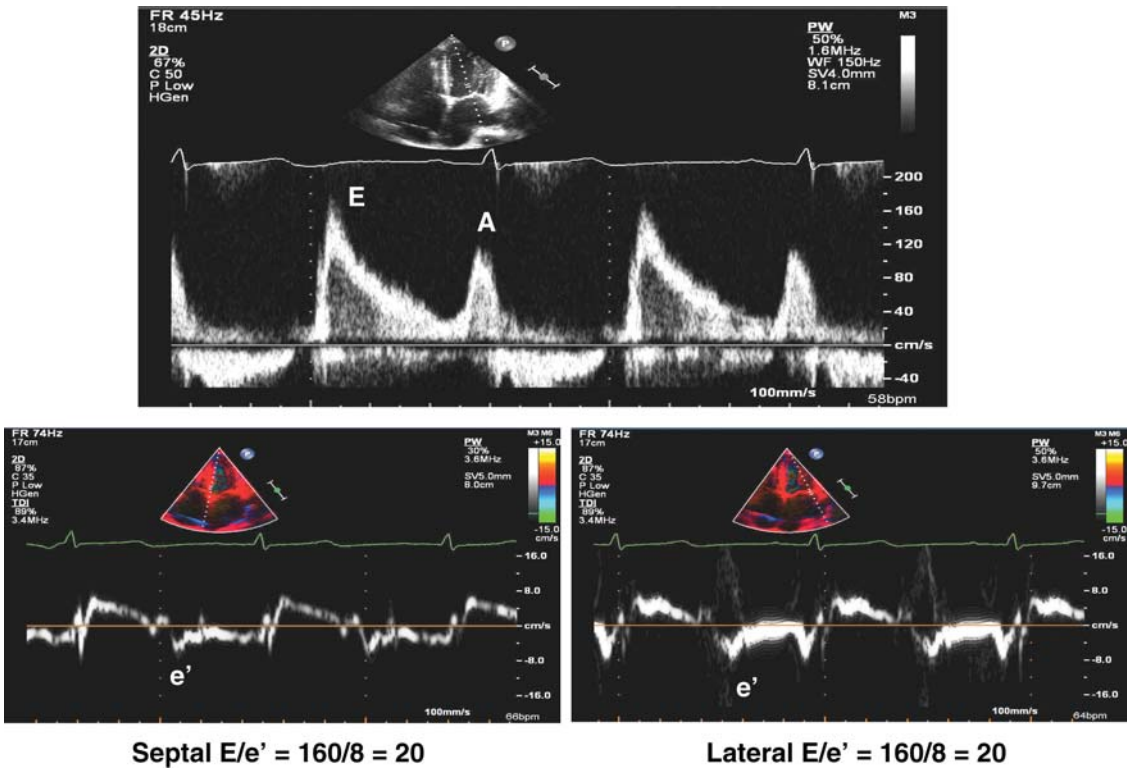


**Figure 19** DTI velocities measured in a patient with impaired LV relaxation and increased LV filling pressures: mitral inflow (top) and mitral annular velocities obtained by DTI at the septal (bottom left) and lateral (bottom right) sides of the annulus. Notice the reduced e′ velocity and the increased E/e′ ratio.

those with regional dysfunction.[73] More recently, $SR_{IVR}$ was shown to have an incremental prognostic value in patients with ST-segment elevation myocardial infarction.[108]

There are other recent indices of LV diastolic function, including left atrial (LA) strain during LV systole[109] and LV untwisting, including the possibility of measuring early and late-diastolic events as respective markers of relaxation and compliance. In addition, there is now better recognition of the presence of subtle systolic abnormalities in LV longitudinal function in patients with heart failure and preserved systolic function, which can be expected given the fact that LV systolic and diastolic function are coupled. This has been demonstrated using strain and torsion and untwisting measurements.[109]

***Unresolved Issues:*** Although the above indices of diastolic function are promising, they have limitations, which include the need for a high signal-to-noise ratio, satisfactory myocardial visualization in the apical views, experience with the acquisition and analysis algorithms, longer time of offline analysis for strain versus velocity measurements, and a lower frame rate for signals acquired by STE.

***Summary and Recommended Indications:*** DTI-derived mitral annular velocities by pulsed-wave Doppler are recommended for the routine clinical evaluation of LV diastolic function.[100] Measurement of diastolic strain and SR may be useful for research applications but is presently not recommended for routine clinical use.

## 3.6. Myocardial Ischemia

Conventional echocardiographic assessment of regional myocardial function is based on the measurement of wall thickening and does not provide information regarding the transmural distribution of contractile performance. The analysis of fiber thickening across the different layers of the myocardial wall is important to differentiate the various patterns of contractile abnormalities that may occur during acute or chronic (hibernation) myocardial ischemia. Ischemic myocardium is characterized by a reduced or missing regional systolic longitudinal and circumferential shortening and radial thickening. Postsystolic shortening after aortic valve closure is a common finding in acute ischemia.[58,110]

***Normal Values:*** There is significant evidence in the literature that global peak systolic strain in the range of $-16\%$ to $-20\%$ and global peak systolic SR $< -0.9$ $sec^{-1}$ are highly sensitive and specific for the identification of patients with prior myocardial infarction.[111]

***Published Findings:*** DTI has been used to quantify the effects of ischemia on myocardial function. Experimentally induced myocardial ischemia in pigs resulted in a significant rapid reduction of systolic velocities, a marked increase in isovolumic relaxation velocity (indicative of postsystolic motion), and an early decrease in the ratio of early to late diastolic velocities within 5 sec of coronary occlusion.[112] Although the decrease in systolic velocity significantly correlated with both systolic shortening and regional myocardial

blood flow during reduction of coronary artery blood flow, systolic velocities slightly overestimated the degree of regional wall motion abnormalities and failed to distinguish ischemia from reperfusion-induced contractile dysfunction. In patients with chronic coronary artery obstruction, abnormalities of longitudinal shortening have been observed using DTI.[113] The functional impairment induced by infarction and ischemia is mirrored by a reduction in peak systolic velocity in the involved myocardium, particularly in the corresponding parts of the mitral annulus, while remote segments may also be affected. However, the differentiation between regional and global changes in contractility is not possible.

In addition to the physiologic insight into longitudinal LV function, the advantage of DTI is the visual display and quantification of myocardial function.[114] Experimental results showed that DTI allows the assessment of regional myocardial function during the cardiac cycle[112] and is sensitive to both inotropic stimulation and ischemic challenge.[115] Clinical studies showed the feasibility of the DTI applied to stress echocardiography, but the reproducibility of the method has been suboptimal,[116] and the accuracy no better than expert visual interpretation.[117,118] In addition, regional assessment is difficult in midventricular segments and virtually impossible at the apex, because the longitudinal systolic wall motion at the apex is minimal, and consequently myocardial velocities are too low and variable to reliably detect apical wall motion abnormalities.[119] Although DTI- derived peak systolic velocity is typically reduced during ischemia, several experimental studies have demonstrated its limited ability to differentiate among different grades of ischemic dysfunction and to distinguish ischemic from postischemic dysfunction.

Experimental studies have shown that DTI-derived SR can be helpful in identifying and quantifying ischemia-induced myocardial abnormalities and in identifying viable myocardium, in which SR is normalized in stunned areas after inotropic challenge with dobut amine or dipyridamole.[5,120–122] Clinical studies have demonstrated the ability of Doppler-derived strain to detect myocardial ischemia during dobutamine stress echocardiography[59] and shown an added predictive value of peak systolic SR measurements.[57]

Two-dimensional STE-derived strain has been validated experimentally, showing good reproducibility of longitudinal and circumferential strain.[15] The sensitivity and specificity of STE-derived radial and circumferential strain for the diagnosis of segmental ventricular dysfunction were shown as accurate means for differentiating normokinetic from hypokinetic or akinetic segments, compared with cardiac magnetic resonance imaging.[123] Global longitudinal strain obtained from apical views was used as an index of cardiac function,[111] with an incremental prognostic value over clinical parameters and LV EF[124]

STE-derived strain seems to be useful for detection of myocardial ischemia in the setting of stress testing and was shown to have good reproducibility because of its mostly automated nature, an especially important advantage for inexperienced observers. Longitudinal and circumferential STE-derived strains were evaluated during dobutamine infusion in anesthetized pigs with varying degrees of coronary occlusion.[125] The effect of coronary occlusion on the different strain components was more pronounced during dobutamine infusion (*Figure 20*).

The first studies in humans showed high levels of feasibility during handgrip stress,[126] and with dobutamine infusion, a similar accuracy to DTI strain in the anterior but not in the posterior circulation.[127]

***Unresolved Issues and Research Priorities:*** Not all clinical studies have unanimously confirmed the advantages highlighted by experimental studies and shown comparable values of SR and tissue velocity imaging for diagnosis of coronary artery disease and comparable accuracy compared with expert reader visual interpretation.[128]

The ability of STE strain to detect earlier phases of the ischemic response in human subjects with chest pain needs to be tested. With DTI, peak amplitudes of velocity and strain variables are influenced by the angle of the incident beam with the myocardial wall and depend on image quality and is frequently difficult to use in apical segments.[68] For both STE-based and DTI-based strain imaging, considerable expertise is needed to obtain sufficient accuracy and reproducibility.

***Summary and Recommended Indications:*** The direct observation of a developing systolic dysfunction combined with a postsystolic shortening indicates acute myocardial ischemia. However, the lack of clinical trials does not allow recommending specific parameters for differentiating various states of acute and chronic ischemia when baseline data are not available.

## 3.7. Fibrosis and Viability

The detection of myocardial fibrosis and viability is dependent on the evaluation of both myocardial tissue characteristics and myocardial shape change within the cardiac cycle. Fibrotic tissue may be either focal (as occurs in patients after myocardial infarction) or diffuse (as may occur in response to increased afterload or metabolic disturbances). Fibrosis is most readily identified using myocardial late enhancement with cardiac magnetic resonance imaging[129] but may also be detected using a variety of echocardiographic techniques, including deformation imaging. Diffuse fibrosis is difficult to measure. Its contribution to increased tissue reflectivity may be measured by calibrated myocardial backscatter (see section 2.4), and it may have a specific tissue signature, sometimes referred to as a "double peak sign," characterized by a pattern consisting of an unsustained early systolic peak followed by a rapid fall in SR close to zero and a second peak during isovolumic relaxation.[130]

Changes in myocardial shape can be assessed using standard imaging, DTI, or STE. The differences among these approaches have been described above. As far as viability assessment, the attraction of the Doppler approach relates to its high temporal resolution, which permits the accurate characterization of brief temporal phenomena such as postsystolic thickening and isovolumic contraction. On the other hand, the attraction of STE is its ability to measure in any dimension, irrespective of the ultrasound beam direction, its relative robustness to signal noise (in particular avoidance of aliasing), and its provision of strain in all dimensions (longitudinal, radial, and circumferential) with the possibility of measuring shear strain between myocardial layers.[52]

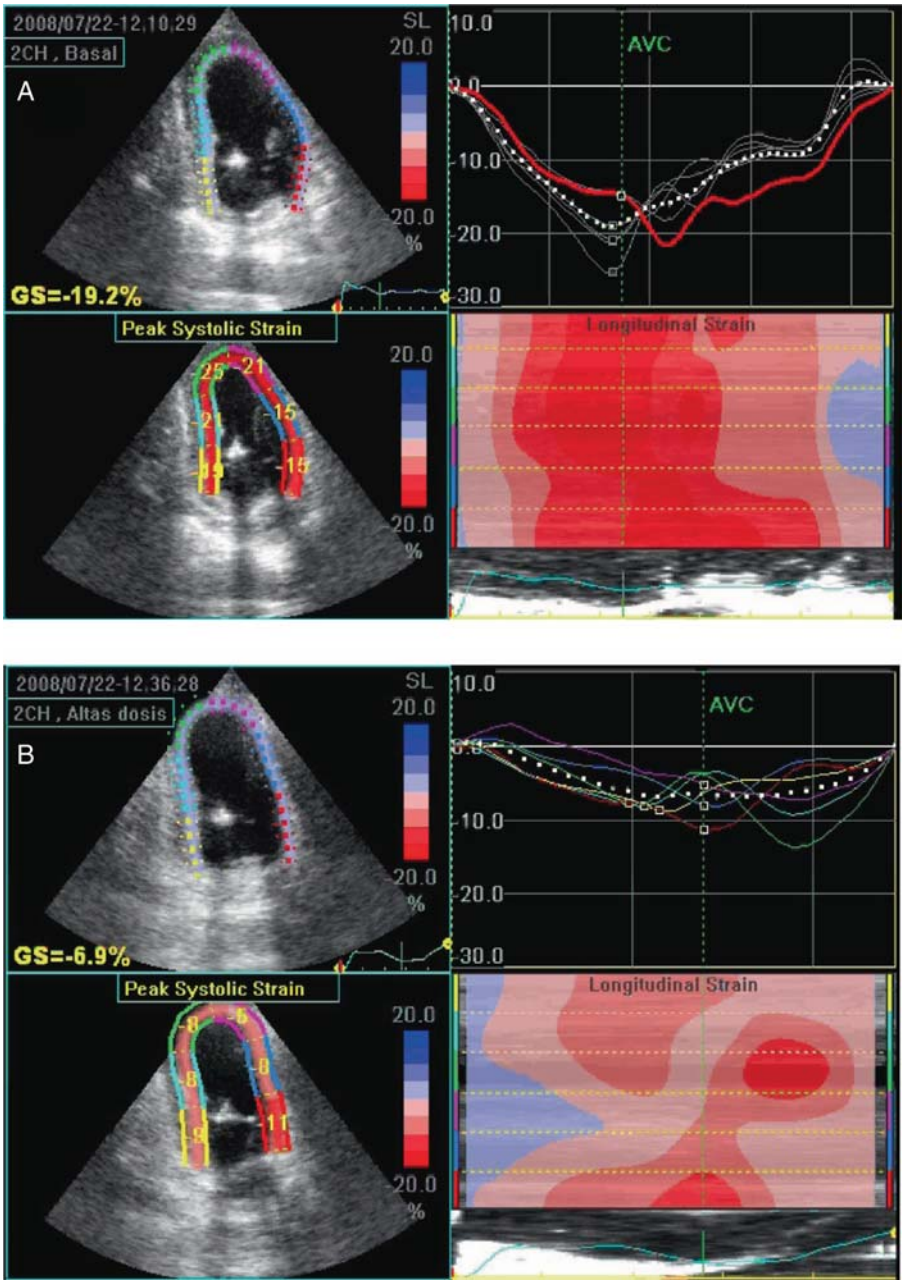


**Figure 20** Two-dimensional speckle-tracking echocardiographic image of an apex obtained in a pig during coronary occlusion at rest (*A*) and at peak dose of dobutamine (*B*), showing decreased global longitudinal strain (GS). The quantitative assessment of velocity and direction of vectors by global strain helps describe the motion in an integrated and quantitative fashion.

The main indications for these techniques have been the recognition and quantification of a global fibrotic process, existing wall motion abnormalities, and the assessment of myocardial viability. Diffuse myocardial fibrosis likely contributes to disturbances of ventricular filling, especially to reduced LV compliance, and may be present in pressure overload such as aortic stenosis,[131] as well as conditions of disturbed metabolism such as diabetes and obesity.[132] Although identifying the components of myocardial dysfunction (such as fibrosis) is an important step in developing targeted therapy for a multifactorial process such as diastolic dysfunction, the therapeutic implications of these specific findings remain undefined.

The recognition of resting wall motion abnormalities due to focal fibrosis is recognized as one of the most difficult aspects of echocardiographic interpretation and the component that most requires training and experience.[133]

***Normal Values:*** Normal longitudinal systolic strains are of the order of $\geq$ 18%, with standard deviations of 2% to 3%.[12] A measurement of $\leq$12% definitely constitutes an abnormal value. There are significant variations even between normal segments,

and the definition of a normal range is limited by inherent variability by site (*Table 5*), between normal individuals, by age, and by hemodynamic conditions.

***Published Findings:*** Clinical studies have documented the reliability of the quantitative approach in comparison with expert readers and in particular emphasized the reduced variation of strain measurement for the recognition of regional wall motion abnormalities compared with visual assessment.[134]

Myocardial viability may be assessed at rest or in response to inotropic stimulation. Akinetic or severely hypokinetic myocardium that shows residual longitudinal strain can be inferred as being viable. In these situations, the problem is often that there is some reduction of subendocardial function at rest, with functional reserve arising from contraction of the mid and epicardial components of the wall. The transmyocardial distribution of thickening can be documented by distinguishing between the different components of myocardial strain. Longitudinal strain becomes compromised at a relatively early stage in the development of coronary disease and a clue to the presence of subendocardial infarction or ischemia may be identified from a discrepancy between longitudinal and radial strain.[135] The degree of radial strain reduction has been used as a marker of increasing transmyocardial extent of scar as well as in the recognition of nontransmural infarction.[123] A recent study suggested that direct measurement of the transmyocardial strain gradient by STE may provide similar information.[136] However, this approach can only deliver valid results if the image resolution in the interrogated direction is sufficient.

The initial validation of the response of the myocardium to an inotropic stimulus such as dobutamine as a marker of viability was performed nearly a decade ago by comparison against positron emission tomographic imaging.[137] This study reported that segments with perfusion metabolism mismatch were associated with regional contractile reserve, as reflected by an increment of SR in response to dobutamine.[137] Subsequent studies documented that an increase in SR in response to dobutamine was associated with subsequent functional recovery of segments, and cutoffs were defined for strain and SR or the changes in these parameters consistent with subsequent functional recovery. Further work in this area has confirmed these cutoffs.[9]

The most reliable echocardiographic sign that myocardium is likely to recover after revascularization is the biphasic response, whereby reduced baseline function is seen to improve with inotropic stimulation (generally with dobutamine stress) but deteriorates when sufficient workload is delivered to exceed perfusion reserve and provoke ischemia. *Figures 21 to 23* show examples of studies suggesting ischemia and viability. Animal experiments have demonstrated that the most reliable marker of contractility response to stress is SR rather than strain.[140] The normal response of SR to increasing doses of dobutamine is a continuing increment, whereas the normal response of strain to dobutamine is an initial increment, followed by a

**Table 5 Normal values of regional longitudinal systolic strain obtained by different techniques and reported in the literature**

| Study | Method | n | Age (y) | Mean strain (%) | Septal (%) | Lateral (%) | Inferior (%) | Anterior (%) |
|---|---|---|---|---|---|---|---|---|
| *Moore et al.*[182] | MRI | 31 | 37 ± 2 | 16 ± 3 | | | | |
| Basal | | | | | 14 ± 3 | 15 ± 3 | 15 ± 3 | 15 ± 3 |
| Midventricular | | | | | 15 ± 3 | 14 ± 4 | 15 ± 3 | 15 ± 3 |
| Apical | | | | | 18 ± 4 | 19 ± 3 | 18 ± 4 | 19 ± 3 |
| *Edvardsen et al.*[183] | MRI | 11 | 41 ± 13 | 18 ± 4 | | | | |
| Basal | | | | | 17 ± 3 | 18 ± 4 | 18 ± 4 | 17 ± 3 |
| Apical | | | | | 19 ± 5 | 17 ± 4 | 19 ± 3 | 18 ± 4 |
| *Edvardsen et al.*[183] | DTI | 33 | 41 ± 13 | 19 ± 4 | | | | |
| Basal | | | | | 17 ± 3 | 18 ± 4 | 20 ± 4 | 19 ± 4 |
| Apical | | | | | 19 ± 4 | 17 ± 3 | 21 ± 2 | 18 ± 5 |
| *Kowalski et al.*[184] | DTI | 40 | 29 ± 5 | 17 ± 5 | | | | |
| Basal | | | | | 21 ± 5 | 13 ± 4 | 15 ± 5 | 17 ± 6 |
| Midventricular | | | | | 21 ± 5 | 14 ± 4 | 16 ± 5 | 17 ± 6 |
| Apical | | | | | 23 ± 4 | 15 ± 5 | 18 ± 5 | 18 ± 6 |
| *Sun et al.*[185] | DTI | 100 | 43 ± 15 | 18 ± 5 | | | | |
| Basal | | | | | 18 ± 5 | 18 ± 7 | 15 ± 6 | 22 ± 8 |
| Midventricular | | | | | 18 ± 1 | 19 ± 5 | 14 ± 5 | 18 ± 6 |
| Apical | | | | | 19 ± 6 | 18 ± 6 | 24 ± 5 | 13 ± 6 |
| *Marwick et al.*[12] | 2D STE | 242 | 51 ± 12 | 19 ± 5 | | | | |
| Basal | | | | | 14 ± 4 | 18 ± 5 | 17 ± 4 | 20 ± 4 |
| Midventricular | | | | | 19 ± 3 | 18 ± 3 | 20 ± 4 | 19 ± 3 |
| Apical | | | | | 22 ± 5 | 19 ± 5 | 23 ± 5 | 19 ± 5 |

plateau or minor decrement as heart rate increases and stroke volume falls. Postsystolic shortening may be a useful marker of viable myocardium, especially if it normalizes in response to dobutamine.

***Unresolved Issues and Research Priorities:*** Although the detection of myocardial fibrosis and evaluation of viability may prove to be an important application of deformation imaging, the interpretation of subtle variations of myocardial thickening and response to dobutamine is difficult, dependent on training and experience, and shows significant variation between readers even when using standardized reading criteria.[141] More research is needed in this area.

***Summary and Recommended Indications:*** The place of deformation analysis in the recognition and evaluation of fibrosis and myocardial viability is a matter of ongoing investigation. At present, the strongest evidence pertains to the combination of strain with low- dose dobutamine stress for the assessment of myocardial viability. Although encouraging data have been obtained with the use of deformation analysis to recognize fibrosis and distinguish nontransmural scar in the setting of resting wall motion

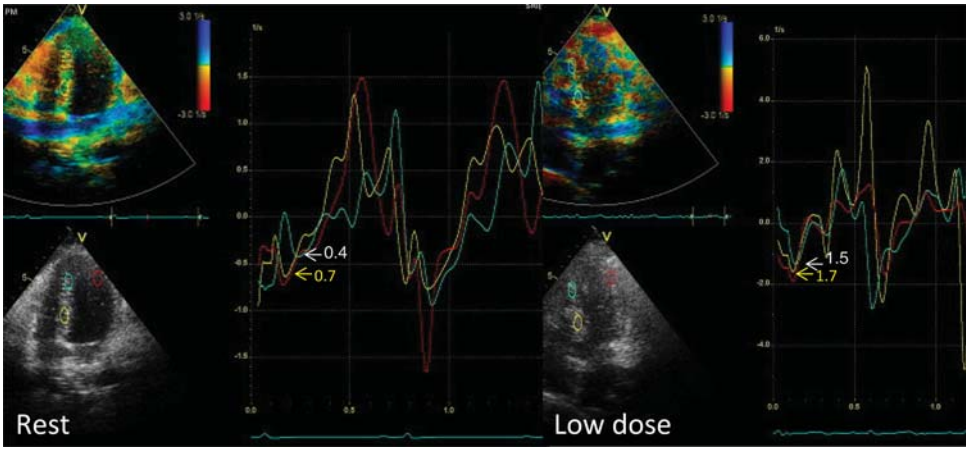


**Figure 21** Application of SR imaging to facilitate the recognition of myocardial viability. At rest, both septal segments show reduced SR, with the apical also showing delay. In response to low-dose dobutamine, both septal segments show increases in SR, which becomes more synchronous. The lateral wall (red) is used as a normal reference segment.

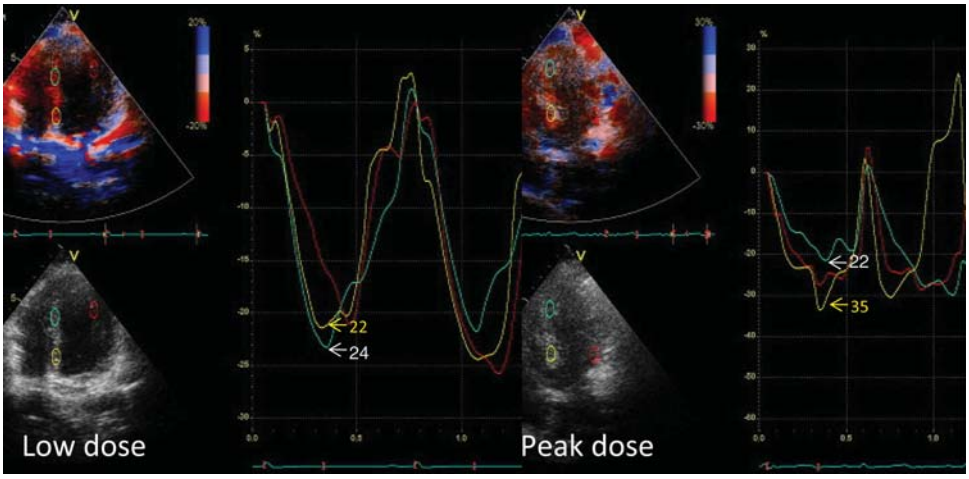


**Figure 22** Application of tissue velocity imaging derived strain to facilitate the recognition of the biphasic response. At low dose, both septal segments show normal strain, with synchrony. At peak-dose dobutamine, the basal septal segment (yellow) shows an increase in strain, but the midapical segment (blue) shows a slight decrease and becomes delayed.

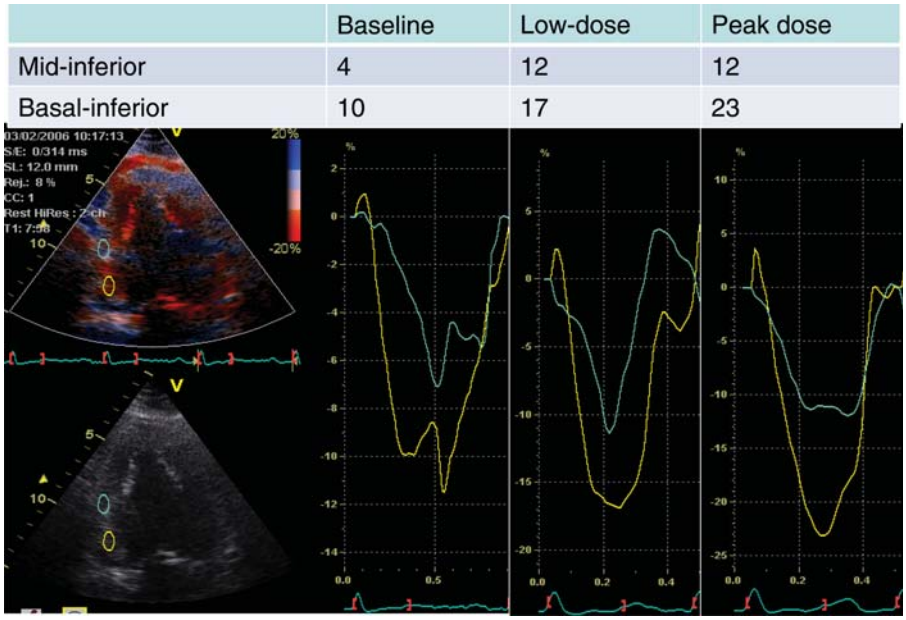


**Figure 23** Application of tissue velocity imaging-derived strain to facilitate the recognition of the uniphasic response. At rest, both inferior segments show reduced strain. At low dose, both have increased. At peak-dose dobutamine, the midinferior segment (blue) has not increased strain, but the basal segment (yellow) has increased further.

abnormalities, clinical use of this methodology is not recommended at this time.

# 4. PHYSIOLOGIC MEASUREMENTS OF RIGHT VENTRICULAR AND LEFT AND RIGHT ATRIAL FUNCTION

## 4.1. Right Ventricle

The RV wall is thinner than the LV myocardium, and the two ventricles have different shapes. This is associated with low pressure in the pulmonary circulation. The thin-walled and compliant right ventricle facilitates quick adaptation to changes in preload. An increase in RV afterload results in an increase in wall stress, unless the thickness of the chamber walls is increased or the internal radius of the chamber is reduced. Normal RV contraction proceeds in a sequential manner, as a peristaltic wave directed from inflow tract to infundibulum. Longitudinal shortening is the major contributor to overall RV performance with an equal contribution of the RV free wall and the interventricular septum. RV function assessment by conventional 2D echocardiography is challenging because of the complex RV geometry and the heavily trabeculated inner wall contour. The load dependency of most conventional echocardiographic parameters adds another challenge for functional assessment.

A simple quantitative approach to assess longitudinal RV function is the measurement of the tricuspid annular plane systolic excursion, which estimates the level of the systolic excursion of the lateral tricuspid valve annulus toward the apex in the four-chamber view. Tricuspid annular plane systolic excursion has demonstrated an excellent correlation with radionuclide ventriculography-derived RV EF and has proved to be a strong predictor of prognosis in heart failure. Nevertheless, it can be angle dependent if an enlarged right ventricle results in off-axis images, and it may also be influenced by translation.

DTI and STE both provide indices of RV function. DTI allows quantitative assessment of RV systolic and diastolic longitudinal motion by means of measurement of myocardial velocities from the apical four- chamber view. Two-dimensional color-coded DTI allows examination of multiple segments simultaneously. Pulsed-wave DTI examines RV function by recording velocities of the tricuspid annulus, which are used as a correlate of RV function, because longitudinal displacement of the RV base accounts for the greater proportion of total RV volume change in comparison with radial shortening in normal ventricles.

Systolic RV function may be assessed by measuring DTI systolic velocities and isovolumic myocardial acceleration, which is calculated by dividing the maximal isovolumic myocardial velocity by the time to peak velocity and has the advantage of being less affected by RV shape and loading conditions than systolic velocities. Experimental studies have identified isovolumic myocardial acceleration as the most reliable contractility index among various velocity parameters by comparison with systolic elastance. In addition to systolic velocities, pulsed-wave DTI can also be used to measure the peak early and late diastolic velocity, allowing evaluation of RV diastolic function and right atrial (RA) pressure by using the ratio between transtricuspid early diastolic velocity (using conventional pulsed-wave Doppler) to the peak early DTI diastolic velocity of the lateral tricuspid annulus.

Besides assessment of velocity, DTI permits measurement of time intervals. As opposed to the left ventricle, isovolumic relaxation time is almost nonexistent in the normal right ventricle (*Figure 24A*), and an increase in right-sided isovolumic relaxation time duration suggests impairment in RV function related to primary RV dysfunction or an increase in RV afterload. The Tei index of the right ventricle may be calculated from pulsed-wave DTI traces and has the advantage of simultaneous recordings of systolic and diastolic velocity patterns compared with conventional Doppler (*Figure 24B*). DTI may also identify RV dyssynchrony by measurement of septum-to-RV free wall delay.

DTI has been validated for its ability to quantify RV myocardial deformation. Although the assessment of longitudinal strain from the apical views is feasible in the clinical setting, the analysis of RV radial deformation from the parasternal window is difficult. It is hampered by near-field artifacts caused by the close proximity to the transducer and by the thin RV wall that requires selection of an extremely small computational distance of $<5$ mm for SR measurements. SR imaging measurements correlate well with sonomicrometry segment length measurements and may be used to quantify RV function under different loading conditions in an experimental model. An acute increase in RV afterload was found to lead to an increase in RV myocardial SR and to a decrease in peak systolic strain, indicating a decrease in RV stroke volume. In addition, the strain profile after pulmonary artery constriction demonstrated a shift of myocardial shortening from early mid to end-systole or even early diastole (postsystolic shortening).[142]

STE also has a great promise in assessing regional and global RV deformation in different directions in terms of both amplitude and timing, with the advantage of being less affected by overall heart motion.[143]

***Normal Values:*** At the level of the tricuspid annulus, in the RV free wall, normal systolic velocity by pulsed DTI is $>12$ cm/sec, although it may be age dependent, similar to normal LV myocardial velocities. A peak systolic velocity $<10$ cm/sec should raise the suspicion of abnormal RV function, especially in younger adults.[144] A peak systolic velocity $<11.5$ cm/sec was found to identify the presence of RV dysfunction or pulmonary hypertension with sensitivity and specificity of 90% and 85%, respectively[145] (*Figure 24A*). In addition, a cutoff value of $<9.5$ cm/sec has been identified as a prognostic risk factor for predicting adverse outcomes in various diseases, including chronic heart failure.[146] Peak S-wave values with pulsed DTI and with color DTI cannot be used interchangeably, because the former measures peak myocardial velocities, while the latter measures mean myocardial velocities, which are 20% lower (*Figure 25*).

***Published Findings:*** *Myocardial Velocity Profiles.* — In a large cohort of normal subjects over a wide age range, it was found

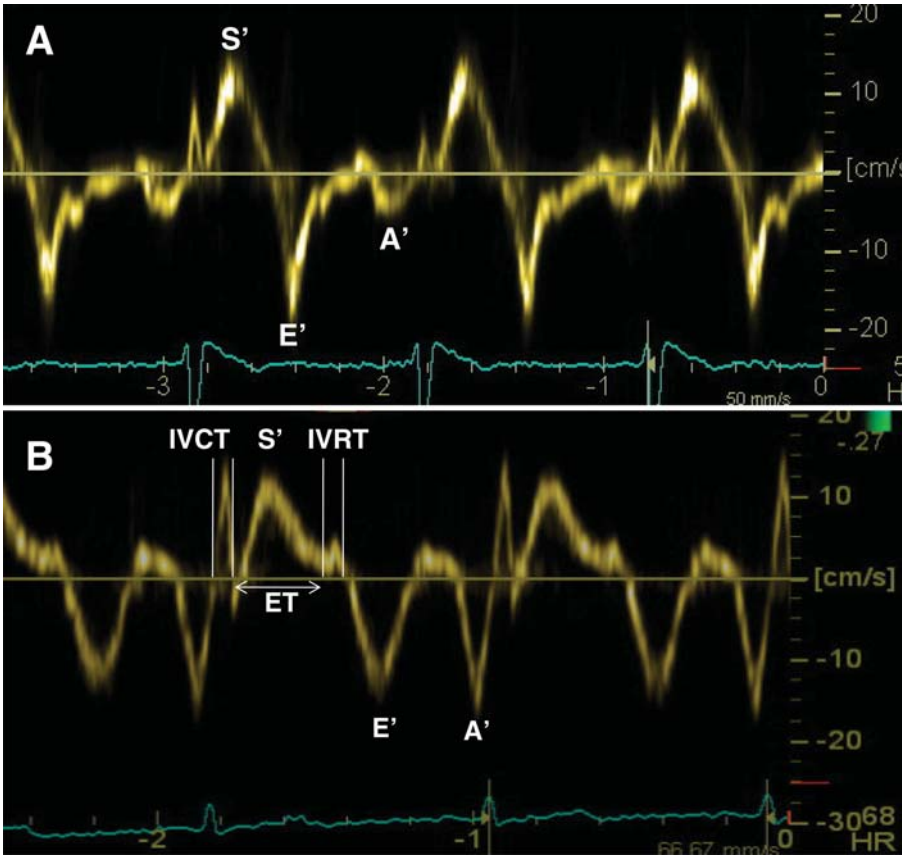


**Figure 24** (*A*) Tricuspid annular velocities assessed using pulsed DTI in a normal subject. (*B*) Measurement of the RV Tei index ([isovolumic contraction time + isovolumic relaxation time])/ejection time).

that systolic RV free wall myocardial velocities were not affected by age, while diastolic velocities were affected, with a progressive decrease in early diastolic velocity. This information is important for interpreting values in patients over a wide range of age groups.[147]

In healthy individuals, RV longitudinal velocities demonstrate a typical base-to-apex gradient with higher velocities at the base (*Figure 26A*). In addition, RV velocities are consistently higher compared with the left ventricle. This can be explained by the differences in loading conditions and compliance with a lower afterload in the right ventricle and the dominance of longitudinal and oblique myocardial fibers in the RV free wall. With RV dysfunction, RV longitudinal velocities decrease and the base-to-apex gradient tends to disappear (*Figure 27*).

The value of the tricuspid annular systolic velocity has been studied in a wide range of pathologic conditions, such as pulmonary hypertension, chronic heart failure, chronic and acute pulmonary embolism, systemic sclerosis, coronary artery disease, congenital heart disease, and various types of cardiomyopathy (*Figure 28*). Under these pathologic conditions, the tricuspid lateral annular systolic and early diastolic velocities are significantly reduced compared with healthy individuals. In patients with heart failure, the reduction

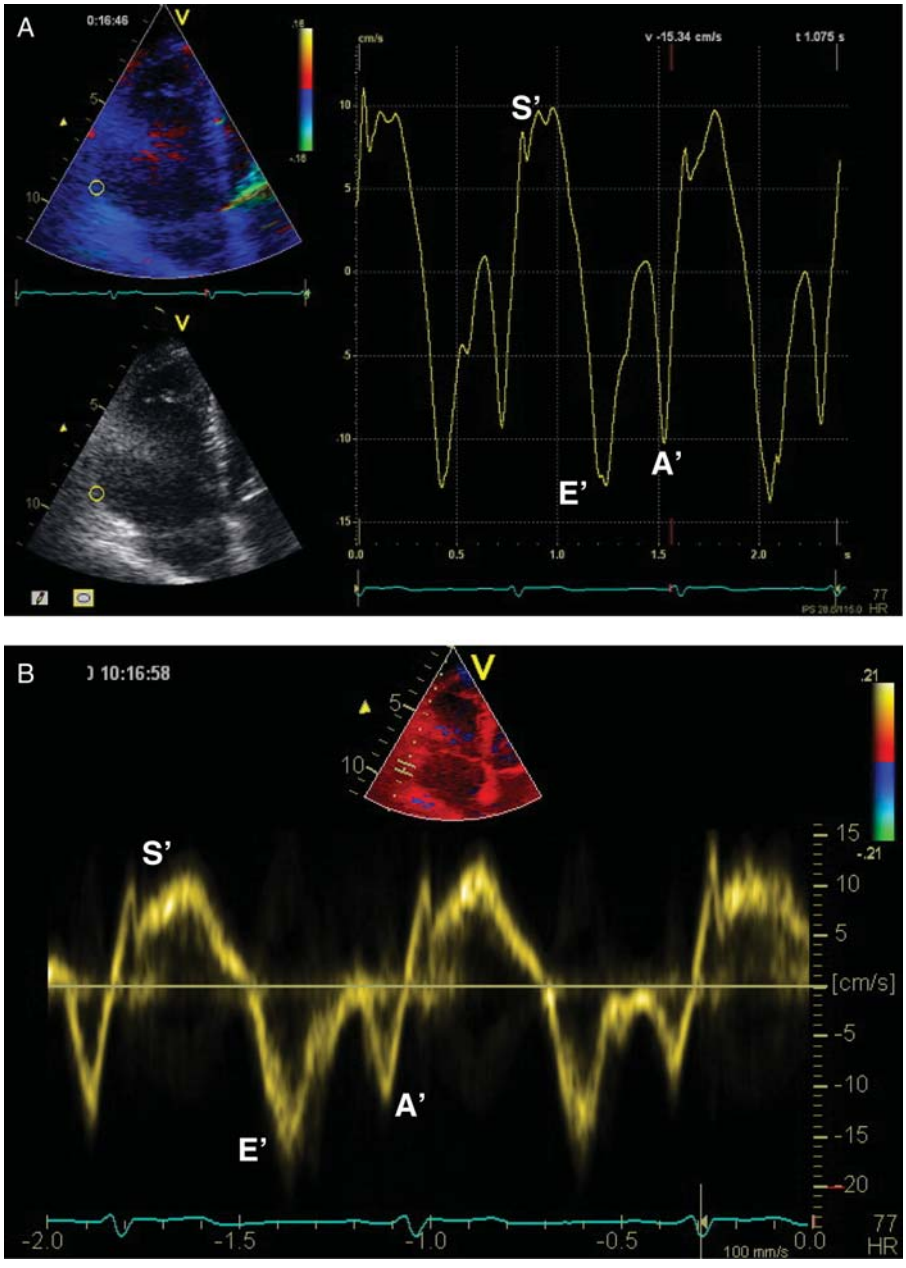


**Figure 25** Myocardial velocity profile of the tricuspid annulus assessed using color DTI (*A*) and pulsed DTI (*B*) in a normal subject. Note the lower velocities obtained with color DTI compared with pulsed DTI.

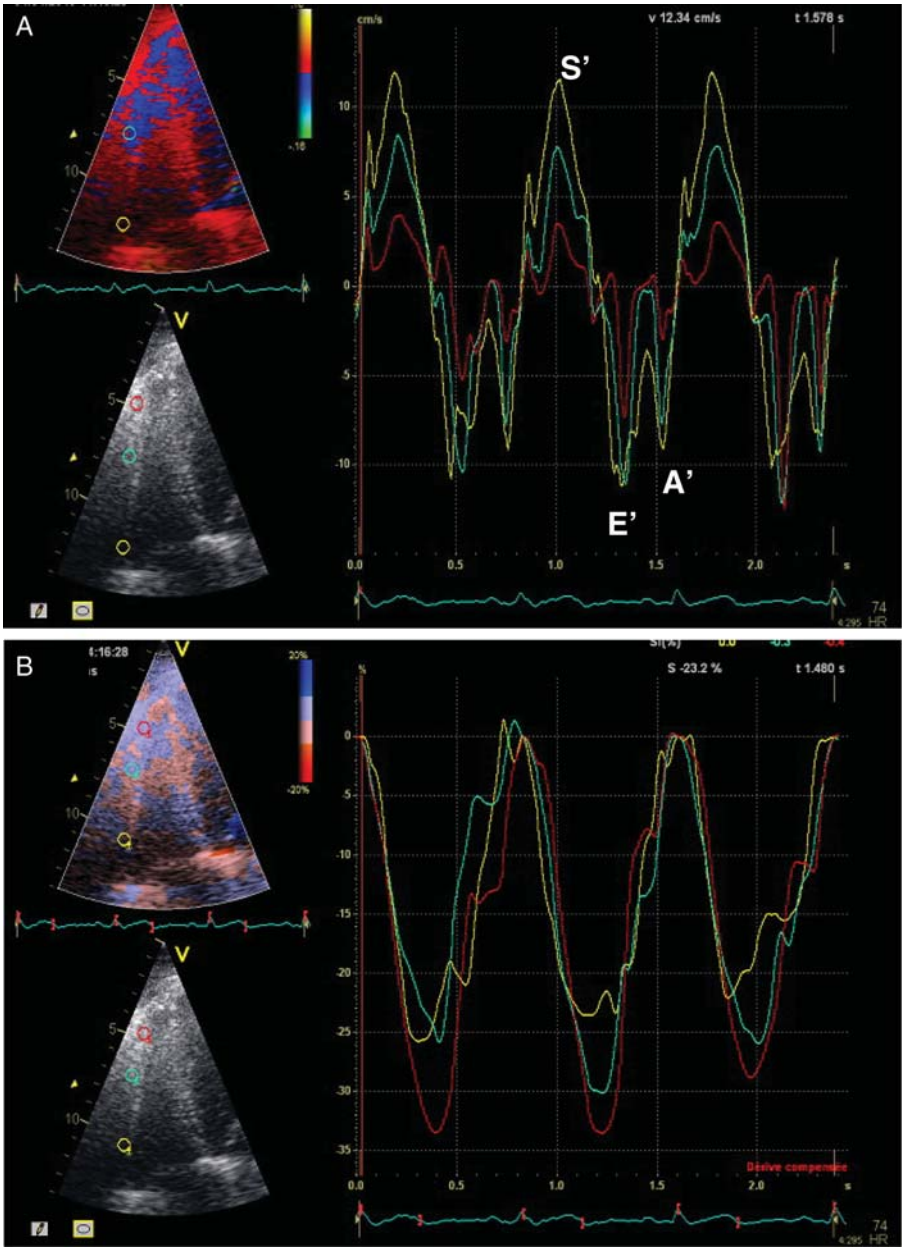


**Figure 26** RV lateral free wall velocities (*A*) and longitudinal strain (*B*) assessed using color DTI in a normal subject. Note the base-to-apex gradient in velocities and apex-to-base gradient in longitudinal strain. Yellow = basal; blue = mid; red = apical.

of tricuspid annular systolic velocity is associated with the severity of RV dysfunction and is a strong predictor of outcomes.[146] In systemic sclerosis and hypertrophic cardiomyopathy, subclinical involvement of the right ventricle is also evident by a reduction of tricuspid annular peak systolic and early diastolic velocities and reversal of tricuspid annular E′/a′ ratios.[148]

*Myocardial Deformation.* — In contrast to the more homogenously distributed deformation properties within the left ventricle, the SR and strain values are less homogeneously distributed in the right ventricle and show a reverse base-to-apex gradient, reaching the highest values in the apical segments and outflow tract (*Figure 26B*).[149] This pattern can be explained by the complex geometry of the thin-walled, crescent-shaped right ventricle and the less homogeneous distribution of regional wall stress compared with the thick-walled, bullet-shaped left ventricle.

DTI-derived and STE-derived strain and SR can be used to assess RV dynamics and were found to be both feasible and roughly comparable.[150] Strain and SR correlate well with radionuclide RV EF. Cutoff points of systolic strain and SR at the basal RV free wall of 25% and $-4$ sec$^{-1}$ yielded sensitivities of 81% and 85% and specificities of 82% and 88%, respectively, for the prediction of RV EF $>50\%$.[151] In patients with RV disease or dysfunction, peak systolic strain and SR are significantly reduced and

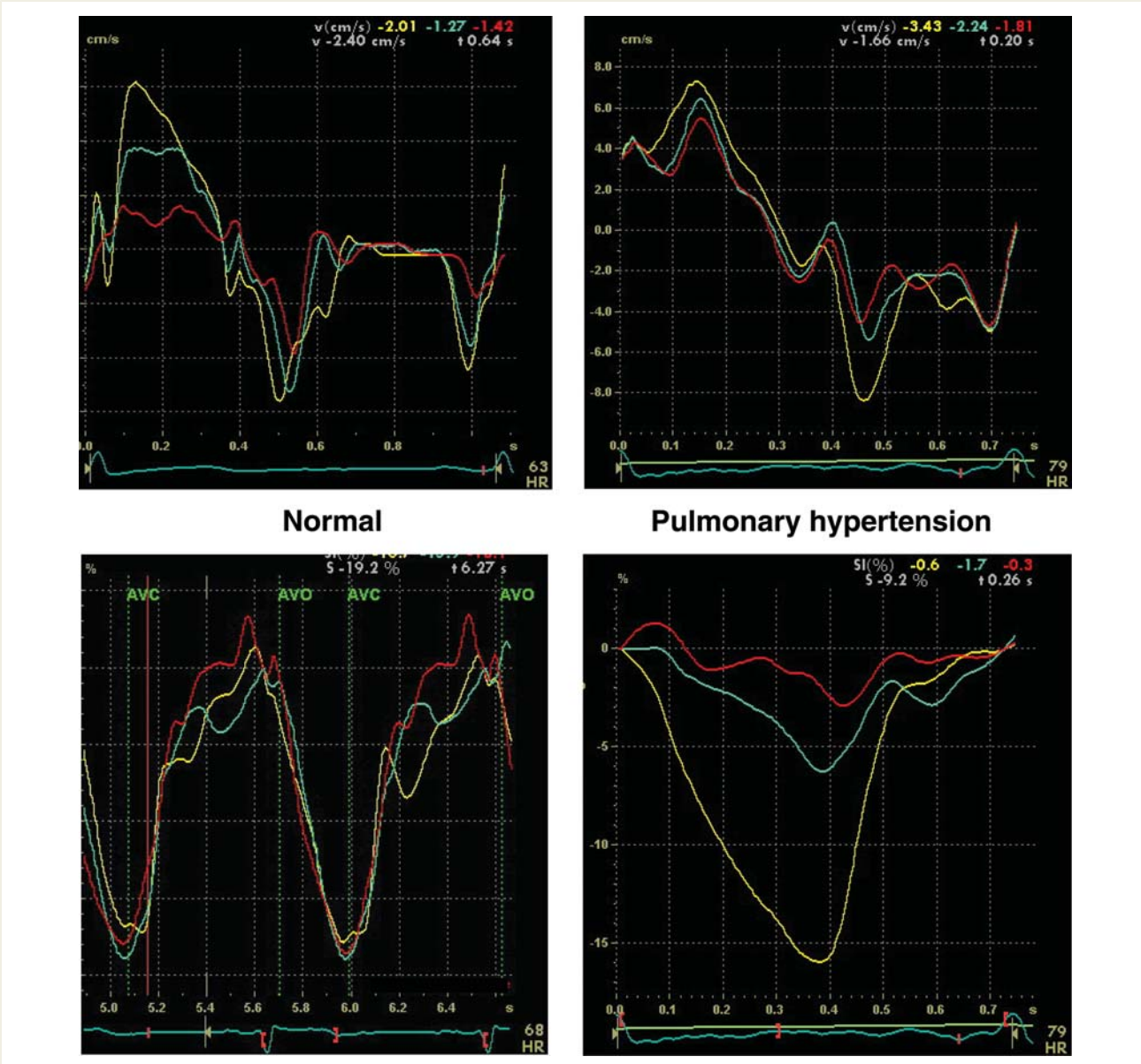


**Figure 27** Myocardial velocities (top) and longitudinal strain (bottom) of the RV lateral free wall assessed using color DTI in a normal subject (left) and in a patient with pulmonary hypertension (right). Although apical (red), mid (blue), and basal (yellow) segments have a similar velocity profile without any base-to-apex gradient, the apical and mid segments exhibit a dramatic decrease in systolic strain compared with the basal segment in the patient with pulmonary hypertension.

delayed compared with individuals with normal RV function (*Figures 26B, 27*, and *29*).

Strain and SR abnormalities of the right ventricle can be detected in pulmonary hypertension, as well as in amyloidosis, congenital heart diseases, and arrhythmogenic RV cardiomyopathy. Doppler-derived strain and SR may identify subtle changes in response to vasodilator treatment[152] and may detect early signs of RV involvement in the course of pulmonary artery hypertension (*Figure 27*).[153] Also, it proved sensitive enough to detect early alterations of RV function in patients with systemic sclerosis and normal pulmonary pres- sures.[154] Strain measurement may prove useful as an early indicator of RV dysfunction. For instance, in asymptomatic children with repaired tetralogy of Fallot, RV strain decreased as pulmonary insufficiency increased.[155] Also, in the setting of perioperative follow-up of RV function, strain has advantages over M-mode or velocity- based parameters, because it is not influenced by a possible change in overall heart motion pattern after pericardectomy.[143]

A recent study in patients with pulmonary hypertension confirmed an inverse relationship between RV pressure and RV free wall longitudinal strain.[156] Furthermore, there was a significant relationship between RV pressure and septal longitudinal strain but not lateral wall strain, suggesting that the longitudinal fibers cannot propagate the impact of RV pressure far into the left

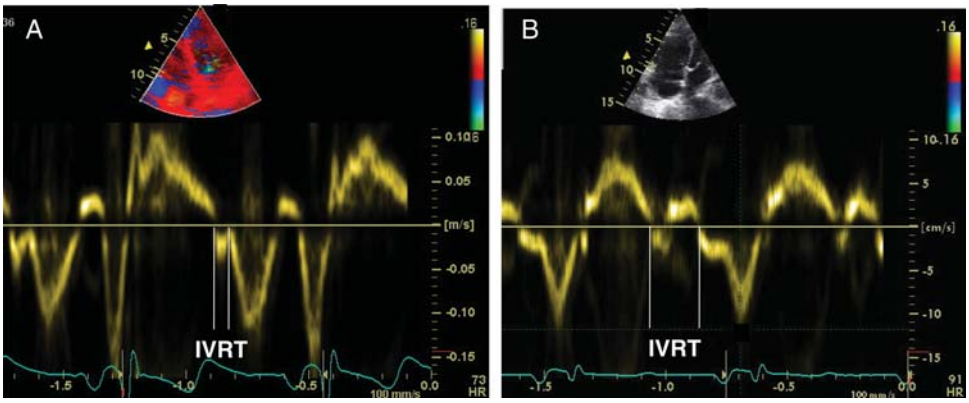


**Figure 28** Myocardial velocity profile of the tricuspid annulus assessed using pulsed DTI in a patient with systemic sclerosis without resting pulmonary hypertension (*A*) and developing later pulmonary hypertension (*B*). Note the increase in the isovolumic relaxation duration.

ventricle. In contrast, circumferential strain was related to RV pressure in both the septum and lateral LV wall, indicating that the circumferential fibers can propagate RV factors throughout the left ventricle.

***Unresolved Issues and Research Priorities:*** The available experience on STE for the assessment of RV function is limited to small single-center studies. The technique seems feasible for the quantitative assessment of RV function and may improve the understanding of the pathophysiology of different diseases. However, its clinical value for patient management remains to be proven.

***Summary and Recommended Indications:*** DTI-derived velocity and deformation parameters have been demonstrated to be reliable and useful, especially in detecting subtle abnormalities and in assessing prognosis. They have recently been proposed as parameters to be included in the follow-up of patients with pulmonary hypertension.[157] Myocardial velocities recorded at the level of the tricuspid annulus are helpful to quantify RV longitudinal motion. They provide useful information in terms of quantification, early detection of subtle myocardial abnormalities, and prognosis.

## 4.2. Left Atrium

The left atrium performs four basic mechanical functions: phase 1, *reservoir* (collection of pulmonary venous flow during LV systole); phase 2, *conduit* (passage of blood to the left ventricle during early diastole); phase 3, *active contractile pump* (15%–30% of LV filling in late diastole); and phase 4, *suction force* (the atrium refills itself in early systole). Through these functions, the left atrium modulates LV filling. LA dilation occurs in response to impaired LV filling and as a consequence of mitral disease and/or atrial fibrillation.

LA function can be separated into a roughly exponential pressure- volume relationship during the reservoir and conduit phases and a counterclockwise pressure-volume loop during atrial contraction and suction. Any comprehensive assessment of LA function should require accurate LA pressure, which can only be indirectly estimated by echocardiography[100] Complicating the situation further are the facts that (1) unlike the left ventricle, there is no true LA isovolumic phase (because the pulmonary vein orifices are always open), and (2) reservoir function is determined as much by LV function (descent of the mitral annulus during systole) as by primary LA properties. Passive and active LA properties can be characterized by combining 3D echocardiographic volumes with invasive pressure measurements in conjunction with changes in loading conditions.[158] By using this method, a reduction of LA systolic loop occurred during circumflex ligation (which induces LA ischemia) but not with left anterior descending coronary artery ligation (which affects only the left ventricle). On a regional basis, LA function can be fundamentally described in terms of stress-strain relationships. Although strain is becoming increasingly accessible by echocardiography, there is no way to estimate wall stress, even invasively. Fortunately, because the left atrium is thin walled, one can reasonably equate LA pressure with wall stress.

***Global and Regional LA Function:*** LA function is currently estimated by 2D measurements of LA volumes, by Doppler analysis of transmitral flow (peak and time velocity integral of a velocity, atrial filling fraction) and by pulmonary vein flow (peak and duration of atrial reverse velocity). Because 2D echocardiography is limited by the use of geometric models and by possible errors due to foreshortening, it may underestimate LA volume compared with cardiac magnetic resonance, while Doppler assessment of LA function and/or the use of the LA ejection force are indirect parameters. Three-dimensional LA volume measurements, which do not require geometric assumptions, can accurately estimate global LA function. Acoustic quantification, an automated border detection technique, provides online continuous LA area or volume over time, but the values obtained are heavily influenced by gain settings, resulting in large interobserver and test- retest variability.

Both DTI and 2D STE allow noninvasive assessment of global LA function and regional deformation of LA walls. Two-dimensional STE also successfully provides LA volume curves during one cardiac cycle, from which various LA mechanical indices can be obtained,[159,160] and allows a direct assessment of LA endocardial contractility and passive deformation. Two

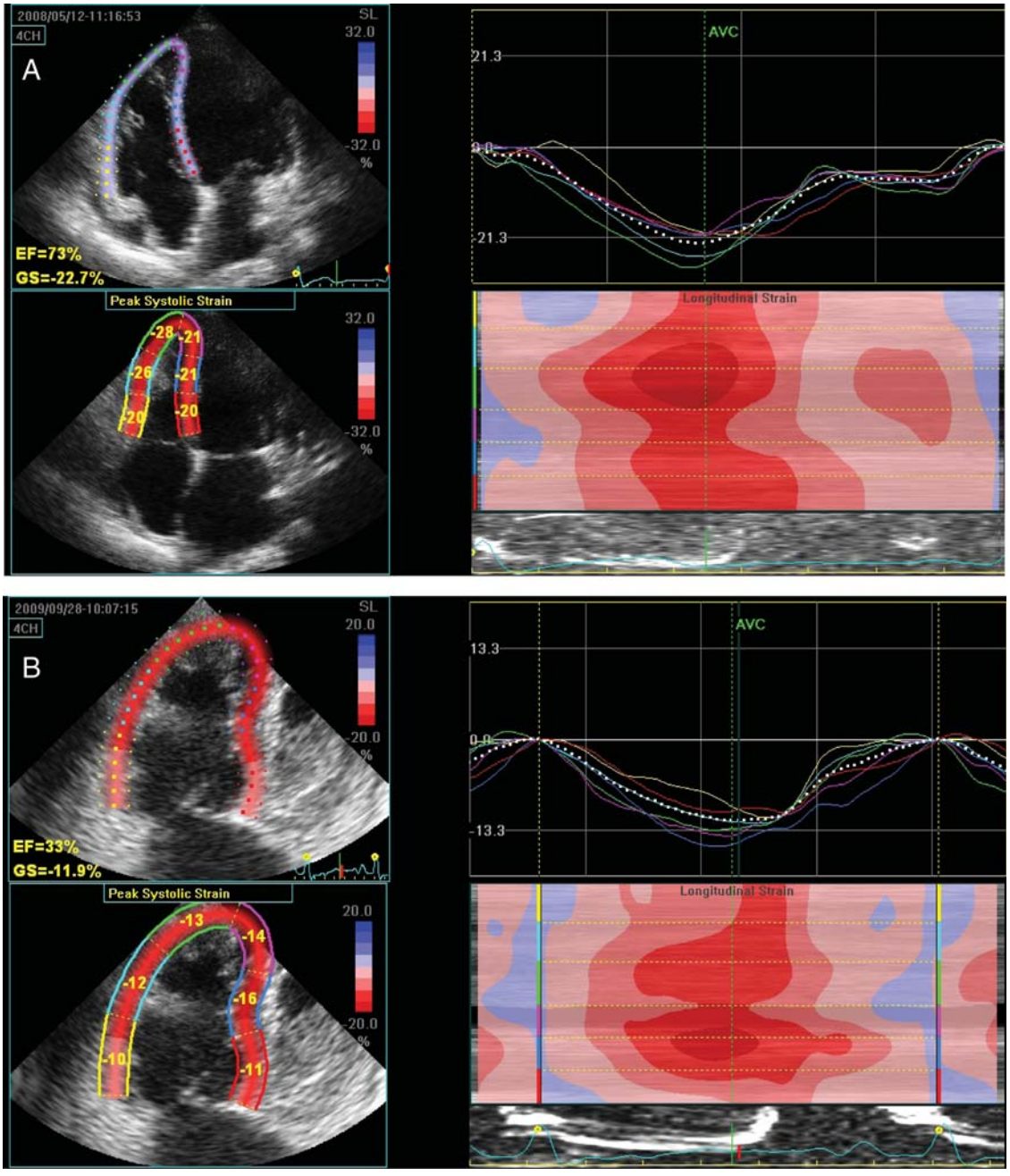


**Figure 29** Longitudinal strain of the right ventricle assessed using STE from an apical four-chamber view in a normal subject (*A*) and in a patient with altered RV function (*B*). *GS*, Global strain.

different modalities have been proposed to quantify atrial deformation by STE (*Figure 30*). The first (total of 12 equidistant regions, six in the apical four-chamber view and six in the apical two-chamber view) takes as a reference point the QRS onset and measures the positive peak atrial longitudinal strain (corresponding to atrial reservoir).[159] The second (total of 15 equidistant regions, six in the apical four-chamber view, six in the apical two- chamber view, and three in the inferoposterior wall in long axis) uses the P wave as the reference point, enabling the measurement of a first negative peak atrial longitudinal strain (corresponding to atrial systole), a second positive peak atrial strain (corresponding to LA conduit function), and their sum.[160]

***Normal Values:*** Two-dimensional speckle-tracking echocardiographic normal values of LA strain have been recently reported.[159–161] By using a 12-segment model and QRS onset as the reference point, the mean peak atrial longitudinal strain of 60 healthy individuals was 42.2 ± 6.1% (5th to 95th percentile range, 32.2%-53.2%).[159] The average values of positive and negative peak strain were 23.2 ± 6.7% and −14.6 ± 3.5%,

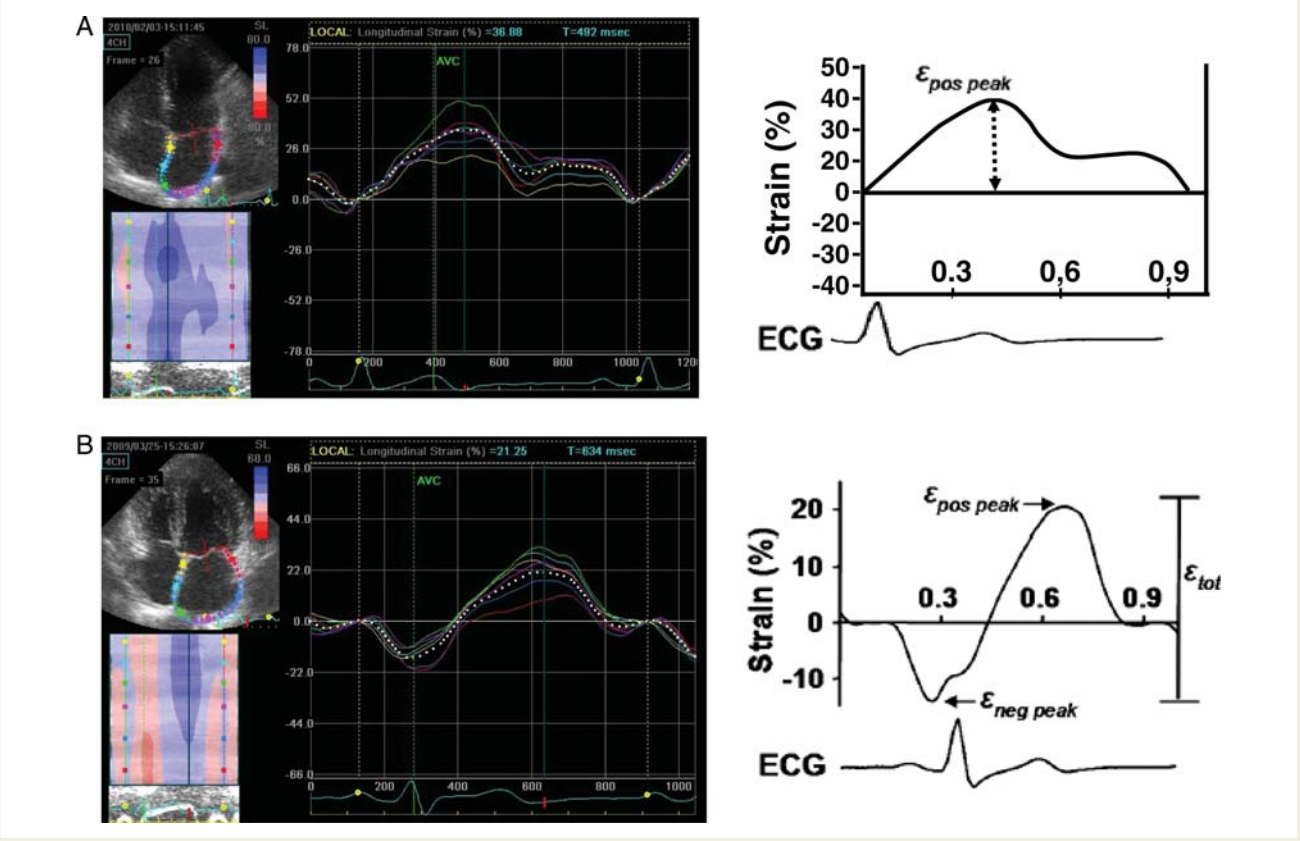


**Figure 30** Two different modalities proposed to quantify regional and global atrial deformation by 2D STE: (*A*) the use of the QRS onset as a reference point and measurement of the positive peak left atrial (LA) longitudinal strain and (*B*) the use of the P wave as the reference point to allow the measurement of a first negative peak LA longitudinal strain (LA systole), of a second positive peak LA strain (LA conduit function), and of their sum.

respectively, in a 15-segment model, which used the P wave as the reference point (64 normal subjects).[161]

***Published Findings:*** Strain and SRs and early diastolic global strain were reported to be reduced in 12 atrial segments in patients with atrial septal occluder devices compared with control subjects.[162] In patients in sinus rhythm who had undergone either cardioversion or catheter ablation for atrial fibrillation, color DTI velocities and strain were lower compared with normal controls, but the ablation group had increased regional and global LA dysfunction.[163] Conversely, LA strain was shown to be increased in patients with mitral regurgitation.[164] Also, strain and SR were used for the evaluation of patients with atrial fibrillation to assess the risk for new atrial fibrillation after cardioversion.[165] Triplane 3D color DTI, which has the advantage of simultaneously recording SRs in three views to minimize beat variation, was used to demonstrate significantly lower peak SRs in patients with hypertension compared with normal controls and athletes.[166] Similar to DTI, STE-derived global LA motion analysis after percutaneous interatrial defect repair showed the expected absence of strain measured at the device site.[167] Decreased negative LA SR is also an independent predictor of episodes of paroxysmal atrial fibrillation in patients in sinus rhythm.[168]

Regional heterogeneity of LA strain and SR values has been reported in healthy subjects, with the highest value in the inferior wall in comparison with mid and superior LA segments.[160] This heterogeneity is confirmed by the observation that DTI-derived SR of the LA inferior wall is one of the best predictors of sinus rhythm maintenance after atrial fibrillation cardioversion and that LA strain is more improved at lateral wall in CRTresponders.[169]

The main strength of LA strain is its feasibility, which is very high with either color DTI[170] or STE (94% in 84 normal subjects).[160] In addition, STE has an important pathophysiologic value, because peak positive global LA strain correlates strongly (inverse relation) with in- vasively determined LV end-diastolic pressure,[109] with Doppler indices of transmitral inflow, pulmonary vein velocities, DTI, and LA volumes.[161]

***Unresolved Issues and Research Priorities:*** The main weakness of LA regional strain measurements is the anatomic effect of the pulmonary vein outlet, which can preclude accurate assessment of LA basal regions, in particular when the pulmonary veins are dilated. Similar confounding effect can be seen in the apical two- chamber view because of the LA appendage, particularly when it is extremely large.

Although regional assessment of LA function could provide more detailed information about LA mechanics, its incremental

value over global LA functional assessment has not been determined, and additional work is needed to elucidate this issue. Also, the normal reference values reported so far for LA strain were obtained in relatively small groups of patients and thus need to be confirmed in larger populations.

***Summary and Recommended Indications:*** Indications for 2D STE of the left atrium include regional LA assessment in patients with LV diastolic dysfunction, evaluation of LA properties after atrial fibrillation to predict the maintenance of sinus rhythm, and evaluation after percutaneous interatrial defect repair. In addition, LA regional strain appears potentially suitable to identify patients at risk for LA failure or arrhythmias and to assess LA characteristics in patients with LA dilation of undetermined cause. However, at the present time, 2D STE of the left atrium does not appear ready for clinical use.

### 4.3. Right Atrium

If the right ventricle is the forgotten ventricle,[171] then the right atrium dwells in true obscurity. Virtually no echocardiographic research has focused on mechanical assessment of RA function per se, with most studies directed at the assessment of mean RA pressure.[172–177] Similar to the left atrium, the right atrium has three distinct phases: reservoir (filling of the right atrium during ventricular systole), conduit (passage of blood into the right ventricle during diastole before the P wave), and active contraction (atrial systole). Thus, one may consider the right atrium to have a passive phase of RA function (reservoir plus conduit) and an active phase of contraction.

***Published Findings:*** The right atrium has received scant attention with the newer methodologies of tissue Doppler and 2D strain. These novel approaches are challenging because of the thinness of the RA wall. One recent study[178] used STE to assess RA free wall strain in patients undergoing CRT. Patients who responded to CRT (as reflected by a reduction of >15% in LV end-systolic volume) were found to have smaller RA sizes ($13.2 \pm 4.4$ vs $19.7 \pm 5.5$ $cm^2/m^2$, $P < .001$) and higher RA strain values ($40.2 \pm 8.9\%$ vs $24.3 \pm 10.2\%$, $P < .001$).

***Summary and Recommended Indications:*** Clearly, there is much more validation work to undertake before RA strain measurements can be considered for routine clinical use.

## 5. CONCLUSIONS

This document represents the consensus of the writing group assembled jointly by the ASE and the EAE to survey the techniques currently available to assess myocardial mechanics. The consensus is that the techniques described in this document significantly contribute to the much needed process of the transformation of echocardiography from a subjective art of image interpretation to a set of objective diagnostic tools. Although the published research provides the evidence basis for potential clinical applications of these techniques in multiple clinical scenarios, the Writing Group believes that in the majority of areas, this methodology is not yet ready for routine clinical use. The consensus is that (1) additional testing is needed in multicenter settings to better establish the diagnostic accuracy of the different parameters and their reproducibility in various disease states, (2) standardization is needed for what should be measured and how measurements should be performed, and (3) standardization among manufacturers is essential, as clinicians should be able to interpret data generated by different equipment irrespective of vendor. Once these conditions are met and the larger echocardiography community gains the necessary experience with these techniques, they promise to become an integral part of the "toolbox" of clinical echocardiography.

## NOTICE AND DISCLAIMER

This report is made available by the ASE and EAE as a courtesy reference source for their members. This report contains recommendations only and should not be used as the sole basis to make medical practice decisions or for disciplinary action against any employee. The statements and recommendations contained in this report are primarily based on the opinions of experts, rather than on scientifically verified data. ASE and EAE make no express or implied warranties regarding the completeness or accuracy of the information in this report, including the warranty of merchantability or fitness for a particular purpose. In no event shall ASE or EAE be liable to you, your patients, or any other third parties for any decision made or action taken by you or such other parties in reliance on this information. Nor does your use of this information constitute the offering of medical advice by ASE or EAE, or create any physician-patient relationship between ASE or EAE and your patients or anyone else.

## REFERENCES


1. Yoshida T, Mori M, Nimura Y, Hikita G, Taka GS, Nakanishi K *et al.* Analysis of heart motion with ultrasonic Doppler method and its clinical application. *Am Heart J* 1961;**61**:61–75.
2. McDicken WN, Sutherland GR, Moran CM, Gordon LN. Colour Doppler velocity imaging of the myocardium. *Ultrasound Med Biol* 1992;**18**:651–4.
3. Sutherland GR, Hatle L, Claus P, D'hooge J, Bijnens BH. Doppler Myocardial imaging—a textbook. Hasselt, Belgium: BSWK; 2006.
4. Heimdal A, Stoylen A, Torp H, Skjaerpe T. Real-time strain rate imaging of the left ventricle by ultrasound. *J Am Soc Echocardiogr* 1998;**11**:1013–9.
5. Urheim S, Edvardsen T, Torp H, Angelsen B, Smiseth OA. Myocardial strain by Doppler echocardiography. Validation of a new method to quantify regional myocardial function. *Circulation* 2000;**102**:1158–64.
6. Leitman M, Lysyansky P, Sidenko S, Shir V, Peleg E, Binenbaum M *et al.* Two-dimensional strain—a novel software for real-time quantitative echo- cardiographic assessment of myocardial function. *J Am Soc Echocardiogr* 2004;**17**: 1021–9.
7. Pirat B, Khoury DS, Hartley CJ, Tiller L, Rao L, Schulz DG *et al.* A novel feature-tracking echocardiographic method for the quantitation of regional myocardial function: validation in an animal model of ische- mia-reperfusion. *J Am Coll Cardiol* 2008;**51**:651–9.
8. Alharthi MS, Jiamsripong P, Calleja A, Sengupta PP, McMahon EM, Khandheria B *et al.* Selective echocardiographic analysis of epicardial and endocardial left ventricular rotational mechanics in an animal model of pericardial adhesions. *Eur J Echocardiogr* 2009;**10**:357–62.
9. Jiamsripong P, Alharthi MS, Calleja AM, McMahon EM, Mookadam F, Khandheria BK *et al.* Quantification of left ventricular twisting mechanics by velocity vector imaging in an animal model of pericardial adhesions. *Ultrasound Med Biol* 2009;**35**:1963–72.
10. Kim DH, Kim HK, Kim MK, Chang SA, Kim YJ, Kim MA *et al.* Velocity vector imaging in the measurement of left ventricular twist mechanics: head-to-head one way comparison between speckle tracking echocardi- ography and velocity vector imaging. *J Am Soc Echocardiogr* 2009;**22**:1344–52.
11. Chen J, Cao T, Duan Y, Yuan L, Yang Y. Velocity vector imaging in assessing the regional systolic function of patients with post myocardial infarction. *Echocardiography* 2007;**24**:940–5.

12. Marwick TH, Leano RL, Brown J, Sun JP, Hoffmann R, Lysyansky P *et al.* Myocardial strain measurement with 2-dimensional speckle-tracking echocardiography: definition of normal range. *JACC Cardiovasc Imaging* 2009;**2**:80–4.
13. Manovel A, Dawson D, Smith B, Nihoyannopoulos P. Assessment of left ventricular function by different speckle-tracking software. *Eur J Echocar- diogr* 2010;**11**: 417–21.
14. Brown J, Jenkins C, Marwick TH. Use of myocardial strain to assess global left ventricular function: a comparison with cardiac magnetic resonance and 3-dimensional echocardiography. *Am Heart J* 2009;**157**:102–5.
15. Amundsen BH, Helle-Valle T, Edvardsen T, Torp H, Crosby J, Lyseggen E *et al.* Noninvasive myocardial strain measurement by speckle tracking echocardiography: validation against sonomicrometry and tagged magnetic resonance imaging. *J Am Coll Cardiol* 2006;**47**:789–93.
16. Teske AJ, De Boeck BW, Melman PG, Sieswerda GT, Doevendans PA, Cramer MJ. Echocardiographic quantification of myocardial function using tissue deformation imaging, a guide to image acquisition and analysis using tissue Doppler and speckle tracking. *Cardiovasc Ultrasound* 2007;**5**:27.
17. Korinek J, Wang J, Sengupta PP, Miyazaki C, Kjaergaard J, McMahon E *et al.* Two-dimensional strain—a Doppler-independent ultrasound method for quantitation of regional deformation: validation in vitro and in vivo. *J Am Soc Echocardiogr* 2005;**18**:1247–53.
18. Korinek J, Kjaergaard J, Sengupta PP, Yoshifuku S, McMahon EM, Cha SS *et al.* High spatial resolution speckle tracking improves accuracy of 2-dimensional strain measurements: an update on a new method in functional echocardiography. *J Am Soc Echocardiogr* 2007;**20**:165–70.
19. Gjesdal O, Hopp E, Vartdal T, Lunde K, Helle-Valle T, Aakhus S *et al.* Global longitudinal strain measured by two-dimensional speckle tracking echocardiography is closely related to myocardial infarct size in chronic ischaemic heart disease. *Clin Sci (Lond)* 2007;**113**:287–96.
20. Holland MR, Houle H, Prater D, Thomenius K, Thomas JD. Improving accuracy and vendor interoperability in advanced ventricular mechanics derived from 2D and 3D echocardiography. *J Am Soc Echocardiogr*. In press.
21. Nesser HJ, Mor-Avi V, Gorissen W, Weinert L, Steringer-Mascherbauer R, Niel J *et al.* Quantification of left ventricular volumes using three- dimensional echocardiographic speckle tracking: comparison with MRI. *Eur Heart J* 2009;**30**: 1565–73.
22. Maffessanti F, Nesser HJ, Weinert L, Steringer-Mascherbauer R, Niel J, Gorissen W *et al.* Quantitative evaluation of regional left ventricular function using three-dimensional speckle tracking echocardiography in patients with and without heart disease. *Am J Cardiol* 2009;**104**:1755–62.
23. de Isla LP, Balcones DV, Fernandez-Golfin C, Marcos-Alberca P, Almeria C, Rodrigo JL *et al.* Three-dimensional-wall motion tracking: a new and faster tool for myocardial strain assessment: comparison with two-dimensional-wall motion tracking. *J Am Soc Echocardiogr* 2009;**22**:325–30.
24. Seo Y, Ishizu T, Enomoto Y, Sugimori H, Yamamoto M, Machino T *et al.* Validation of 3-dimensional speckle tracking imaging to quantify regional myocardial deformation. *Circ Cardiovasc Imaging* 2009;**2**:451–9.
25. Baccouche H, Maunz M, Beck T, Fogarassy P, Beyer M. Echocardio- graphic assessment and monitoring of the clinical course in a patient with Tako-Tsubo cardiomyopathy by a novel 3D-speckle-tracking-strain analysis. *Eur J Echocardiogr* 2009;**10**:729–31.
26. Tanaka H, Hara H, Saba S, Gorcsan J III. Usefulness of three-dimensional speckle tracking strain to quantify dyssynchrony and the site of latest mechanical activation. *Am J Cardiol* 2010;**105**:235–42.
27. Miller JG, Sobel BE. Cardiac ultrasonic tissue characterization. *Hosp Pract (Off Ed)* 1982;**17**:143–51.
28. Perez JE, Miller JG, Wickline SA, Holland MR, Waggoner AD, Barzilai B *et al.* Quantitative ultrasonic imaging: tissue characterization and instantaneous quantification of cardiac function. *Am J Cardiol* 1992;**69(suppl)**: p104H–11.
29. D'hooge J, Bijnens B, Jamal F, Pislaru C, Pislaru S, Thoen J *et al.* High frame rate myocardial integrated backscatter. Does this change our understanding of this acoustic parameter? *Eur J Echocardiogr* 2000;**1**:32–41.
30. Komuro K, Yamada S, Mikami T, Yoshinaga K, Noriyasu K, Goto K *et al.* Sensitive detection of myocardial viability in chronic coronary artery disease by ultrasonic integrated backscatter analysis. *J Am Soc Echocardiogr* 2005;**18**:26–31.
31. Marini C, Picano E, Varga A, Marzullo P, Pingitore A, Paterni M. Cyclic variation in myocardial gray level as a marker of viability in man. A videodensitometry study. *Eur Heart J* 1996;**17**:472–9.
32. Aghini-Lombardi F, Di BV, Talini E, Di CA, Monzani F, Antonangeli L *et al.* Early textural and functional alterations of left ventricular myocardium in mild hypothyroidism. *Eur J Endocrinol* 2006;**155**:3–9.
33. Maceira AM, Barba J, Varo N, Beloqui O, Diez J. Ultrasonic backscatter and serum marker of cardiac fibrosis in hypertensives. *Hypertension* 2002;**39**:923–8.
34. Picano E, Pelosi G, Marzilli M, Lattanzi F, Benassi A, Landini L *et al.* In vivo quantitative ultrasonic evaluation of myocardial fibrosis in humans. *Circulation* 1990; **81**:58–64.
35. Kubota T, Kawasaki M, Takasugi N, Takeyama U, Ishihara Y, Okubo M *et al.* Evaluation of left atrial degeneration for the prediction of atrial fibrillation: usefulness of integrated backscatter transesophageal echocardiog- raphy. *JACC Cardiovasc Imaging* 2009;**2**:1039–47.
36. Finch-Johnston AE, Gussak HM, Mobley J, Holland MR, Petrovic O, Perez JE *et al.* Cyclic variation of integrated backscatter: dependence of time delay on the echocardiographic view used and the myocardial segment analyzed. *J Am Soc Echocardiogr* 2000;**13**:9–17.
37. Ashikaga H, van der Spoel TI, Coppola BA, Omens JH. Transmural myo- cardial mechanics during isovolumic contraction. *JACC Cardiovasc Imaging* 2009;**2**: 202–11.
38. Covell JW. Tissue structure and ventricular wall mechanics. *Circulation* 2008;**118**: 699–701.
39. Sengupta PP, Korinek J, Belohlavek M, Narula J, Vannan MA, Jahangir A *et al.* Left ventricular structure and function: basic science for cardiac imaging. *J Am Coll Cardiol* 2006;**48**:1988–2001.
40. Smiseth OA, Remme EW. Regional left ventricular electric and mechanical activation and relaxation. *J Am Coll Cardiol* 2006;**47**:173–4.
41. Crosby J, Hergum T, Remme EW, Torp H. The effect of including myo- cardial anisotropy in simulated ultrasound images of the heart. *IEEE Trans Ultrason Ferroelectr Freq Control* 2009;**56**:326–33.
42. Wickline SA, Verdonk ED, Miller JG. Three-dimensional characterization of human ventricular myofiber architecture by ultrasonic backscatter. *J Clin Invest* 1991;**88**:438–46.
43. Remme EW, Lyseggen E, Helle-Valle T, Opdahl A, Pettersen E, Vartdal T *et al.* Mechanisms of preejection and postejection velocity spikes in left ventricular myocardium: interaction between wall deformation and valve events. *Circulation* 2008;**118**:373–80.
44. Sengupta PP, Khandheria BK, Korinek J, Wang J, Jahangir A, Seward JB *et al.* Apex-to-base dispersion in regional timing of left ventricular shortening and lengthening. *J Am Coll Cardiol* 2006;**47**:163–72.
45. Sengupta PP, Tajik AJ, Chandrasekaran K, Khandheria BK. Twist mechanics of the left ventricle: principles and application. *JACC Cardiovasc Imaging* 2008;**1**:366–76.
46. Notomi Y, Lysyansky P, Setser RM, Shiota T, Popovic ZB, Martin- Miklovic MG *et al.* Measurement of ventricular torsion by two- dimensional ultrasound speckle tracking imaging. *J Am Coll Cardiol* 2005;**45**:2034–41.
47. Bansal M, Leano RL, Marwick TH. Clinical assessment of left ventricular systolic torsion: effects of myocardial infarction and ischemia. *J Am Soc Echocardiogr* 2008; **21**:887–94.
48. Geyer H, Caracciolo G, Abe H, Wilansky S, Carerj S, Gentile F *et al.* Assessment of myocardial mechanics using speckle tracking echocardiogra- phy: fundamentals and clinical applications. *J Am Soc Echocardiogr* 2010;**23**:351–69.
49. Kuznetsova T, Herbots L, Richart T, D'hooge J, Thijs L, Fagard RH *et al.* Left ventricular strain and strain rate in a general population. *Eur Heart J* 2008;**29**: 2014–23.
50. Dalen H, Thorstensen A, Aase SA, Ingul CB, Torp H, Vatten LJ *et al.* Seg- mental and global longitudinal strain and strain rate based on echocardi- ography of 1266 healthy individuals: the HUNT study in Norway. *Eur J Echocardiogr* 2010; **11**:176–83.
51. Nagueh SF, Middleton KJ, Kopelen HA, Zoghbi WA, Quinones MA. Doppler tissue imaging: a noninvasive technique for evaluation of left ventricular relaxation and estimation of filling pressures. *J Am Coll Car- diol* 1997;**30**:1527–33.
52. Marwick TH. Measurement of strain and strain rate by echocardiogra- phy: ready for prime time? *J Am Coll Cardiol* 2006;**47**:1313–27.
53. Jurcut R, Wildiers H, Ganame J, D'hooge J, De BJ, Denys H *et al.* Strain rate imaging detects early cardiac effects of pegylated liposomal Doxoru- bicin as adjuvant therapy in elderly patients with breast cancer. *J Am Soc Echocardiogr* 2008;**21**:1283–9.
54. Sengupta PP, Mohan JC, Mehta V, Arora R, Pandian NG, Khandheria BK. Accuracy and pitfalls of early diastolic motion of the mitral annulus for diagnosing constrictive pericarditis by tissue Doppler imaging. *Am J Cardiol* 2004;**93**:886–90.
55. Cardim N, Oliveira AG, Longo S, Ferreira T, Pereira A, Reis RP *et al.* Doppler tissue imaging: regional myocardial function in hypertrophic cardiomyopathy and in athlete's heart. *J Am Soc Echocardiogr* 2003;**16**:223–32.
56. Bijnens B, Claus P, Weidemann F, Strotmann J, Sutherland GR. Investigating cardiac function using motion and deformation analysis in the setting of coronary artery disease. *Circulation* 2007;**116**:2453–64.
57. Bjork IC, Rozis E, Slordahl SA, Marwick TH. Incremental value of strain rate imaging to wall motion analysis for prediction of outcome in patients undergoing dobutamine stress echocardiography. *Circulation* 2007;**115**:1252–9.

58. Kukulski T, Jamal F, Herbots L, D'hooge J, Bijnens B, Hatle L *et al.* Identification of acutely ischemic myocardium using ultrasonic strain measurements. *A clinical study in patients undergoing coronary angio- plasty. J Am Coll Cardiol* 2003;**41**:810–9.
59. Voigt JU, Exner B, Schmiedehausen K, Huchzermeyer C, Reulbach U, Nixdorff U *et al.* Strain-rate imaging during dobutamine stress echocar- diography provides objective evidence of inducible ischemia. *Circulation* 2003;**107**:2120–6.
60. Weidemann F, Jung P, Hoyer C, Broscheit J, Voelker W, Ertl G *et al.* Assessment of the contractile reserve in patients with intermediate coronary lesions: a strain rate imaging study validated by invasive myocardial fractional flow reserve. *Eur Heart J* 2007;**28**:1425–32.
61. Faber L, Prinz C, Welge D, Hering D, Butz T, Oldenburg O *et al.* Peak systolic longitudinal strain of the lateral left ventricular wall improves after septal ablation for symptomatic hypertrophic obstructive cardiomyopa- thy: a follow-up study using speckle tracking echocardiography. *Int J Car- diovasc Imaging*. In press.
62. Jasaityte R, Dandel M, Lehmkuhl H, Hetzer R. Prediction of short-term outcomes in patients with idiopathic dilated cardiomyopathy referred for transplantation using standard echocardiography and strain imaging. *Transplant Proc* 2009; **41**:277–80.
63. Singh GK, Cupps B, Pasque M, Woodard PK, Holland MR, Ludomirsky A. Accuracy and reproducibility of strain by speckle tracking in pediatric subjects with normal heart and single ventricular physiology: a two-dimensional speckle-tracking echocardiography and magnetic resonance imaging correlative study. *J Am Soc Echocardiogr* 2010;**23**:1143–52.
64. Koopman LP, Slorach C, Hui W, Manlhiot C, McCrindle BW, Friedberg MK *et al.* Comparison between different speckle tracking and color tissue Doppler techniques to measure global and regional myo- cardial deformation in children. *J Am Soc Echocardiogr* 2010;**23**:919–28.
65. Lorch SM, Ludomirsky A, Singh GK. Maturational and growth-related changes in left ventricular longitudinal strain and strain rate measured by two-dimensional speckle tracking echocardiography in healthy pedi- atric population. *J Am Soc Echocardiogr* 2008;**21**:1207–15.
66. de Kort E, Thijssen JM, Daniels O, de Korte CL, Kapusta L. Improvement of heart function after balloon dilation of congenital valvar aortic stenosis: a pilot study with ultrasound tissue Doppler and strain rate imaging. *Ultrasound Med Biol* 2006;**32**:1123–8.
67. Notomi Y, Setser RM, Shiota T, Martin-Miklovic MG, Weaver JA, Popovic ZB *et al.* Assessment of left ventricular torsional deformation by Doppler tissue imaging: validation study with tagged magnetic resonance imaging. *Circulation* 2005;**111**:1141–7.
68. Helle-Valle T, Crosby J, Edvardsen T, Lyseggen E, Amundsen BH, Smith HJ *et al.* New noninvasive method for assessment of left ventricular rotation: speckle tracking echocardiography. *Circulation* 2005;**112**:3149–56.
69. Takeuchi M, Nakai H, Kokumai M, Nishikage T, Otani S, Lang RM. Age- related changes in left ventricular twist assessed by two-dimensional speckle-tracking imaging. *J Am Soc Echocardiogr* 2006;**19**:1077–84.
70. Burns AT, La GA, Prior DL, Macisaac AI. Left ventricular untwisting is an important determinant of early diastolic function. *JACC Cardiovasc Imaging* 2009;**2**: 709–16.
71. Notomi Y, Srinath G, Shiota T, Martin-Miklovic MG, Beachler L, Howell K *et al.* Maturational and adaptive modulation of left ventricular torsional biomechanics: Doppler tissue imaging observation from infancy to adulthood. *Circulation* 2006; **113**:2534–41.
72. Park SJ, Miyazaki C, Bruce CJ, Ommen S, Miller FA, Oh JK. Left ventricular torsion by two-dimensional speckle tracking echocardiography in patients with diastolic dysfunction and normal ejection fraction. *J Am Soc Echocardiogr* 2008; **21**:1129–37.
73. Wang J, Khoury DS, Thohan V, Torre-Amione G, Nagueh SF. Global di- astolic strain rate for the assessment of left ventricular relaxation and filling pressures. *Circulation* 2007;**115**:1376–83.
74. Takeuchi M, Nishikage T, Nakai H, Kokumai M, Otani S, Lang RM. The assessment of left ventricular twist in anterior wall myocardial infarction using two-dimensional speckle tracking imaging. *J Am Soc Echocardiogr* 2007;**20**:36–44.
75. Borg AN, Harrison JL, Argyle RA, Ray SG. Left ventricular torsion in primary chronic mitral regurgitation. *Heart* 2008;**94**:597–603.
76. Bertini M, Marsan NA, Delgado V, van Bommel RJ, Nucifora G, Borleffs CJ *et al.* Effects of cardiac resynchronization therapy on left ventricular twist. *J Am Coll Cardiol* 2009;**54**:1317–25.
77. Takeuchi M, Borden WB, Nakai H, Nishikage T, Kokumai M, Nagakura T *et al.* Reduced and delayed untwisting of the left ventricle in patients with hypertension and left ventricular hypertrophy: a study using two- dimensional speckle tracking imaging. *Eur Heart J* 2007;**28**:2756–62.
78. Sengupta PP, Krishnamoorthy VK, Abhayaratna WP, Korinek J, Belohlavek M, Sundt TM III *et al.* Disparate patterns of left ventricular mechanics differentiate constrictive pericarditis from restrictive cardio- myopathy. *JACC Cardiovasc Imaging* 2008;**1**:29–38.
79. Greenberg NL, Vandervoort PM, Firstenberg MS, Garcia MJ, Thomas JD. Estimation of diastolic intraventricular pressure gradients by Doppler M- mode echocardiography. *Am J Physiol Heart Circ Physiol* 2001;**280**:H2507–15.
80. Rovner A, Smith R, Greenberg NL, Tuzcu EM, Smedira N, Lever HM *et al.* Improvement in diastolic intraventricular pressure gradients in patients with HOCM after ethanol septal reduction. *Am J Physiol Heart Circ Physiol* 2003;**285**: H2492–9.
81. Rovner A, Greenberg NL, Thomas JD, Garcia MJ. Relationship of dia- stolic intraventricular pressure gradients and aerobic capacity in patients with diastolic heart failure. *Am J Physiol Heart Circ Physiol* 2005;**289**:H2081–8.
82. Notomi Y, Popovic ZB, Yamada H, Wallick DW, Martin MG, Oryszak SJ *et al.* Ventricular untwisting: a temporal link between left ventricular relaxation and suction. *Am J Physiol Heart Circ Physiol* 2008;**294**:H505–13.
83. Vardas PE, Auricchio A, Blanc JJ, Daubert JC, Drexler H, Ector H *et al.* Guidelines for cardiac pacing and cardiac resynchronization therapy: The Task Force for Cardiac Pacing and Cardiac Resynchronization Therapy of the European Society of Cardiology. Developed in collaboration with the European Heart Rhythm Association. *Eur Heart J* 2007;**28**:2256–95.
84. Bader H, Garrigue S, Lafitte S, Reuter S, Jais P, Haissaguerre M *et al.* Intra- left ventricular electromechanical asynchrony. A new independent predictor of severe cardiac events in heart failure patients. *J Am Coll Cardiol* 2004;**43**:248–56.
85. Abraham J, Abraham TP. Is echocardiographic assessment of dyssyn- chrony useful to select candidates for cardiac resynchronization therapy? Echocardiography is useful before cardiac resynchronization therapy if QRS duration is available. *Circ Cardiovasc Imaging* 2008;**1**:79–84.
86. Bax JJ, Gorcsan J III. Echocardiography and noninvasive imaging in cardiac resynchronization therapy: results of the PROSPECT (Predictors of Response to Cardiac Resynchronization Therapy) study in perspective. *J Am Coll Cardiol* 2009;**53**:1933–43.
87. Sanderson JE. Echocardiography for cardiac resynchronization therapy selection: fatally flawed or misjudged? *J Am Coll Cardiol* 2009;**53**:1960–4.
88. Anderson LJ, Miyazaki C, Sutherland GR, Oh JK. Patient selection and echocardiographic assessment of dyssynchrony in cardiac resynchronization therapy. *Circulation* 2008;**117**:2009–23.
89. Voigt JU, Schneider TM, Korder S, Szulik M, Gurel E, Daniel WG *et al.* Apical transverse motion as surrogate parameter to determine regional left ventricular function inhomogeneities: a new, integrative approach to left ventricular asynchrony assessment. *Eur Heart J* 2009;**30**:959–68.
90. Szulik M, Tillekaerts M, Vangeel V, Ganame J, Willems R, Lenarczyk R *et al.* Assessment of apical rocking: a new, integrative approach for selection of candidates for cardiac resynchronization therapy. *Eur J Echocar- diogr* 2010;**11**:863–9.
91. Gorcsan J III, Abraham T, Agler DA, Bax JJ, Derumeaux G, Grimm RA *et al.* Echocardiography for cardiac resynchronization therapy: recommendations for performance and reporting—a report from the American Society of Echocardiography Dyssynchrony Writing Group endorsed by the Heart Rhythm Society. *J Am Soc Echocardiogr* 2008;**21**:191–213.
92. Lim P, Buakhamsri A, Popovic ZB, Greenberg NL, Patel D, Thomas JD *et al.* Longitudinal strain delay index by speckle tracking imaging: a new marker of response to cardiac resynchronization therapy. *Circulation* 2008;**118**:1130–7.
93. Gorcsan J III, Tanabe M, Bleeker GB, Suffoletto MS, Thomas NC, Saba S *et al.* Combined longitudinal and radial dyssynchrony predicts ventricular response after resynchronization therapy. *J Am Coll Cardiol* 2007;**50**:1476–83.
94. Ypenburg C, van Bommel RJ, Delgado V, Mollema SA, Bleeker GB, Boersma E *et al.* Optimal left ventricular lead position predicts reverse remodeling and survival after cardiac resynchronization therapy. *J Am Coll Cardiol* 2008;**52**:1402–9.
95. Chung ES, Leon AR, Tavazzi L, Sun JP, Nihoyannopoulos P, Merlino J *et al.* Results of the Predictors of Response to CRT (PROSPECT) trial. *Circulation* 2008;**117**:2608–16.
96. Beshai JF, Grimm RA, Nagueh SF, Baker JH, Beau SL, Greenberg SM *et al.* Cardiac-resynchronization therapy in heart failure with narrow QRS complexes. *N Engl J Med* 2007;**357**:2461–71.
97. Oyenuga O, Hara H, Tanaka H, Kim HN, Adelstein EC, Saba S *et al.* Usefulness of echocardiographic dyssynchrony in patients with borderline QRS duration to assist with selection for cardiac resynchronization therapy. *JACC Cardiovasc Imaging* 2010;**3**:132–40.
98. Miyazaki C, Powell BD, Bruce CJ, Espinosa RE, Redfield MM, Miller FA *et al.* Comparison of echocardiographic dyssynchrony assessment by tissue velocity and strain imaging in subjects with or without systolic dysfunction and with or without left bundle-branch block. *Circulation* 2008;**117**:2617–25.
99. Miyazaki C, Redfield MM, Powell BD, Lin GM, Herges RM, Hodge DO *et al.* Dyssynchrony indices to predict response to cardiac resynchronization therapy: a comprehensive, prospective single-center study. *Circ Heart Fail* 2010;**3**:565–73.
100. Nagueh SF, Appleton CP, Gillebert TC, Marino PN, Oh JK, Smiseth OA *et al.* Recommendations for the evaluation of left ventricular diastolic function by echocardiography. *J Am Soc Echocardiogr* 2009;**22**:107–33.

101. Abraham TP, Belohlavek M, Thomson HL, Pislaru C, Khandheria B, Seward JB *et al.* Time to onset of regional relaxation: feasibility, variability and utility of a novel index of regional myocardial function by strain rate imaging. *J Am Coll Cardiol* 2002;**39**:1531–7.
102. Pislaru C, Bruce CJ, Anagnostopoulos PC, Allen JL, Seward JB, Pellikka PA *et al.* Ultrasound strain imaging of altered myocardial stiffness: stunned versus infarcted reperfused myocardium. *Circulation* 2004;**109**:2905–10.
103. Park TH, Nagueh SF, Khoury DS, Kopelen HA, Akrivakis S, Nasser K *et al.* Impact of myocardial structure and function postinfarction on dia- stolic strain measurements: implications for assessment of myocardial viability. *Am J Physiol Heart Circ Physiol* 2006;**290**:H724–31.
104. Park SM, Miyazaki C, Prasad A, Bruce CJ, Chandrasekaran K, Rihal C *et al.* Feasibility of prediction of myocardial viability with Doppler tissue imaging following percutaneous coronary intervention for ST elevation anterior myocardial infarction. *J Am Soc Echocardiogr* 2009;**22**:183–9.
105. Kato T, Noda A, Izawa H, Nishizawa T, Somura F, Yamada A *et al.* Myocardial velocity gradient as a noninvasively determined index of left ventricular diastolic dysfunction in patients with hypertrophic cardiomyopathy. *J Am Coll Cardiol* 2003;**42**:278–85.
106. Wakami K, Ohte N, Sakata S, Kimura G. Myocardial radial strain in early diastole is useful for assessing left ventricular early diastolic function: comparison with invasive parameters. *J Am Soc Echocardiogr* 2008;**21**:446–51.
107. 107 Dokainish H, Sengupta R, Pillai M, Bobek J, Lakkis N. Usefulness of new diastolic strain and strain rate indexes for the estimation of left ventricular filling pressure. *Am J Cardiol* 2008;**101**:1504–9.
108. Shanks M, Ng AC, van de Veire NR, Antoni ML, Bertini M, Delgado V *et al.* Incremental prognostic value of novel left ventricular diastolic indexes for prediction of clinical outcome in patients with ST-elevation myocardial infarction. *Am J Cardiol* 2010;**105**:592–7.
109. Wakami K, Ohte N, Asada K, Fukuta H, Goto T, Mukai S *et al.* Correlation between left ventricular end-diastolic pressure and peak left atrial wall strain during left ventricular systole. *J Am Soc Echocardiogr* 2009;**22**:847–51.
110. Voigt JU, Lindenmeier G, Exner B, Regenfus M, Werner D, Reulbach U *et al.* Incidence and characteristics of segmental postsystolic longitudinal shortening in normal, acutely ischemic, and scarred myocardium. *J Am Soc Echocardiogr* 2003;**16**:415–23.
111. Reisner SA, Lysyansky P, Agmon Y, Mutlak D, Lessick J, Friedman Z. Global longitudinal strain: a novel index of left ventricular systolic function. *J Am Soc Echocardiogr* 2004;**17**:630–3.
112. Derumeaux G, Ovize M, Loufoua J, Andre-Fouet X, Minaire Y, Cribier A *et al.* Doppler tissue imaging quantitates regional wall motion during myocardial ischemia and reperfusion. *Circulation* 1998;**97**:1970–7.
113. Bolognesi R, Tsialtas D, Barilli AL, Manca C, Zeppellini R, Javernaro A *et al.* Detection of early abnormalities of left ventricular function by he- modynamic, echo-tissue Doppler imaging, and mitral Doppler flow techniques in patients with coronary artery disease and normal ejection fraction. *J Am Soc Echocardiogr* 2001;**14**:764–72.
114. Hatle L, Sutherland GR. Regional myocardial function—a new approach. *Eur Heart J* 2000;**21**:1337–57.
115. Gorcsan J III, Strum DP, Mandarino WA, Gulati VK, Pinsky MR. Quantitative assessment of alterations in regional left ventricular contractility with color-coded tissue Doppler echocardiography. *Comparison with so- nomicrometry and pressure-volume relations. Circulation* 1997;**95**:2423–33.
116. Fraser AG, Payne N, Madler CF, Janerot-Sjoberg B, Lind B, Grocott- Mason RM *et al.* Feasibility and reproducibility of off-line tissue Doppler measurement of regional myocardial function during dobutamine stress echocardiography. *Eur J Echocardiogr* 2003;**4**:43–53.
117. Madler CF, Payne N, Wilkenshoff U, Cohen A, Derumeaux GA, Pierard LA *et al.* Non-invasive diagnosis of coronary artery disease by quantitative stress echocardiography: optimal diagnostic models using off-line tissue Doppler in the MYDISE study. *Eur Heart J* 2003;**24**:1584–94.
118. Pasquet A, Yamada E, Armstrong G, Beachler L, Marwick TH. Influence of dobutamine or exercise stress on the results of pulsed-wave Doppler assessment of myocardial velocity. *Am Heart J* 1999;**138**:753–8.
119. Cain P, Short L, Baglin T, Case C, Bosch HG, Marwick TH. Development of a fully quantitative approach to the interpretation of stress echocardi- ography using radial and longitudinal myocardial velocities. *J Am Soc Echocardiogr* 2002; **15**:759–67.
120. Marciniak M, Claus P, Streb W, Marciniak A, Boettler P, McLaughlin M *et al.* The quantification of dipyridamole induced changes in regional deformation in normal, stunned or infarcted myocardium as measured by strain and strain rate: an experimental study. *Int J Cardiovasc Imaging* 2008;**24**:365–76.
121. Jamal F, Strotmann J, Weidemann F, Kukulski T, D'hooge J, Bijnens B *et al.* Noninvasive quantification of the contractile reserve of stunned myocardium by ultrasonic strain rate and strain. *Circulation* 2001;**104**:1059–65.
122. Weidemann F, Dommke C, Bijnens B, Claus P, D'hooge J, Mertens P *et al.* Defining the transmurality of a chronic myocardial infarction by ultrasonic strain-rate imaging: implications for identifying intramural viability: an experimental study. *Circulation* 2003;**107**:883–8.
123. Becker M, Bilke E, Kuhl H, Katoh M, Kramann R, Franke A *et al.* Analysis of myocardial deformation based on pixel tracking in two dimensional echocardiographic images enables quantitative assessment of regional left ventricular function. *Heart* 2006;**92**:1102–8.
124. Antoni ML, Mollema SA, Delgado V, Atary JZ, Borleffs CJ, Boersma E *et al.* Prognostic importance of strain and strain rate after acute myocardial infarction. *Eur Heart J* 2010;**31**:1640–7.
125. Reant P, Labrousse L, Lafitte S, Bordachar P, Pillois X, Tariosse L *et al.* Experimental validation of circumferential, longitudinal, and radial 2-di- mensional strain during dobutamine stress echocardiography in ischemic conditions. *J Am Coll Cardiol* 2008;**51**:149–57.
126. Stefani L, Toncelli L, Di TV, Vono MC, Cappelli B, Pedrizzetti G *et al.* Supernormal functional reserve of apical segments in elite soccer players: an ultrasound speckle tracking handgrip stress study. *Cardiovasc Ultrasound* 2008;**6**:14.
127. Hanekom L, Cho GY, Leano R, Jeffriess L, Marwick TH. Comparison of two-dimensional speckle and tissue Doppler strain measurement during dobutamine stress echocardiography: an angiographic correlation. *Eur Heart J* 2007;**28**: 1765–72.
128. Ingul CB, Stoylen A, Slordahl SA, Wiseth R, Burgess M, Marwick TH. Automated analysis of myocardial deformation at dobutamine stress echo- cardiography: an angiographic validation. *J Am Coll Cardiol* 2007;**49**:1651–9.
129. Kim RJ, Wu E, Rafael A, Chen EL, Parker MA, Simonetti O *et al.* The use of contrast-enhanced magnetic resonance imaging to identify reversible myocardial dysfunction. *N Engl J Med* 2000;**343**:1445–53.
130. Weidemann F, Niemann M, Herrmann S, Kung M, Stork S, Waller C *et al.* A new echocardiographic approach for the detection of non- ischaemic fibrosis in hypertrophic myocardium. *Eur Heart J* 2007;**28**:3020–6.
131. Weidemann F, Herrmann S, Stork S, Niemann M, Frantz S, Lange V *et al.* Impact of myocardial fibrosis in patients with symptomatic severe aortic stenosis. *Circulation* 2009;**120**:577–84.
132. Mizushige K, Yao L, Noma T, Kiyomoto H, Yu Y, Hosomi N *et al.* Alteration in left ventricular diastolic filling and accumulation of myocardial collagen at insulin-resistant prediabetic stage of a type II diabetic rat model. *Circulation* 2000;**101**: 899–907.
133. Picano E, Lattanzi F, Orlandini A, Marini C, L'Abbate A. Stress echocardiography and the human factor: the importance of being expert. *J Am Coll Cardiol* 1991;**17**: 666–9.
134. Liel-Cohen N, Tsadok Y, Beeri R, Lysyansky P, Agmon Y, Feinberg MS *et al.* A new tool for automatic assessment of segmental wall motion based on longitudinal 2D strain: a multicenter study by the Israeli Echocardiography Research Group. *Circ Cardiovasc Imaging* 2010;**3**:47–53.
135. Chan J, Hanekom L, Wong C, Leano R, Cho GY, Marwick TH. Differentiation of subendocardial and transmural infarction using two-dimensional strain rate imaging to assess short-axis and long-axis myocardial function. *J Am Coll Cardiol* 2006;**48**:2026–33.
136. Becker M, Ocklenburg C, Altiok E, Futing A, Balzer J, Krombach G *et al.* Impact of infarct transmurality on layer-specific impairment of myocar- dial function: a myocardial deformation imaging study. *Eur Heart J* 2009;**30**:1467–76.
137. Hoffmann R, Altiok E, Nowak B, Heussen N, Kuhl H, Kaiser HJ *et al.* Strain rate measurement by Doppler echocardiography allows improved assessment of myocardial viability in patients with depressed left ventricular function. *J Am Coll Cardiol* 2002;**39**:443–9.
138. Hanekom L, Jenkins C, Short L, Marwick TH. Accuracy of strain rate techniques for identification of viability at dobutamine stress echo: a follow-up study after revascularization. *J Am Coll Cardiol* 2004;**43**:p360A.
139. Vitarelli A, Montesano T, Gaudio C, Conde Y, Cimino E, D'angeli I *et al.* Strain rate dobutamine echocardiography for prediction of recovery after revascularization in patients with ischemic left ventricular dysfunction. *J Card Fail* 2006; **12**:268–75.
140. Greenberg NL, Firstenberg MS, Castro PL, Main M, Travaglini A, Odabashian JA *et al.* Doppler-derived myocardial systolic strain rate is a strong index of left ventricular contractility. *Circulation* 2002;**105**:99–105.
141. Hoffmann R, Marwick TH, Poldermans D, Lethen H, Ciani R, van der MP *et al.* Refinements in stress echocardiographic techniques improve inter-institutional agreement in interpretation of dobutamine stress echocardiograms. *Eur Heart J* 2002;**23**:821–9.
142. Jamal F, Bergerot C, Argaud L, Loufouat J, Ovize M. Longitudinal strain quantitates regional right ventricular contractile function. *Am J Physiol Heart Circ Physiol* 2003;**285**:H2842–7.

143. Giusca S, Dambrauskaite V, Scheurwegs C, D'hooge J, Claus P, Herbots L *et al.* Deformation imaging describes right ventricular function better than longitudinal displacement of the tricuspid ring. *Heart* 2010;**96**:281–8.
144. Rudski LG, Lai WW, Afilalo J, Hua L, Handschumacher M, Chandrasekaran K *et al.* Guidelines for the echocardiographic assessment of the right heart in adults: a report from the American Society of Echocardiography. *J Am Soc Echocardiogr* 2010;**23**:685–713.
145. Meluzin J, Spinarova L, Bakala J, Toman J, Krejci J, Hude P *et al.* Pulsed Doppler tissue imaging of the velocity of tricuspid annular systolic motion; a new, rapid, and non-invasive method of evaluating right ventricular systolic function. *Eur Heart J* 2001;**22**:340–8.
146. Damy T, Viallet C, Lairez O, Deswarte G, Paulino A, Maison P *et al.* Comparison of four right ventricular systolic echocardiographic parameters to predict adverse outcomes in chronic heart failure. *Eur J Heart Fail* 2009;**11**:818–24.
147. Lindqvist P, Waldenstrom A, Henein M, Morner S, Kazzam E. Regional and global right ventricular function in healthy individuals aged 20-90 years: a pulsed Doppler tissue imaging study: Umea General Population Heart Study. *Echocardiography* 2005;**22**:305–14.
148. Huez S, Roufosse F, Vachiery JL, Pavelescu A, Derumeaux G, Wautrecht JC *et al.* Isolated right ventricular dysfunction in systemic sclerosis: latent pulmonary hypertension? Eur Respir J 2007;**30**:928–36.
149. Weidemann F, Eyskens B, Jamal F, Mertens L, Kowalski M, D'hooge J *et al.* Quantification of regional left and right ventricular radial and longitudinal function in healthy children using ultrasound-based strain rate and strain imaging. *J Am Soc Echocardiogr* 2002;**15**:20–8.
150. Teske AJ, De Boeck BW, Olimulder M, Prakken NH, Doevendans PA, Cramer MJ. Echocardiographic assessment of regional right ventricular function: a head-to-head comparison between 2-dimensional and tissue Doppler-derived strain analysis. *J Am Soc Echocardiogr* 2008;**21**:275–83.
151. Vitarelli A, Conde Y, Cimino E, Stellato S, D'orazio S, D'angeli I *et al.* Assessment of right ventricular function by strain rate imaging in chronic obstructive pulmonary disease. *Eur Respir J* 2006;**27**:268–75.
152. Borges AC, Knebel F, Eddicks S, Panda A, Schattke S, Witt C *et al.* Right ventricular function assessed by two-dimensional strain and tissue Dopp- ler echocardiography in patients with pulmonary arterial hypertension and effect of vasodilator therapy. *Am J Cardiol* 2006;**98**:530–4.
153. Pirat B, McCulloch ML, Zoghbi WA. Evaluation of global and regional right ventricular systolic function in patients with pulmonary hypertension using a novel speckle tracking method. *Am J Cardiol* 2006;**98**:699–704.
154. Matias C, Isla LP, Vasconcelos M, Almeria C, Rodrigo JL, Serra V *et al.* Speckle-tracking-derived strain and strain-rate analysis: a technique for the evaluation of early alterations in right ventricle systolic function in patients with systemic sclerosis and normal pulmonary artery pressure. *J Cardiovasc Med (Hagerstown)* 2009;**10**:129–34.
155. Eyskens B, Brown SC, Claus P, Dymarkowski S, Gewillig M, Bogaert J *et al.* The influence of pulmonary regurgitation on regional right ventricular function in children after surgical repair of tetralogy of Fallot. *Eur J Echocardiogr* 2010;**11**: 341–5.
156. Puwanant S, Park M, Popovic ZB, Tang WH, Farha S, George D *et al.* Ventricular geometry, strain, and rotational mechanics in pulmonary hypertension. *Circulation* 2010;**121**:259–66.
157. Badano LP, Ginghina C, Easaw J, Muraru D, Grillo MT, Lancellotti P *et al.* Right ventricle in pulmonary arterial hypertension: haemodynamics, structural changes, imaging, and proposal of a study protocol aimed to assess remodelling and treatment effects. *Eur J Echocardiogr* 2010;**11**:27–37.
158. Bauer F, Jones M, Qin JX, Castro P, Asada J, Sitges M *et al.* Quantitative analysis of left atrial function during left ventricular ischemia with and without left atrial ischemia: a real-time 3-dimensional echocardiographic study. *J Am Soc Echocardiogr* 2005;**18**:795–801.
159. Cameli M, Caputo M, Mondillo S, Ballo P, Palmerini E, Lisi M *et al.* Feasibility and reference values of left atrial longitudinal strain imaging by two-dimensional speckle tracking. *Cardiovasc Ultrasound* 2009;**7**:6.
160. Vianna-Pinton R, Moreno CA, Baxter CM, Lee KS, Tsang TS, Appleton CP. Two-dimensional speckle-tracking echocardiography of the left atrium: feasibility and regional contraction and relaxation differences in normal subjects. *J Am Soc Echocardiogr* 2009;**22**:299–305.
161. Saraiva RM, Demirkol S, Buakhamsri A, Greenberg N, Popovic ZB, Thomas JD *et al.* Left atrial strain measured by two-dimensional speckle tracking represents a new tool to evaluate left atrial function. *J Am Soc Echocardiogr* 2010;**23**:172–80.
162. Boyd AC, Cooper M, Thomas L. Segmental atrial function following percutaneous closure of atrial septum using occluder device. *J Am Soc Echocardiogr* 2009;**22**:508–16.
163. Boyd AC, Schiller NB, Ross DL, Thomas L. Differential recovery of regional atrial contraction after restoration of sinus rhythm after intraoper- ative linear radiofrequency ablation for atrial fibrillation. *Am J Cardiol* 2009;**103**:528–34.
164. Borg AN, Pearce KA, Williams SG, Ray SG. Left atrial function and deformation in chronic primary mitral regurgitation. *Eur J Echocardiogr* 2009;**10**:833–40.
165. Di Salvo G, Caso P, Lo PR, Fusco A, Martiniello AR, Russo MG *et al.* Atrial myocardial deformation properties predict maintenance of sinus rhythm after external cardioversion of recent-onset lone atrial fibrillation: a color Doppler myocardial imaging and transthoracic and transesopha- geal echocardiographic study. *Circulation* 2005;**112**:387–95.
166. Sun P, Wang ZB, Li JX, Nie J, Li Y, He XQ *et al.* Evaluation of left atrial function in physiological and pathological left ventricular myocardial hypertrophy by real-time triplane strain rate imaging. *Clin Cardiol* 2009;**32**:676–83.
167. Di Salvo G, Pacileo G, Castaldi B, Gala S, Morelli C, D'Andrea A *et al.* Two-dimensional strain and atrial function: a study on patients after percutaneous closure of atrial septal defect. *Eur J Echocardiogr* 2009;**10**:256–9.
168. Tsai WC, Lee CH, Lin CC, Liu YW, Huang YY, Li WT *et al.* Association of left atrial strain and strain rate assessed by speckle tracking echocardi- ography with paroxysmal atrial fibrillation. *Echocardiography* 2009;**26**:1188–94.
169. D'Andrea A, Caso P, Romano S, Scarafile R, Riegler L, Salerno G *et al.* Different effects of cardiac resynchronization therapy on left atrial function in patients with either idiopathic or ischaemic dilated cardiomyopa- thy: a two-dimensional speckle strain study. *Eur Heart J* 2007;**28**:2738–48.
170. Sirbu C, Herbots L, D'hooge J, Claus P, Marciniak A, Langeland T *et al.* Feasibility of strain and strain rate imaging for the assessment of regional left atrial deformation: a study in normal subjects. *Eur J Echocardiogr* 2006;**7**:199–208.
171. Rigolin VH, Robiolio PA, Wilson JS, Harrison JK, Bashore TM. The forgotten chamber: the importance of the right ventricle. *Cathet Cardiovasc Diagn* 1995; **35**:18–28.
172. Brennan JM, Blair JE, Goonewardena S, Ronan A, Shah D, Vasaiwala S *et al.* Reappraisal of the use of inferior vena cava for estimating right atrial pressure. *J Am Soc Echocardiogr* 2007;**20**:857–61.
173. Gullace G, Savoia MT. Echocardiographic assessment of the inferior vena cava wall motion for studies of right heart dynamics and function. *Clin Cardiol* 1984; **7**:393–404.
174. Kircher BJ, Himelman RB, Schiller NB. Noninvasive estimation of right atrial pressure from the inspiratory collapse of the inferior vena cava. *Am J Cardiol* 1990;**66**:493–6.
175. Moreno FL, Hagan AD, Holmen JR, Pryor TA, Strickland RD, Castle CH. Evaluation of size and dynamics of the inferior vena cava as an index of right-sided cardiac function. *Am J Cardiol* 1984;**53**:579–85.
176. Nagueh SF, Kopelen HA, Zoghbi WA. Relation of mean right atrial pressure to echocardiographic and Doppler parameters of right atrial and right ventricular function. *Circulation* 1996;**93**:1160–9.
177. Ommen SR, Nishimura RA, Hurrell DG, Klarich KW. Assessment of right atrial pressure with 2-dimensional and Doppler echocardiography: a simultaneous catheterization and echocardiographic study. *Mayo Clin Proc* 2000;**75**:24–9.
178. D'Andrea A, Scarafile R, Riegler L, Salerno G, Gravino R, Cocchia R *et al.* Right atrial size and deformation in patients with dilated cardiomyopathy undergoing cardiac resynchronization therapy. *Eur J Heart Fail* 2009;**11**:1169–77.
179. Voigt JU. QuantifizierungderMyokardfunktion. In: Flachskampf FA editor. Praxis der Echokardiographie. 3rd ed. Stuttgart, Germany: Thieme; 2010.
180. Voigt JU. Quantification of left ventricular function and synchrony using tissue Doppler, strain imaging, and speckle tracking. In: Galiuto L, Badano LP, Fox K, Sicari R, Zamorano JL editors. *EAR textbook of echocardiography*. Oxford, UK: Oxford University Press; 2010.
181. Camm AJ, Luscher TF, Serruys PW. The ESC textbook of cardiovascular medicine. Oxford, UK: Oxford University Press; 2009. 99–147.
182. Moore CC, Lugo-Olivieri CH, McVeigh ER, Zerhouni EA. Three-dimensional systolic strain patterns in the normal human left ventricle: characterization with tagged MR imaging. Radiology 2000;**214**:453–66.
183. Edvardsen T, Gerber BL, Garot J, Bluemke DA, Lima JA, Smiseth OA. Quantitative assessment of intrinsic regional myocardial deformation by Doppler strain rate echocardiography in humans: validation against three-dimensional tagged magnetic resonance imaging. *Circulation* 2002;**106**:50–6.
184. Kowalski M, Kukulski T, Jamal F, D'hooge J, Weidemann F, Rademakers F *et al.* Can natural strain and strain rate quantify regional myocardial deformation? A study in healthy subjects. *Ultrasound Med Biol* 2001;**27**:1087–97.
185. Sun JP, Popovic ZB, Greenberg NL, Xu XF, Asher CR, Stewart WJ *et al.* Noninvasive quantification of regional myocardial function using Doppler-derived velocity, displacement, strain rate, and strain in healthy volunteers: effects of aging. *J Am Soc Echocardiogr* 2004;**17**:132–8.